Student thesis series INES nr 533

Increasing forest mortality and its drivers: Simulating central European forests under climate change

Marieke Scheel

2021

Department of

Physical Geography and Ecosystem Science

Lund University

Sölvegatan 12

S-223 62 Lund

Marieke Scheel (2021).

Increasing forest mortality and its drivers: Simulating central European forests under climate change (English)

Ökande skogsdödlighet och dess drivkrafter: Simulering av centraleuropeiska skogar under klimatförändringar (Swedish)

Bachelor degree thesis, 15 credits in Physical Geography and Ecosystem Analysis

Department of Physical Geography and Ecosystem Science, Lund University

Level: Bachelor of Science (BSc)

Course duration: *November* 2020 until *January* 2021

Disclaimer

Increasing forest mortality and its drivers: Simulating central European forests under climate change

---

Marieke Scheel

Bachelor thesis, 15 credits, in Physical Geography and Ecosystem Analysis

Supervisor 1: Benjamin Smith

Department of Physical Geography and Ecosystem Science

Supervisor 2: Thomas Pugh

Department of Physical Geography and Ecosystem Science

Exam committee:

Examiner 1: Anders Ahlström,

Department of Physical Geography and Ecosystem Science

Examiner 2: Martin Berggren

Department of Physical Geography and Ecosystem Science

Acknowledgements

Firstly, I would like to thank my supervisors Thomas Pugh and Benjamin Smith for their guidance and thorough feedback. Thanks as well to Thomas Pugh for suggesting the thesis topic and helping to shape it. Also, I thank my fellow classmates for the great feedback sessions and their moral support, while working together in the computer lab. Thanks to my family for supporting me and putting up with me while finishing this thesis.

Abstract

Increasing tree growth and mortality rates in Europe are still poorly understood and have been attributed to a variety of drivers. This study aimed to relate increasing forest mortality rates in six central European countries to climate drivers (CO_2 concentration, temperature and precipitation) from 1985-2015, using a process-based vegetation model. For this, the direct (e.g. mortality due to water scarcity) and indirect (e.g. enhanced competition leading to increased mortality) effects of changes in climate drivers on mortality were assessed. Using the LPJ-GUESS dynamic vegetation model (DVM), a dataset showing increased canopy mortality rates was aimed to be reproduced. Factorial simulations excluding changes in individual drivers were run to identify causes of simulated trends. The lack of relationship between simulated and observed canopy mortality rates were suggested to be linked to simplifications of the model. Also, a link to land use changes and increased harvest intensity, which cannot be captured by a model simulating natural vegetation is suggested. In most countries examined, an increased tree mortality could partially be attributed to increased competition, caused by faster tree growth and crowding. An exception was Switzerland, where a negative trend in canopy mortality was associated with its vegetation being simulated at a higher altitude and treeline advance was suggested to be responsible for decreasing mortality rates and increasing NPP. The main driver of increased competition mortality was identified to be the increase in CO_2 concentration. Interestingly, changes in seasonal precipitation patterns caused an increase in water availability and a small increase in competition. Increasing nitrogen deposition partially increased competition trends, but it remains uncertain at which scale. Temperature (mainly increasing stress mortality) was the largest driver of mortality followed by CO_2 concentration (mainly increasing competition mortality due to higher productivity induced by 'CO_2 fertilisation'), however, this assessment includes a large uncertainty. Further studies distinguishing between vitality mortality caused by direct and indirect resource stress (through neighbourhood crowding) are recommended to decrease that uncertainty. This study contributes to the understanding of the current changes in the global carbon cycle and sink, can help to adapt forest management practices to those changes and improves the understanding of the LPJ-GUESS model.

Key Words: *Forest mortality, central Europe, competition, CO_2, temperature, precipitation, DVM, LPJ-GUESS, simulation, reproducing data*

Popular Summary

European forests grow and die faster than in the past. This has been caused by many different drivers that have changed because of climate change. In this study it was investigated if the increase in tree mortality in European forests from 1985-2015 was caused by higher stress among trees because resources decreased (stress mortality) or because resources increased causing trees to grow and compete with each other for limited resources. The role of CO_2 concentration, temperature and precipitation was assessed for the changes in resource availabilities in forests. A dynamic vegetation model (LPJ-GUESS), that simulates vegetation based on climate conditions, was run to be able to link changes to individual drivers. By comparing simulations with change in individual driver 'switched off' to a simulation aiming to reproduce observed vegetation trends, one could identify causes of tree mortality trends. The trends in simulated tree crown death (canopy mortality) were shown to not be related to the trends revealed by an observational dataset. This discrepancy was attributed to simplifications of the model and by land use changes and increased timber harvest intensity in the dataset that are not captured by a model not simulating human impact through e.g., harvest. The increase in tree mortality was partially shown to be related to increased competition, since trees were displayed to grow faster, which leads to trees being outcompeted faster (competition mortality). A decrease in canopy mortality in Switzerland was the exception and was suggested to be caused by its vegetation being simulated at a higher altitude. There, vegetation is generally more stressed and only vegetation that can cope with those conditions can grow there (usually smaller, herbaceous vegetation). Due to climate change the conditions are becoming more favourable for different vegetation so that more species start to grow in higher altitudes (tree line advance). Decreasing tree mortality rates were suggested to be caused by growth conditions improving. The main driver of increased competition mortality was identified to be the increase in CO_2 concentration, which positively impacts vegetation productivity through 'CO_2 fertilisation'. Changes in precipitation during the different seasons caused an increase in water availability and a small increase in competition. Temperature (mainly increasing stress mortality) was shown to be the largest driver of mortality followed by CO_2 concentration (mainly increasing competition mortality), however, this assessment includes a large uncertainty. This study contributes to the understanding of the current changes in the global carbon cycle and sink, can help to adapt forest management practices to those changes and improves the understanding of the LPJ-GUESS model.

Table of Contents

Abbreviations

AT - Austria

CH - Switzerland

CZ - the Czech Republic

DE - Germany

LAI - Leaf area index
A unitless measure of leaf area (m^2) per ground area (m^2)

LPJ-GUESS - Lund-Potsdam-Jena General Ecosystem Simulator
A Dynamic Vegetation Model, version used in this study refers to Smith et al. (2014)

NPP - Net Primary Productivity
The net carbon gain of plants. It is a balance between the carbon gained through photosynthesis and carbon lost by respiration. (NPP = Gross Primary Productivity – plant respiration)

PFT - Plant Functional Type
Plant types are grouped based on their growth form, bioclimatic limits for growth, photosynthetic pathway, plant phenology, plant allometry and life history strategy (Smith 2001).

PL - Poland

SK – Slovakia

1 Introduction

1.1 Background

Worldwide forest growth rates have been observed to accelerate (Notaro et al. 2005; Mellert et al. 2008; McMahon et al. 2010; Pretzsch et al. 2014b; Bontemps et al. 2020). Drivers that have been associated with increasing growth rates include atmospheric CO_2 concentrations (Bellassen et al. 2011; Friend et al. 2014), increasing temperatures (Myneni et al. 1997) and atmospheric nitrogen (N) depositions (De Vries et al. 2006; Laubhann et al. 2009). Photosynthesis rates increase due to CO_2 fertilisation, which enhances NPP and accelerates growth rates (Ainsworth and Long 2005). Furthermore, water-use efficiency increases with higher CO_2 concentrations (Frank et al. 2015). The observed increase in temperatures over the last decades, has been linked with a lengthening of the growing season (Myneni et al. 1997), increased nitrogen fixation rates and heightening of metabolic rates (Friend et al. 2014). However, the latter process is only enhanced with increasing temperatures until passing a certain temperature threshold (Hyvönen et al. 2007). Nitrogen deposition rates were in particular high in central Europe because of its extensive industrialisation (Hyvönen et al. 2007). Policy changes and implementations of regulations have caused a decrease in N deposition in Europe since the 1990s (Schmitz et al. 2019) but not worldwide (Fowler et al. 2015). Higher N deposition has mainly accelerated growth by increasing LAI (Hyvönen et al. 2007).

Additionally, tree mortality rates in forests worldwide have been found to increase (van Mantgem et al. 2009; Luo and Chen 2015; Neumann et al. 2017; Senf et al. 2018; Hubau et al. 2020). These findings have been mainly attributed to increased stress due to climate change, such as detrimental changes in precipitation patterns (Archambeau et al. 2020) and water stress caused by increasing temperatures that cause soil drying (Vilà-Cabrera et al. 2011). However, other factors have been shown to also contribute to observed changes. Forest demography in Europe is shown to have changed since the 1950s, with forest stands becoming increasingly more juvenile and hence showing increasing carbon accumulation rates (Ciais et al. 2008; Vilén et al. 2012). Furthermore, the ratio of harvest relative to the available woody biomass (which has been increasing) has been decreasing in Europe since the 1950s (Ciais et al. 2008). Also, disturbances like windthrow, forest fires and bark beetles have caused increasing damage in European forests and are projected to increase further in the future (Schelhaas et al. 2003; Seidl et al. 2014).

However, the observed increase in tree mortality and forest growth have been accompanied by changes in forest dynamics, including changes in competition (Ruiz-Benito et al. 2013; Luo and Chen 2015; Etzold et al. 2019; Needham et al. 2020; Rozendaal et al. 2020). Trees compete over resources (water, light and nutrients) and the weakest trees get outcompeted and die. This process is known as self-thinning and is, as shown in fig. 1, a function of biomass (B) and stand density (N) (Westoby 1984). A young stand consisting of a large number of trees will have a relatively low total biomass. Such a stand will according to the self-thinning rule initially develop rather vertically until neighbourhood crowding sets in. That will make resources limited and self-thinning starts, as depicted in fig. 1, following the self-thinning line. Then the number of trees will decrease while the amount of biomass increases, trees hence getting larger in size but fewer in number.

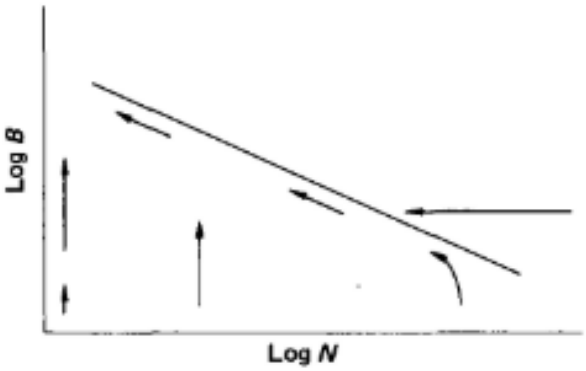

Figure 1. B is the biomass and N is the density, the arrows show the 'direction' of development of forests. This figure is reprinted from Westoby (1984), with permission from Elsevier.

Accelerated forest growth leads to a current forest stand of a certain age to consist of fewer trees that are larger in height than in a forest stand of the same age in the past (Pretzsch et al. 2014b). Therefore, it can be concluded that higher growth rates speed up self-thinning, reflected in higher mortality rates (Luo and Chen 2015; Lu et al. 2019). It is, hence, unclear how much better growth conditions (e.g., through CO_2 fertilisation or an extended growing season) and worse growth conditions (e.g., water or other resource stress) contribute to observed increases in tree mortality.

Both an acceleration in growth rates, as well as an increase in mortality rates were observed in Europe in several studies. The slope of self-thinning lines (Fig. 1) in European forests has been observed to remain constant, while intercepts moved up and stands moved along the self-thinning line faster (due to a changed turnover rate and growth velocity, while resource stock stayed the same) (Pretzsch et al. 2014b). Another study showed trees to move along self-thinning lines faster, but the slope of self-thinning lines furthermore shifted upwards, indicating an additional increase in growing stock (Pretzsch et al. 2014a). The latter was suggested to be mainly caused by the increasing temperatures (Pretzsch et al. 2014a). However, Dulamsuren et al. (2017) found growth rates of European beech to only increase at high elevations and to decline at low elevations in Germany since the 1980s. Thus, suggesting the increasing growth rates to be linked to altitude. Archambeau et al. (2020) found that increasing droughts increased mortality rates of beech and Scots pine along the entire European latitudinal gradient. But while mortality of Scots pine was mainly caused by competition (that increased with water stress), mortality of beech was mostly driven by the intensity of a drought. This study shows how resource stress can impact vegetation directly or indirectly via competition. The latter links back to higher resource availability potentially inducing self-thinning.

Senf et al. (2018) showed that the annual canopy mortality rate (loss of canopy in m^2/ total area of canopy in m^2) in Austria, the Czech Republic, Germany, Poland, Slovakia, and Switzerland more than doubled (increased by 2.4% yr^{-1}) between 1984 and 2016 (Fig. 2, Fig. 9). Those six countries were selected because of their diversity regarding biophysical gradients and forest management. The study analysed Landsat time series and matched it spatially with ESA images to estimate canopy mortality rates. In each country 4000 Landsat pixels (of 30m resolution) were randomly sampled and analysed by a human interpreter according to the TimeSync approach (Cohen et al. 2010). Canopy mortality was distinguished as being non-stand-replacing or stand-replacing and non-stand replacing canopy mortality was observed to increase more strongly (Fig. 2). However, a clear attribution of the drivers of the observed canopy mortality increase in Senf et al. (2018) is lacking. As the countries differed in forest types and management, the increase in canopy mortality rates was suggested to be caused by the broad

scale processes of increasing temperatures, increasing growing stocks due to forest recovery from past land uses and potentially by changes in total annual precipitation. To improve the interpretation of the observed canopy mortality trends, wood removal rates, inventories (mortality of individual trees) and disturbances (windthrow, bark beetles) were analysed. Canopy mortality rates were shown to correlate positively with wood removal rates, bark beetles and windthrow, while a negative correlation with stem mortality rates was calculated (loss of numbers of tree trunks). Moreover, stem mortality rates showed a slight and uncertain decrease over the time period. Senf et al. (2018) suggested that changes of land use and especially increased harvest rates are the major agents responsible for the increased canopy mortality in Europe. The intensified tree harvest was assumed to mainly happen as thinning (opposed to as clear-cut) due to changes in silvicultural practices. Generally, Senf et al. (2018) concluded that stands with a high growing stock or large forest area were affected more strongly by mortality, with less (but larger) trees dying in those stands than in the past. This was interpreted to suggest that decreasing carbon residence time and higher mortality rates might cancel out the increase in forest growth.

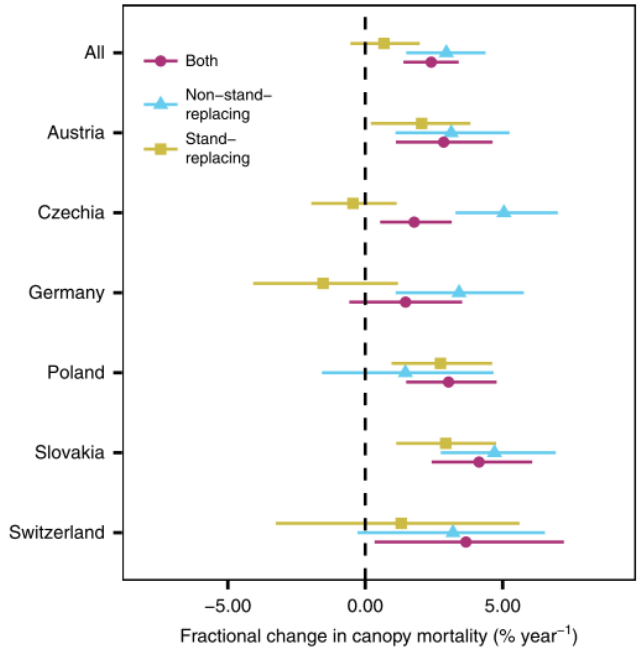

Figure. 2. 'Changes in stand-replacing and non-stand-replacing canopy mortality. Mortality is considered stand-replacing if there are no live trees after the mortality event at the level of a 30m pixel. Points indicate the median of the posterior probability distributions, and bars extent to the 95% credible interval' (Senf et al. 2018). This figure is reprinted from Senf et al. (2018).

The carbon stored in terrestrial biomass and soils is roughly three times as much as CO_2 stored in the Earth's atmosphere (Körner 2003). About 90% of the carbon stored in biomass is stored in forests (Körner 2003), thereby highlighting the important role of forests in the carbon cycle. Therefore, the suggested decrease of the carbon sink in European forests due to increased growth rates and turnover time (Senf et al. (2018); (Brienen et al. 2020) would negatively impact the global carbon storage and risk accelerating climate change. It is therefore of increasing importance to clearly understand the drivers of the observed increases in canopy mortality (Senf et al. 2018).

Vegetation models can be used to understand the mechanisms driving changes in vegetation functions and structures, like LAI, growth rates or mortality rates. A dynamic vegetation model (DVM) simulates vegetation establishment and growth in a simplified manner and typically at a coarse spatial scale (Prentice et al. 2007) (e.g., 0.5x0.5 degrees in LPJ-GUESS (Smith et al. 2014)). For this, vegetation properties (e.g., LAI, growth rate, life-history strategy, etc.) are simulated as being driven by climate data. The climate data can be adapted to the purpose of a simulation, e.g., used to assess how vegetation will react to climate change or study which driver causes a certain observed vegetation trend. Mortality trends in both models and observations can be quantified as canopy mortality (loss of tree crown in m^2), carbon mortality (loss of biomass in carbon) and stem mortality (loss of numbers of tree individuals). Models are a useful complement to field studies when investigating mechanisms and drivers of forest change. This is because, it is often very time and work intensive to collect data in the field, so that field research is more limited in temporal and spatial scale than using models. Also, the number of observed quantities (e.g., canopy mortality) is more limited in field than in a model, since the work and time in the field doubles if another quantity (e.g., stem mortality) is observed.

1.2 Aim and research questions

This study aims to assess the extent to which increases in competition cause observed increases in tree mortality in forests in six central European countries (Austria, the Czech Republic, Germany, Poland, Slovakia, and Switzerland) from 1985 to 2015, using a process-based vegetation model. Also, the role of CO_2 concentration, temperature and precipitation will be assessed. The following research questions shall be answered:

1. Can a canopy mortality trend comparable to observations be reproduced with a process-based forest model?
2. Is there evidence for an increase in competition when simulating forest development in central Europe?
3. Can an increased tree mortality be attributed to increased competition?
4. What is the relative contribution of changes in temperature, CO_2 concentration and precipitation in driving changes in tree mortality?

2 Methods

2.1 Model

2.1.1 Model description

In this study the Dynamic Vegetation Model LPJ-GUESS version 4.0 (subversion revision r8877) (Smith et al. 2001; Hickler et al. 2012; Smith et al. 2014) was used. The following description refers – if not otherwise indicated – to Smith et al. (2014). The recommended settings of the model were used.

In the model, each 'location' that is simulated is represented by a grid cell of 0.5°x0.5°. The vegetation is simulated as woody plants and herbaceous undergrowth that grow while competing for space to access the resources light, water and nitrogen. The model version incorporates an interactive nitrogen cycle so that the simulation incorporates constraints of nitrogen on plant growth. Vegetation for each grid cell is simulated for multiple replicate patches (each patch has a size of 0.1 ha) within the grid cell that represent 'random samples' of

the wider vegetation landscape, to account for stochasticity (Fig. 3). Soil type and climate within each patch are assumed to be identical. The simulated plant individuals are grouped into Plant Functional Types (PFTs) that are defined based on their growth form, bioclimatic limits for growth, photosynthetic pathway, plant phenology, plant allometry (woody plants only) and life-history strategy (woody plants only). Within each PFT and patch, one or more interacting age classes or cohorts of trees are simulated.

The conducted simulations always start without any established vegetation. Then, a defined spin-up time follows, in which the first years of available historical data are used as driver data (trends removed), so that vegetation, soil and litter carbon and nitrogen pools can accumulate and will be close to an equilibrium with the following phase, the historical phase. In the historical phase, climate data from an individually defined time span will be used to simulate vegetation.

In the model, faster processes are implemented daily, while slower processes are implemented annually (Fig. 3). The drivers are temperature, precipitation, radiation, wind, relative humidity, CO_2 concentration, Nitrogen deposition and soil physical properties (Fig. 3). The biomass accumulation is calculated based on the net primary production (NPP), which is allocated to leaves, fine roots and sapwood (for woody PFTs) according to the allometry defined for each woody PFT. The sapwood is the transport vessel of trees allowing to transport water and photosynthetic assimilate.

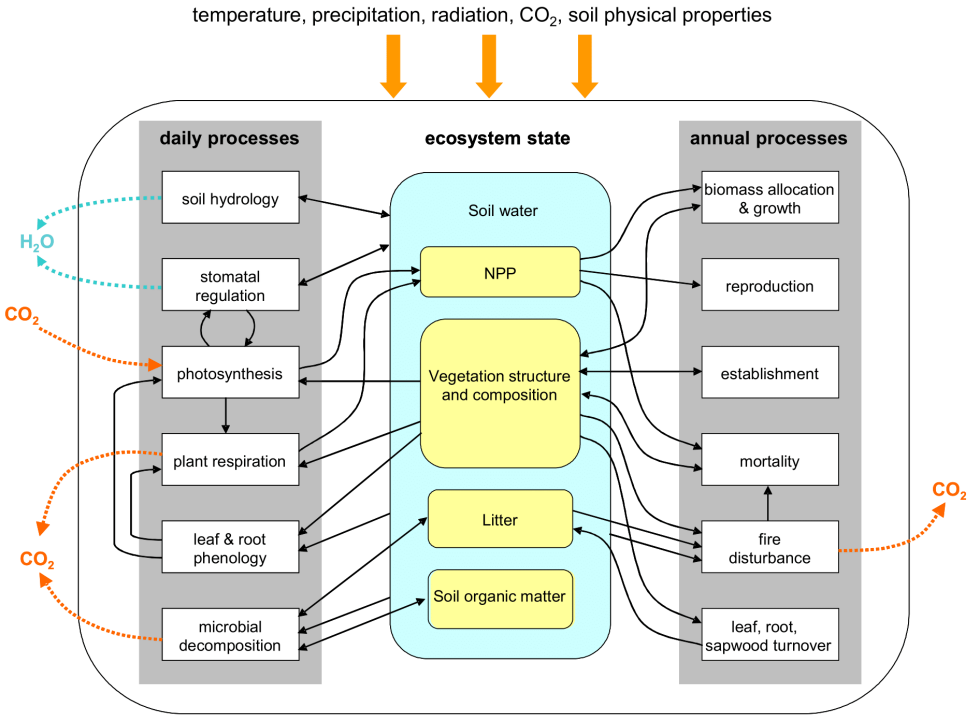

Figure 3. Vegetation dynamics in the model LPJ-GUESS are simulated as dependent on fast and slow processes that interact with each other. This figure is reproduced from Smith (2001).

Growth and mortality are, influenced by age, current resource availability and life history strategy of each PFT, simulated as stochastic processes.

Allometric tree growth is simulated in the model as a rigid process following PFT specific constraints. Diameter of the stem increases with height after

$$H = k_2 D^{\frac{2}{3}}. \quad (1)$$

H is the height in m, k_2 is a PFT-specific constant and D is the stem diameter in m. Additionally, the cross-section of the sapwood is assumed to follow the following relationship to the total leaf area

$$LA = k_{LA:SA} SA. \quad (2)$$

LA is the annual maximum leaf area of an individual in m², $k_{LA:SA}$ is a constant specific for each PFT and SA is the sapwood cross-sectional area in m².

Furthermore, crown area and stem diameter are simulated to be in the following relationship:

$$CA = k_1 D^{1.6}. \quad (3)$$

CA is the crown area in m², k_1 is a PFT-specific constant and D is the stem diameter in m. This relationship captures mortality that occurs due to self-thinning. The crown area can increase until a maximum of shade intolerant PFTs of 50m². Regardless the size, all trees are assumed to form part of the canopy.

The likelihood of death of an individual plant cohort increases with age according to:

$$m_{min} = -\frac{3 \ln 0.001}{age_{\max}} \left(\frac{age}{age_{\max}}\right)^2. \quad (4)$$

Age refers to the current age of the cohort and age_{max} to its maximum expected life span. Moreover, a low growth efficiency will lead to a higher mortality risk according to

$$mort_{greff} = \frac{k_1}{1 + k_2 (\frac{\Delta C}{LA})}, \quad (5)$$

where k_1 and k_2 are PFT-specific constants, ΔC is the annual increase in biomass C and LA is the total leaf area (Pugh et al. 2020). $Mort_{greff}$ is a scalar, where 1 equals a 100% likelihood of mortality. Additionally, vitality mortality that is not captured by growth efficiency will occur as self-thinning. This is defined to occur if

$$\sum_{PFT} A_{PFT} > A_{\max}. \quad (6)$$

A_{PFT} is the ground area occupied by a particular PFT, while A_{max} is defined as the maximum ground area all PFTs are allowed to cover in a grid cell (Pugh et al. 2020).

Disturbances are simulated stochastically and affect a particular patch with a likelihood of 0.01 yr^{-1}. Wildfires are simulated based on available fuel, weather and population density (Rabin et al. 2017) and result based on the first two factors in a partial biomass destruction.

2.1.2 Model set-up

The following description refers – if not otherwise indicated – to Smith et al. (2014). The simulations of this study were conducted in the 'cohort' mode, in which each PFT cohort is represented by one average individual (Fig. 4). Therefore, the model simulates all individual plants of the same age class in one patch to be identical. Vegetation in each grid cell was simulated for 50 replicate patches. Saplings of all diameters are included in this set-up (theoretical net photosynthesis at the ground determines initial sapling size).

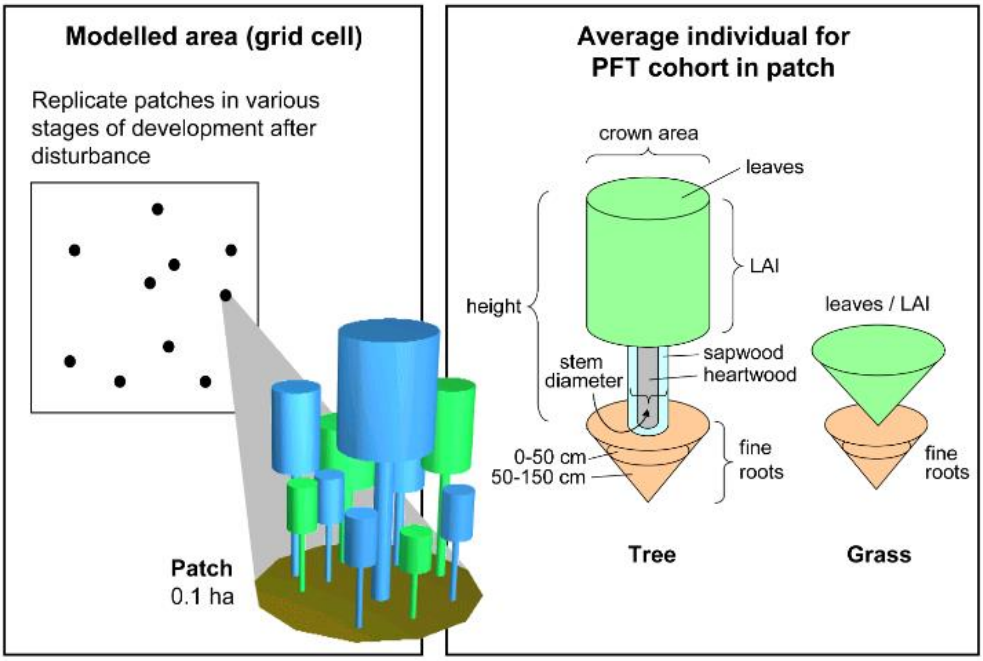

Figure 4. Vegetation in the model LPJ-GUESS is simulated in the 'cohort' mode by simulating a number of replicate patches. Each Plant Functional type (PFT) cohort is represented by an average individual. This figure is reproduced from Smith et al. (2014).

The spin-up time was set to 500 years in all simulations (recommended). In the historical phase, climate data and CO_2 concentrations from 1901 to 2015 were used as inputs. The climate data stems from CRUNCEP (v. 7) (Viovy 2018) and is atmospheric forcing data that is commonly used as model input in the spatial resolution of 0.5° x 0.5°. The input variables precipitation, temperature, radiation, windspeed and humidity were at a monthly temporal resolution, which was scaled down to a daily resolution by the model using either a weather generator or interpolation.

2.2 Selection and description of the simulated sites

A set of locations as input for LPJ-GUESS was obtained from the forest cover dataset by (Hansen et al. 2013). A threshold of 10% closed-canopy forest cover (FAO 2012) was applied, and six 0.5° x 0.5° grid cells were randomly selected for Austria, the Czech Republic, Germany, Poland, Slovakia and Switzerland (Fig. 5) using ArcGIS (ESRI 2012). Only grid cells that were entirely in one country were considered, to ensure that the result only represents the vegetation in that particular country. Six cells per country were chosen as six was the highest number of cells that fulfilled the two criteria described above in all countries. The study by Senf et al. (2018) analysed 4000 pixels (30m resolution) in each country for canopy mortality. As this study is time limited and to make the results comparable in accuracy to the estimated canopy mortality by Senf et al. (2018), the same number of cells was used for each country. Due to the much larger spatial resolution of the model, the number of samples is much lower than that analysed by Senf et al. (2018).

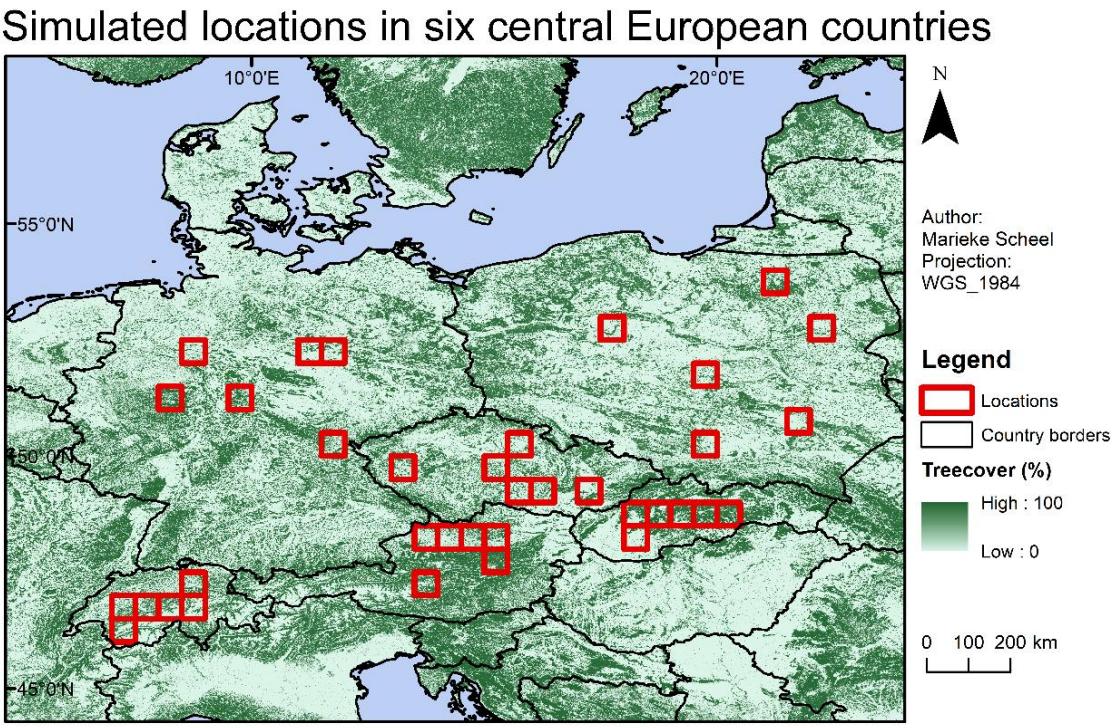

Figure 5. Six locations in six countries that were randomly selected to be simulated using the LPJ-GUESS model are shown in their spatial extend size of 0.5° x 0.5°. The green raster displays the canopy cover in percent in 2000 and stems from Hansen et al. (2013). The administrative boundaries stem from Eurostat (2020).

The median elevation of the six grid cells in each country are below high altitudes (defined here as >1000 m a.s.l.) in all countries but Switzerland (Fig. 6). Additionally, the sites in Austria vary considerably in elevation, with some sites at an altitude of above 1500 m. However, the median elevation of the sites in Austria is at about 500 m, while the median elevation of the sites in Switzerland is nearly at 1500 m. Moreover, the median of the simulated sites in Slovakia is above 500 m a.s.l., while the median of the sites in all other countries is below that.

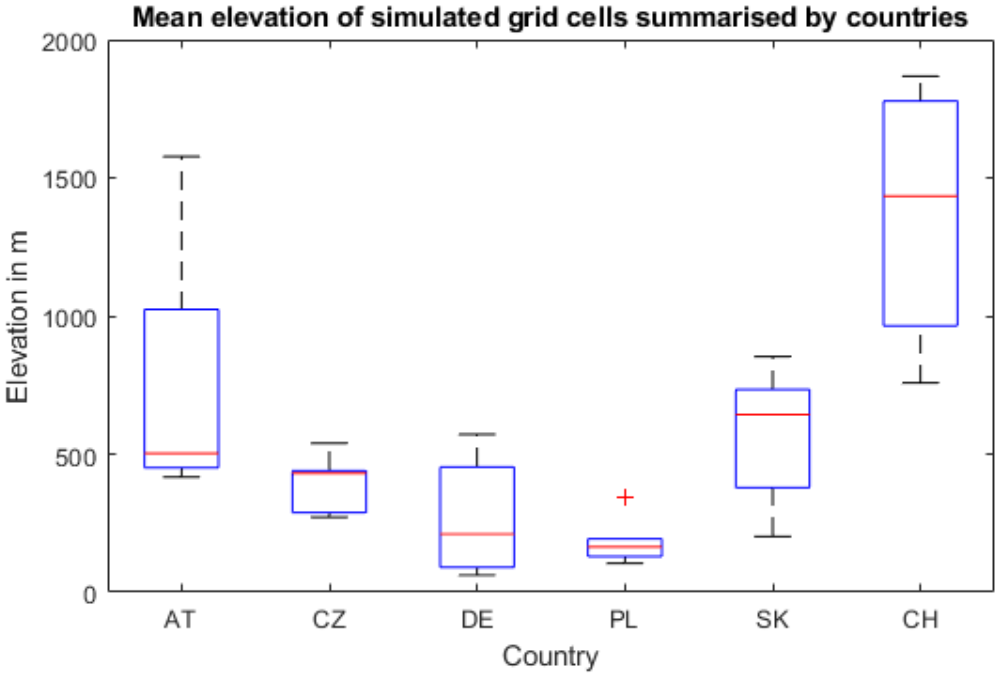

Figure 6. The mean elevation of the 36 grid cells grouped by countries is shown, calculated using data provided by European Environmental Agency (2017). The bottom and top of the blue boxes are at the 75th and 25th percentile respectively of each 'sample', the red line in the box is the median, the ends of the dashed-black lines are the minimum and maximum values (excluding outliers) and the red plus represents outliers.

The mean annual air temperature and total annual precipitation in six European countries was calculated by taking the mean of the climate data for the selected six locations in each country (provided by Viovy (2018)). The average annual temperature in the respective countries was increasing between 1985 and 2015 (Fig. 7). The mean annual temperature range for Switzerland was between ca. 4°C and 6°C, while it was roughly between 6.5°C and 10°C for all other countries. The linear regression models fitted to the temperature values show significant upward trends, with $p<0.01$ (Table S1). Total annual precipitation, however, was relatively stable in all countries in the time period 1985 to 2015 and does not show significant trends, with $p>0.01$ (Table S1). The total annual precipitation was less than 1100mm in all countries but Switzerland, where it was around 1800mm. Seasonal changes in precipitation patterns cannot be gathered from fig. 7.

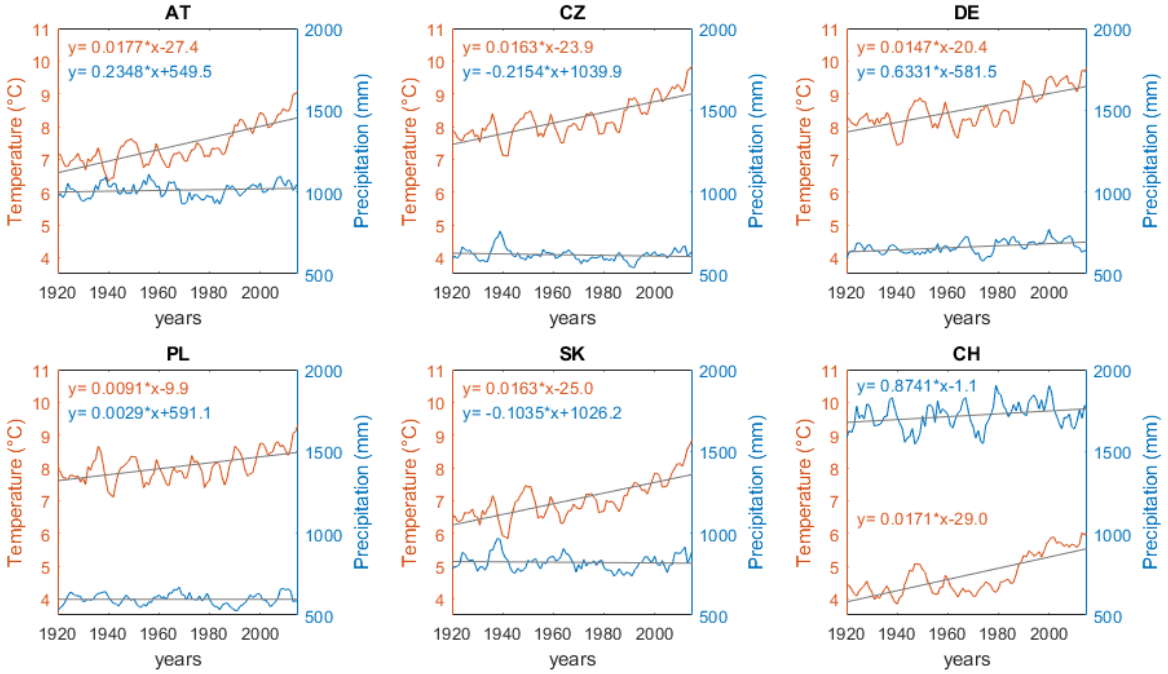

Figure 7. The mean annual air temperature and total annual precipitation in six European countries (represented by six grid cells respectively) is shown. A moving average of 5 years was applied. The grey lines are fitted linear regression models and are described by the equation in the colour of the respective variable the models are fitted for.

2.3 Data and analysis

2.3.1 Simulation settings

LPJ-GUESS was run for the 36 selected locations (Table S2, Fig. 5) with five different driver settings. Firstly, the 'historical simulation' (here denoted **SIMhist**) was run, in which the historical climate data from 1901-2015 was used. After the historical simulation, the model was run four more times, with change in one or more driving variables disabled as follows:

- Temperature fixed to the 30-year mean centred on 1920 (mean of temperature 1906-1935) in that location (**SIMtemp**)
- Precipitation fixed to the 30-year mean centred on 1920 (mean of precipitation 1906-1935) in that location (**SIMprecip**)
- CO_2 concentration fixed to the level of 1920 (**SIMCO2**)
- All drivers but nitrogen deposition fixed to the level (or 30-year mean for temperature and precipitation) of 1920 (**SIMall**)

The simulations with precipitation and temperature fixed to the 30-year mean of 1920 still allow monthly and annual variations around the mean. The year 1920 was the earliest year to which it was possible to fix the drivers with the existing model version. An early year was preferable, to be able to fix the drivers to values as close to pre-industrial conditions as possible, as the study aims at attributing changes in vegetation caused by changing drivers due to climate change. For simplicity, it will be referred to all simulations with fixed drivers, as fixed to 1920.

Where possible, it was decided to rather turn one driver off, to see a change compared to the historical simulation, rather than turn all drivers off but one, as the drivers interact with each other. For example, increased temperatures allow a higher nitrogen fixation rate, while increased nitrogen deposition rates are found to partially increase carbon sequestration rates and thereby allow for higher photosynthetic activity (Fowler et al. 2015; Flechard et al. 2020). The simulations were fixed to 30-year means of temperature and precipitation to avoid fixing the driver to an extreme year and to allow for annual variability. This was not necessary for the CO_2 concentration, since it shows a monotonic annual increase. To estimate the effect of driver interactions all drivers but N deposition were fixed to 1920 in SIMall. The model version did not allow for nitrogen deposition to be fixed to a year.

2.3.2 Evaluation of the model

In this study MATLAB R2019b (The MathWorks Inc. 2019) and ArcMap 10.5.1 (ESRI 2012) were used to analyse data. MS Excel (Microsoft Corporation 2018) was used to format some tables and figures. The model was evaluated by comparing the simulated biomass density in each location in 2010 to a dataset provided by Thurner et al. (2013) that describes the forest carbon density in Europe in 2010 (Table 1). As not all of the simulated biomass density is necessarily forest biomass density (e.g., herbaceous undergrowth), the values of each grid cell are scaled using the percentage of woody PFTs of LAI in 2010, as shown in the following.

$$\rho_{\text{forest biomass}} = \rho_{\text{total biomass}} \times \left(\frac{\text{LAI}_{\text{woody}}}{\text{LAI}_{\text{total}}}\right) \quad (7)$$

$\rho_{\text{forest biomass}}$ is the forest biomass density (kg [C] $m^{-2}yr^{-1}$) and $\rho_{\text{total biomass}}$ is the total forest biomass density (kg [C] $m^{-2}yr^{-1}$). LAI_{woody} is the LAI of all woody PFTs, while LAI_{total} is the LAI of all PFTs. Additionally, as human impact through e.g., agriculture or urban areas is not considered in the model and vegetation is simulated based on climate and soil type (Smith et al. 2014), each grid cell in central Europe is simulated to be covered by forest wherever environmental conditions allow it. In contrast, the biomass density by Thurner et al. (2013) is an average over the entire grid cell, including areas of low biomass density because of agriculture or urban areas. Therefore, the simulated biomass density was scaled by the percentage of tree cover in each respective area in 2000, provided by Hansen et al. (2013) (Table 1), as shown in the following.

$$\rho_{\text{scaled forest biomass}} = \rho_{\text{forest biomass}} \times \text{tree cover} \quad (8)$$

$\rho_{\text{scaled forest biomass}}$ is the forest biomass density (kg [C] $m^{-2}yr^{-1}$) scaled by tree cover of a grid cell. Tree cover is the percentage of a grid cell covered by forest in 2000 according to Hansen et al. (2013).

The biomass density data was compared using the Spearman's rank correlation test. Generally, to compare datasets in this study, the data values were tested for normality using the Shapiro-Wilk test to decide whether to use the parametric Pearson correlation test or the non-parametric Spearman's rank correlation test. If any dataset was not normally distributed, correlation was tested using the latter to ensure that the values are comparable.

Furthermore, the model was evaluated for how well the 'samples' (locations) represent the countries. For this, the biomass density values of all simulated grid cell in a country were averaged to obtain the mean biomass density in kg [C] $m^{-2}yr^{-1}$ in each country. As for the evaluation on grid cell level, before the biomass density values were aggregated to country-level, they were scaled down to only represent woody PFTs (eq. 7) and were scaled down to exclude anthropogenically used areas (eq. 8). These mean values were then multiplied by each countries' forest area (provided by Senf et al. (2018)) (Table 1) to obtain the total biomass simulated in each country. The simulated biomass values were then compared to the average biomass density per country in kg [C] m^{-2} yr^{-1}, calculated based on the estimated average forest biomass density of all grid cells in the country by Thurner et al. (2013) (Table 1), multiplied by the forest area in each country (provided by Senf et al. (2018) (Table 1)) using the Spearman's rank correlation.

2.3.3 Comparison of the simulated canopy mortality to a dataset

The simulated canopy mortality values were compared to the canopy mortality estimated by Senf et al. (2018) in the six countries in the time period 1985-2015 (Table 1). The simulated mortality values were accumulated to country level by averaging them, as the random locations are assumed to all represent mortality values in the country equally well. The country-level values were compared to each other using the Spearman's rank correlation.

2.3.4 Further analyses

The stem, canopy and carbon mortality, the NPP, the quantified cause of carbon loss and the Leaf Area Index (LAI) were analysed for each simulation regarding their changes in mean and trend compared to the historical simulation. Furthermore, all mortality values were compared to NPP, precipitation, temperature and CO_2 concentration in the historical simulation using the Spearman's rank correlation. In all other simulations only the NPP was compared to the mortality rates. To estimate the interactive forces of the drivers, the mortality trends in SIMall were furthermore compared to the mortality trends of the difference between SIMhist and the sum of the differences between SIMhist and SIMtemp, SIMprecip and SIMCO2 respectively. Furthermore, the significance of changes in mortality rates between SIMhist and all other simulations were tested using the Wilcoxon signed-rank test. All country values were derived by taking the mean of the values of the six grid cells in the respective country.

Different mortality variables were analysed because they each are useful for detecting different aspects of changes in forest stand structure. Canopy and carbon mortality are more sensitive towards the death of large, carbon-rich trees. Stem mortality, on the other hand, is more sensitive to capture mortality of younger trees, as the amount of sapling stems in a given area is typically much higher than the amount of adult tree stems, due to the increased need for above- and below-ground resources with increased size.

In this study NPP was used as an indicator for competition, as an increase in NPP is assumed to increase the speed of all processes in a forest. Hence trees grow faster, compete with each other faster and self-thinning occurs at an increased speed (Pretzsch et al. 2014b). However, as changes in forest structure and species-composition can change competition in an ecosystem due to different resource demands and growing optima of species (Kunstler et al. 2012; Nagel et al. 2019), the trends in LAI per PFT over time were also analysed.

The carbon loss due to competition is captured both as self-thinning (eq. 6) and growth efficiency (eq. 5), as described in section 2.1. Therefore, those two causes of carbon loss were summed up as carbon loss due to vitality mortality (following Pugh et al. (2020)). While self-thinning is directly an effect of competition, mortality due to growth efficiency can also occur due to stress caused by resource limitation like drought or shading.

The analysis of the carbon loss was focused on the detection of vitality and background mortality, as this study focuses on trends of mortality over time and not annual variability caused by stand-replacing disturbances. Furthermore, stand-replacing disturbances are simulated purely stochastically, so the model is not expected to exhibit trends in their rate, other than by chance alone. However, as disturbances are in reality coupled with climate conditions (Seidl et al. 2014), they can often cause mortality trends.

Table 1. Description of datasets used in this study. If the accuracy of data was assessed, it is given here.

Reference	Data	Description	Accuracy
Senf et al. (2018)	Annual canopy mortality rate for central European temperate forest per country, 1984-2016	Estimated from Landsat time series interpretation from six European countries: Austria, the Czech Republic, Germany, Poland, Slovakia, and Switzerland; 4000 pixels (30m resolution) were analysed in each of the 6 countries for canopy mortality; a tree was assumed dead at a defoliation of 100%	
Senf et al. (2018)	Total forest area per country in km²	Supplementary material	
Thurner et al. (2013)	Forest carbon density of Northern Hemisphere temperate and boreal forests, 2010	Estimated using radar remote sensing	Standard deviation of the biomass value is provided for each grid cell (0.01°x0.01°), derived from growing stock volume data
Hansen et al. (2013)	Forest canopy cover dataset, 2000	Estimated using imagery generated by the Landsat 7 thematic mapper plus (ETM+)	

		sensor; Canopy cover is defined as canopy closure for all vegetation with a height larger than 5m	
Eurostat (2020)	Administrative boundaries of European countries	Shapefiles	
European Environmental Agency (2017)	Digital Elevation Model of Europe	Raster	+/- 7 meters RMSE

3 Results

3.1 Evaluation of Model LPJ-GUESS

The simulation of forest biomass density for 2010 by the LPJ-GUESS model yielded similar values to the radar remote sensing based estimate by Thurner et al. (2013) (Fig. 8a). The biomass density values in kg [C] m^{-2} in 2010 were averaged per grid cell and marked by country. As shown by the dashed red line, the regression line, lower values were slightly overestimated in the simulation, while higher values (above 10 kg [C] m^{-2}) seemed to be underestimated. Particularly, biomass density values for Austria (light green) and Switzerland (cyan) appeared to be underestimated by the model when comparing the values to the 1:1 line (dashed black). The uncertainty estimated by Thurner et al. (2013) was relatively large, thus the error bars crossed the 1:1 line in 23 out of 36 locations (Fig. 8a). The simulated and estimated biomass values were significantly (α=0.05) correlated (p=1.01e-07, R^2=0.69, RMSE= 6.89 kg [C] m^{-2}).

The total forest biomass per country appeared to be generally overestimated on country level by the simulation (Fig. 8b) compared to values based on Thurner et al. (2013). This became apparent when regarding the fitted dashed red line and there seemed an increasing trend for higher biomass values. However, for Austria and Poland the forest biomass values based on the simulation and Thurner et al. (2013) were very close to the 1:1 line (dashed black line). Nonetheless, the error bars only crossed the 1:1 line in 2 out of 6 countries (PL, AT). The correlations between forest biomass values estimated based on the simulation and based on Thurner et al. (2013) were significant (α=0.05, p=0.0352, R^2= 0.71, RMSE= 0.29 Pg [C]).

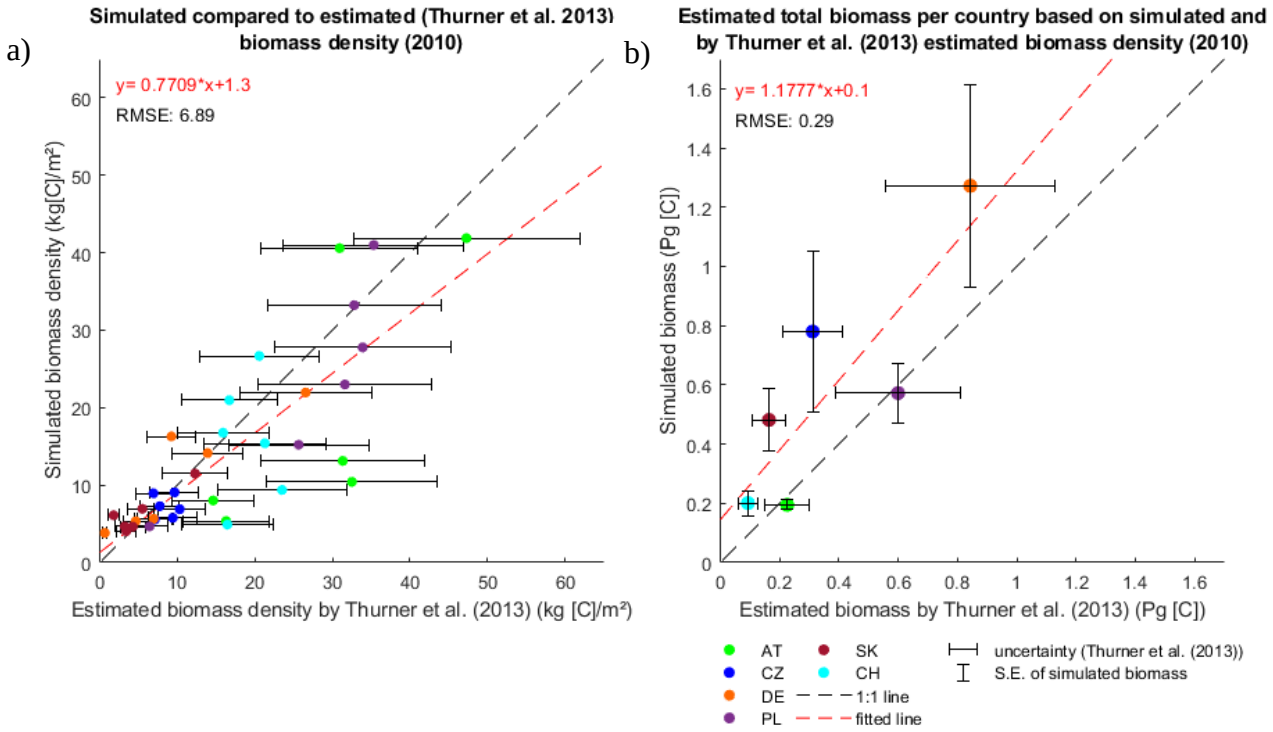

Figure 8. a) Forest biomass density (in kg [C] m^{-2}) simulated using the LPJ-GUESS model was evaluated against data provided by Thurner et al. (2013). The simulated biomass density was scaled using the percentage of canopy cover at the site, provided by Hansen et al. (2013). b) Total biomass (in Pg [C]) per country calculated using the average biomass (in kg [C] m^{-2}) for each country and multiplying it with the total area of forest for each respective country (data given by Senf et al. (2018)). The average biomass for each country was calculated averaging the simulated value of six grid cells in each country and averaging data provided by Thurner et al. (2013). The horizontal error bar is the S.E. of the simulated biomass. The uncertainty of the observed biomass (density) is shown by the vertical error bars. The dashed red line shows the regression line (plotted using the MATLAB (The MathWorks Inc. 2019) function 'polyfit'), and the dashed black line displays the 1:1 line.

3.2 Comparison of canopy mortality to dataset

The simulated canopy mortality on country level was generally about 3% yr^{-1} higher than the canopy mortality estimated by Senf et al. (2018) (Fig. 9). All countries showed a positive trend for the latter and all countries, but Switzerland, showed a positive trend for the simulation. The canopy mortality from the simulation showed a negative trend of -0.0213% yr^{-1} for Switzerland and a positive trend of above 0.01% yr^{-1} for all other countries but the Czech Republic (0.002% yr^{-1}). The positive trend estimated by Senf et al. (2018) was stronger for all countries with a total average across all countries of 0.031% yr^{-1} compared to an average of 0.006% yr^{-1} for the simulated trends of all countries. The simulated canopy mortality values had generally for all countries a much higher amplitude of interannual variability than the estimated ones by Senf et al. (2018). The latter had overall smaller amplitudes but also much more variation in amplitudes between the countries. No significant spatiotemporal correlation could be shown for any of the countries when comparing the simulated canopy mortality to the estimated from Senf et al. (2018) (α=0.05, AT: p=0.2, CZ: p=0.7, DE: p=0.1, PL: p=0.3, SK: p=0.2, CH: p=0.1).

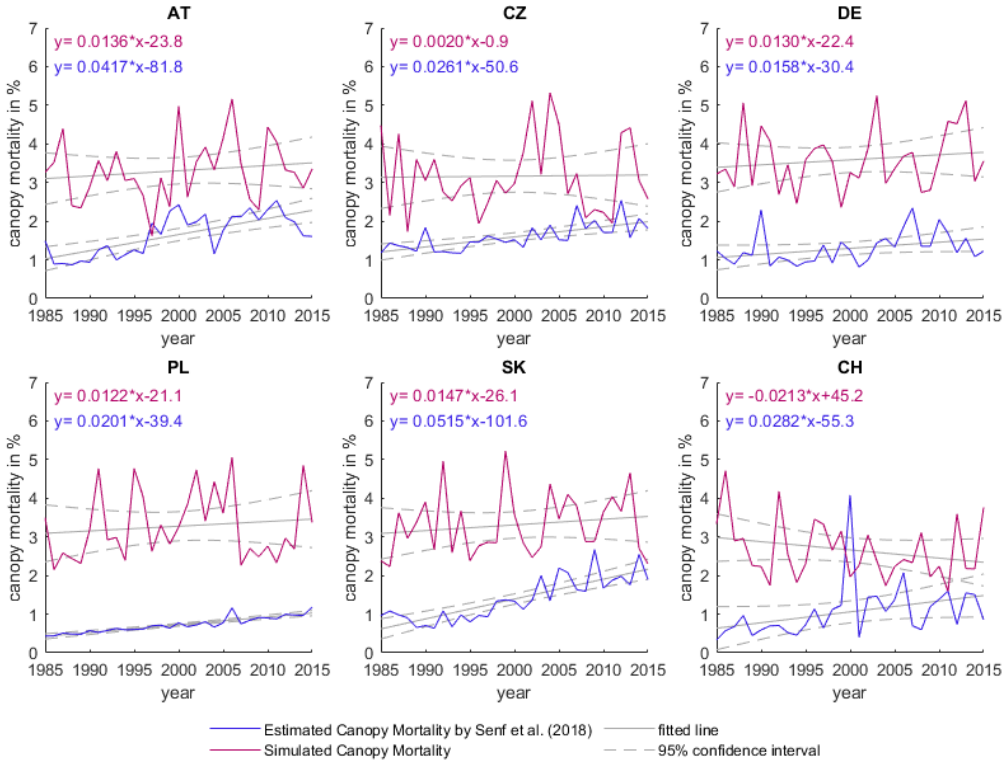

Figure 9. The canopy mortality in six central European countries estimated by Senf et al. (2018) from 1985-2015 is displayed in blue and the simulated canopy mortality in that time period in purple. The continuous grey line is the regression line and the dashed grey lines show the 95% confidence interval. They were plotted using the MATLAB functions 'polyfit' and 'polyval'. The linear equations of the regression lines are displayed in the respective colours.

3.3 Driver Analysis

3.3.1 Analysis of drivers causing changes in NPP and mortality

3.3.1.1 Historical simulation (SIMhist)

In the historical simulation a positive trend in NPP was shown for all countries (Fig. 10, Table 2). This trend was particularly strong in Switzerland, where the increase of 0.0054 kg [C] $m^{-2}yr^{-}1$ was more than double of the average annual increase of 0.0020 kg [C] $m^{-2}yr^{-1}$ of all simulated countries. The NPP was generally the highest in Switzerland, followed by the NPP in Austria that was higher in 1985 but did not experience an increase as strongly as the NPP in Switzerland's forests. Overall, the Czech Republic and Poland showed the lowest NPP, but the highest annual variability. The average NPP of all countries in this simulation was 0.71 kg [C] $m^{-2}yr^{-1}$ (Table S3).

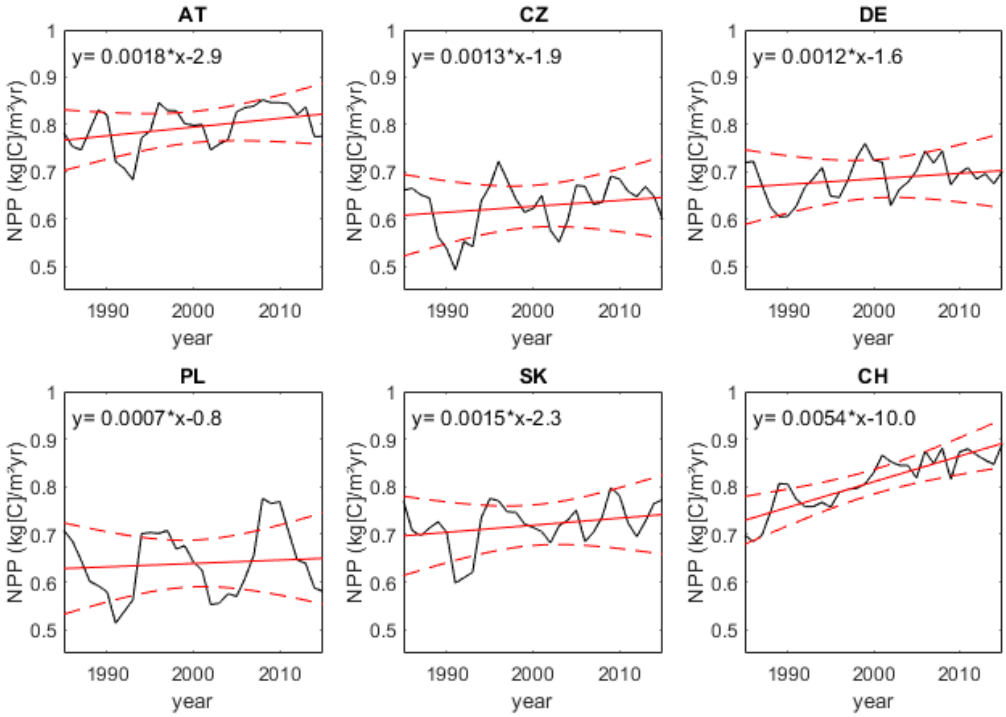

Figure 10. NPP of the SIMhist is displayed in black with a moving average of 3 years applied. The continuous red line is the regression line and the dashed red lines show the 95% confidence interval. They were plotted using the MATLAB (The MathWorks Inc. 2019) functions 'polyfit' and 'polyval'. The linear equation of the regression line is displayed in the upper left corner of each subplot.

Table 2. NPP trends in the time period 1985-2015 are shown as relative values to the historical simulation.

Annual NPP change (kg [C] $m^{-2}yr^{-1}$)					
	SIMhist	**SIMtemp**	**SIMprecip**	**SIMCO2**	**SIMall**
AT	0.0018	*0.0001*	*0.0003*	*-0.0025*	*-0.0018*
CZ	0.0013	*0.0019*	*-0.0001*	*-0.0019*	*-0.0005*
DE	0.0012	*0.0009*	*-0.0012*	*-0.0022*	*-0.0009*
PL	0.0007	*0.0007*	*0.0001*	*-0.0016*	*-0.0008*
SK	0.0015	*-0.0003*	*-0.0010*	*-0.0019*	*-0.0022*
CH	0.0054	*-0.0033*	*-0.0007*	*-0.0029*	*-0.0044*
AVERAGE	**0.0020**	***0.0000***	***-0.0004***	***-0.0021***	***-0.0018***

The tree mortality of the simulations was displayed as percentage of stem, canopy and carbon loss. As seen in Fig. 11, the stem mortality was higher than carbon and canopy mortality in all countries, ranging mostly between 4-8% yr^{-1}. The mean stem mortality of all countries was 5.6% yr^{-1} (Table S4). Canopy and carbon mortality, on the other hand, were mostly ranging between 2-4% yr^{-1}, with a mean of 2.9% yr^{-1} and 2.5% yr^{-1} respectively (Table S4). This means that the interannual variability of stem mortality was also higher than that of canopy and carbon mortality. Furthermore, the stem mortality showed the largest positive trend of all mortality

variables for all countries but Switzerland, with an annual increase of up to 0.07% in the Czech Republic (Fig. 11, Table S5, Fig. 12). Canopy mortality also showed positive trends for all countries (increase below 0.02% yr^{-1}) but Switzerland, while carbon mortality only showed a positive trend for Germany, Poland and Slovakia (increase below 0.02% yr^{-1}) (Table S5). The carbon mortality in forests in Austria and the Czech Republic decreased slightly over the time period (below -0.01% yr^{-1}) (Table S5). In Switzerland, all forest mortality rates declined over time with stem mortality that decreased the most with -0.0387% yr^{-1} and carbon mortality that decreased the least with -0.0127% yr^{-1} (Table S5).

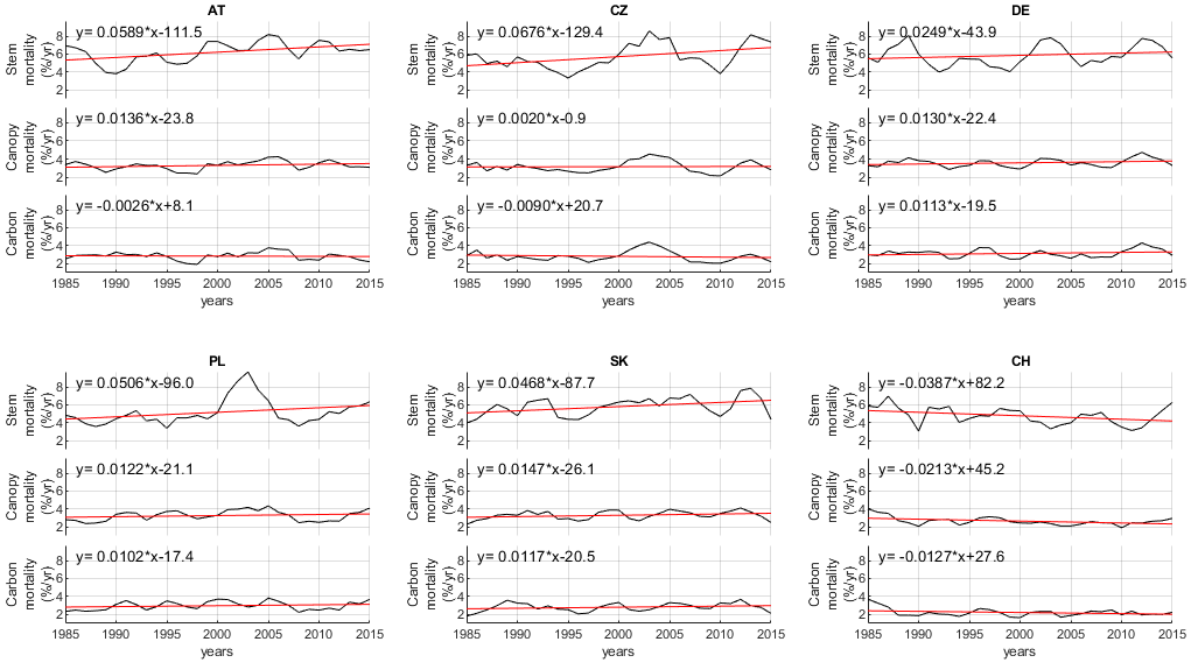

Figure 11. Stem, carbon and canopy mortality of the SIMhist are displayed over the time period 1985-2015 for each country. The red line shows the regression line. It was plotted using the MATLAB (The MathWorks Inc. 2019) function 'polyfit'. A running mean of 3 years was applied. The linear equations of the regression lines are displayed in the upper left corner of each subplot.

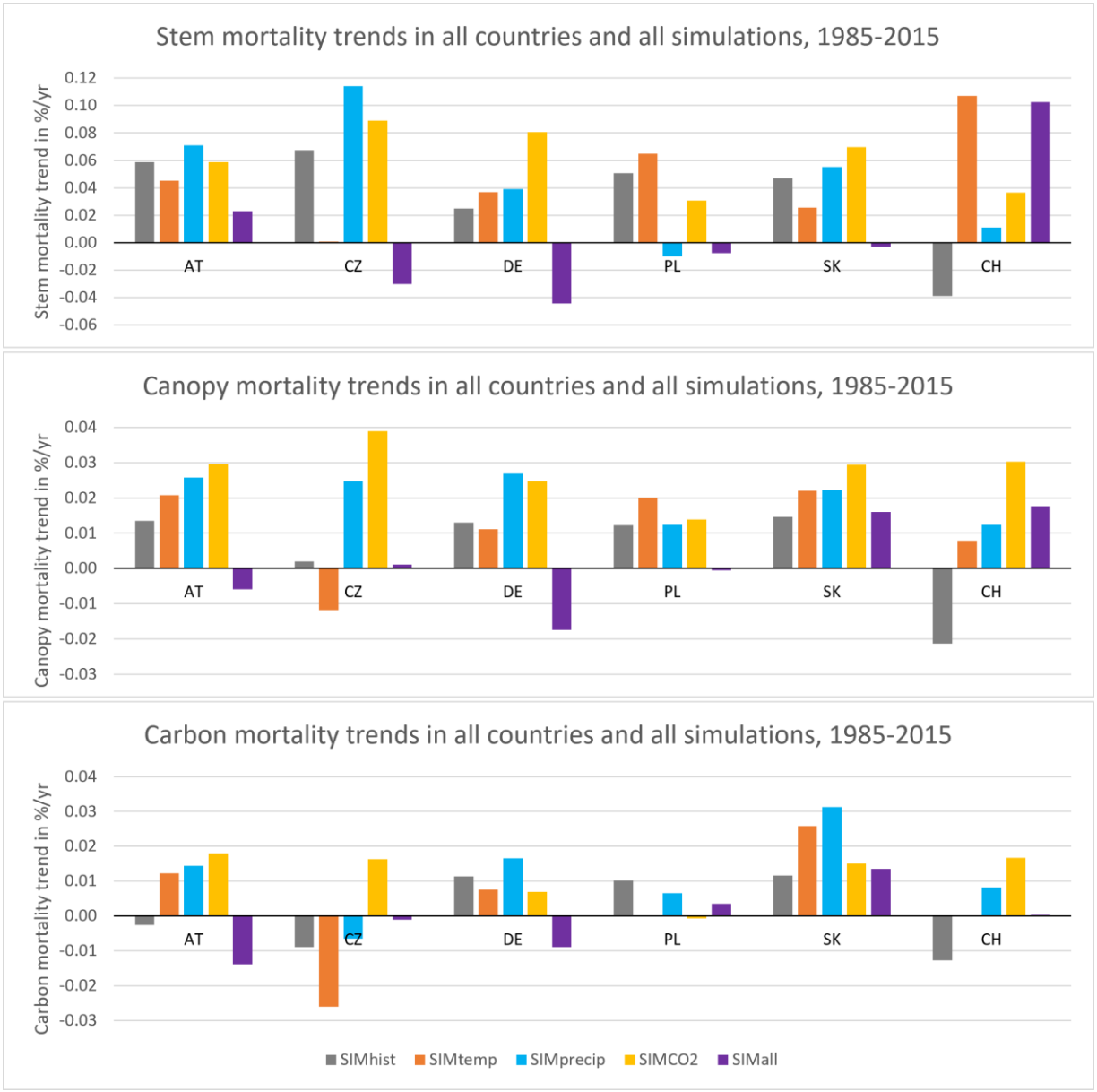

Figure 12. Stem, carbon and canopy mortality trends of all simulation over the time period 1985-2015 are displayed for each country.

Correlation between the observed carbon, canopy and stem mortality and all drivers were tested using the Spearman rank test. However, only two significant correlations (α=0.05) could be found, namely between canopy mortality and precipitation (p=0.03, R_s^2=0.15) and between carbon mortality and NPP (p=0.03, R_s^2=0.15) in Germany (Table S7). As seen in Fig. 13, the NPP plotted against the carbon mortality also did not show any apparent visual trends.

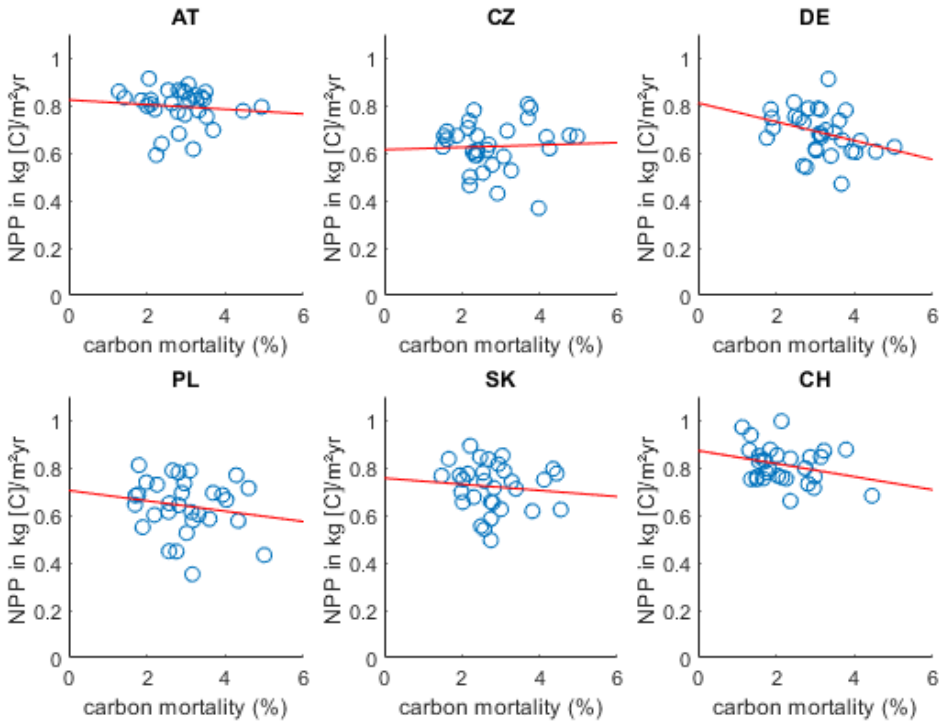

Figure 13. NPP and carbon mortality of the SIMhist in the time period 1985-2015 were plotted against each other for all locations. The red line shows the regression line, plotted using the MATLAB (The MathWorks Inc. 2019) function 'polyfit'. A significant correlation was found only in Germany.

3.3.1.2 Simulation with fixed temperature (SIMtemp)

The simulation with temperatures fixed to levels of 1920 showed that the average annual NPP of all countries in that simulation did not vary considerably from that observed in the historical simulation (Fig. S1; Table 2). Additionally, a positive trend could also be observed in this simulation, with the same average NPP increase of 0.0020 kg [C] $m^{-2}yr^{-1}$ of all simulated countries compared to the historical simulation. However, the NPP trend increased slightly in all countries but Switzerland and Slovakia. The NPP in Switzerland showed a much lower increase than in the historical simulation and was in this simulation close to the average NPP increase of 0.0020 kg [C] $m^{-2}yr^{-1}$ of all countries (decreased by 0.0033 kg [C] $m^{-2}yr^{-1}$ compared to the SIMhist). Also, the NPP in the Czech Republic showed a positive trend that was more than double the positive trend shown in the historical simulation (increased by 0.0019 kg [C] $m^{-2}yr^{-1}$ compared to 0.0013 kg [C] $m^{-2}yr^{-1}$ in the historical simulation). The mean NPP did not change considerably compared to the historical simulation, besides a decrease of 0.13 kg [C] $m^{-2}yr^{-1}$ in the mean NPP in Switzerland (Table S3).

The average trend of all mortality rates showed a small increase in strength compared to the historical simulation, the largest average increase of all countries was +0.0070% yr^{-1} for the stem mortality (Fig. S2; Table S5, Fig. 12). Also, the increases in average strength of trends in all countries in carbon and canopy mortality were more than double the trend initially seen for those variables in the historical simulation (increased by 0.0018% yr^{-1} and 0.0059% yr^{-1} respectively) (Table S5). The negative mortality rates for Switzerland all decreased in strength, the stem mortality rate in this simulation increased by 0.1456 % yr^{-1} compared to the historical simulation and showed the strongest positive trend in stem mortality of all countries (Table S5). The mean canopy and carbon mortality stayed relatively similar to the historical simulation with increases and decreases of less than 0.5% yr^{-1} (Table S4). The mean stem mortality in this

simulation showed a larger variability, with increases and decreases of less than 1% yr^{-1} for all countries but Switzerland and Slovakia (Table S5). The mean stem mortality in Switzerland nearly doubled with an increase of 4% yr^{-1} compared to the historical simulation (Table S4). However, the Wilcoxon signed-rank test showed only significant changes (α=0.05) between stem mortality of SIMtemp and SIMhist in Slovakia and Switzerland and only in Switzerland for carbon mortality (Table S6). The canopy mortality changed significantly in all countries and in all simulations (Table S6).

No significant correlation between NPP and mortality was found in any country when temperature was fixed to levels of 1920 (Table S8).

3.3.1.3 Simulation with fixed precipitation (SIMprecip)

The NPP simulated with precipitation fixed to levels of 1920 showed a decrease in the average NPP trend by 0.0004 kg [C] $m^{-2}yr^{-1}$ compared to the increase of 0.0020 kg [C] $m^{-2}yr^{-1}$ observed in the historical simulation (Fig. S3; Table 2). The trend in annual NPP stagnated particularly in Germany and Slovakia. Therefore, no trend in the NPP in this simulation could be observed in Germany from 1985 to 2015 and only a very small positive trend of 0.0005 kg [C] $m^{-2}yr^{-1}$ was seen in Slovakia. A large positive trend in NPP could still be observed in Switzerland, with only a small decrease of 0.0007 kg [C] $m^{-2}yr^{-1}$ compared to the historical simulation. The positive NPP trend of 0.0018 kg [C] $m^{-2}yr^{-1}$ seen in the historical simulation for Austria increased slightly within this simulation by 0.0003 kg [C] $m^{-2}yr^{-1}$. The mean NPP of this simulation did not differ considerably from the historical simulation (difference <0.04 kg [C] $m^{-2}yr^{-1}$) (Table S3).

The mortality rates for the SIMprecip showed an increase of positive trend strengths for the average mortality variables of all countries (Fig. S4; Table S5, Fig. 12). The largest increase could be seen in the country average of canopy mortality (0.0150% yr^{-1}) and carbon mortality (0.0103% yr^{-1}) (Table S5). Compared to the historical simulation only the trend in carbon and stem mortality in Poland decreased (Table S5). Negative trends could only be observed for the carbon mortality in the Czech Republic and the stem mortality in Poland (Table S5). The mean canopy mortality of all countries but Slovakia and Switzerland increased slightly (<0.5% yr^{-1}) compared to that of the historical simulation (Table S4). For the latter two, it decreased slightly (<0.5% yr^{-1}) (Table S4). The same was observed for the mean carbon mortality (Table S4). The mean stem mortality, however, increased by more than 1% yr^{-1} Poland, while it decreased slightly in all other countries (<0.5% yr^{-1} but Austria and the Czech Republic (increased by <0.5% yr^{-1}) (Table S4). The Wilcoxon signed-rank test showed significant changes (α=0.05) between stem mortality of SIMprecip and SIMhist in Poland only (Table S6).

No significant correlation between NPP and mortality was found in any country in the simulation with precipitation fixed to 1920 (Table S8).

3.3.1.4 Simulation with fixed CO_2 concentration (SIMCO2)

For the simulation with CO_2 concentration fixed to the level of 1920, the average annual NPP trend decreased for all countries compared to the NPP trend observed in the historical simulation (Fig. 14; Table 2). The average annual NPP trend of all countries but Switzerland became negative (up to -0.0010 kg [C] $m^{-2}yr^{-1}$) in this simulation. In Switzerland it decreased compared to the historical simulation by 0.0029 kg [C] $m^{-2}yr^{-1}$ and showed thereby still a strong positive trend. Overall, the average annual NPP trend of all countries became slightly negative with -0.0002 kg [C] $m^{-2}yr^{-1}$ (decrease of 0.0022 kg [C] $m^{-2}yr^{-1}$ compared to the historical

simulation). The mean NPP decreased between 0.5 kg [C] $m^{-2}yr^{-1}$ and 0.9 kg [C] $m^{-2}yr^{-1}$ in all countries compared to the historical simulation (Table S3).

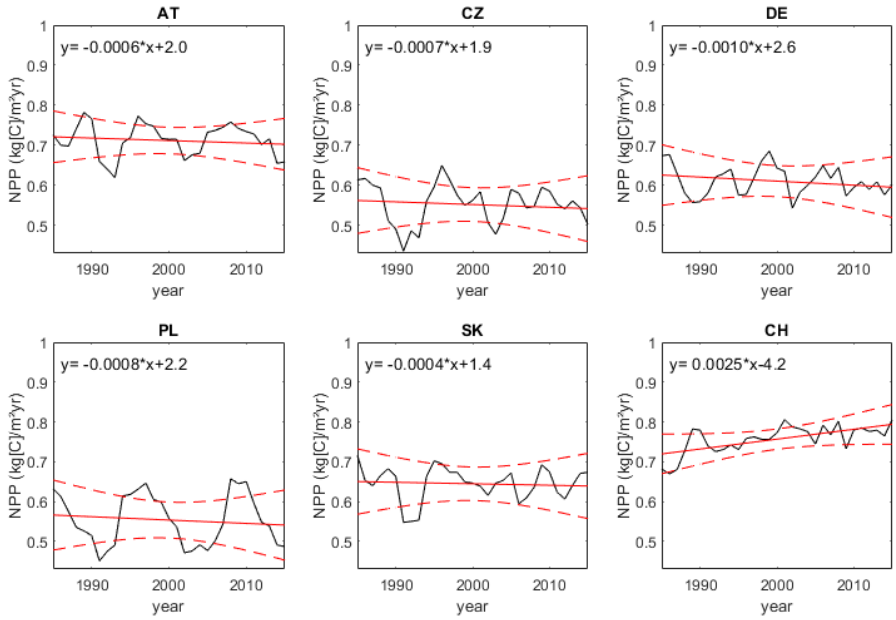

Figure 14. NPP is displayed in black with a moving average of 3 years applied. The continuous red line is the regression line and the dashed red lines show the 95% confidence interval. They were plotted using the MATLAB (The MathWorks Inc. 2019) functions 'polyfit' and 'polyval'. The linear equation of the regression line is displayed in the upper left corner of each subplot.

Considering the average of all countries, all mortality variable trends increased in the simulation with CO_2 concentration levels fixed to 1920 compared to the historical simulation (Fig. 15; Table S5, Fig. 12). Regarding the average of all countries, the stem mortality trend increased the most with +0.0259% yr^{-1} (Table S5). The average trend in canopy mortality of all countries increased by 0.0021% yr^{-1} and the average trend in carbon mortality of all countries increased by 0.0106% yr^{-1} (Table S5). This simulation led to the largest increase in average mortality trends of all countries compared to the historical simulation (Table S5). Trends in tree mortality increased most in Switzerland, with a relative increase of 0.0752% yr^{-1} of stem mortality, of 0.0525% yr^{-1} of canopy mortality and of 0.0294% yr^{-1} of carbon mortality (Table S5). The mean of the mortality rates of all countries, however, decreased on all countries compared to the historical simulation, with the average of all countries decreasing by 0.7% yr^{-1} (Table S4). Using the Wilcoxon signed-rank test, significant changes (α=0.05) between stem mortality of SIMCO2 and SIMhist were shown in Austria and the Czech Republic and only in Austria for carbon mortality (Table S6).

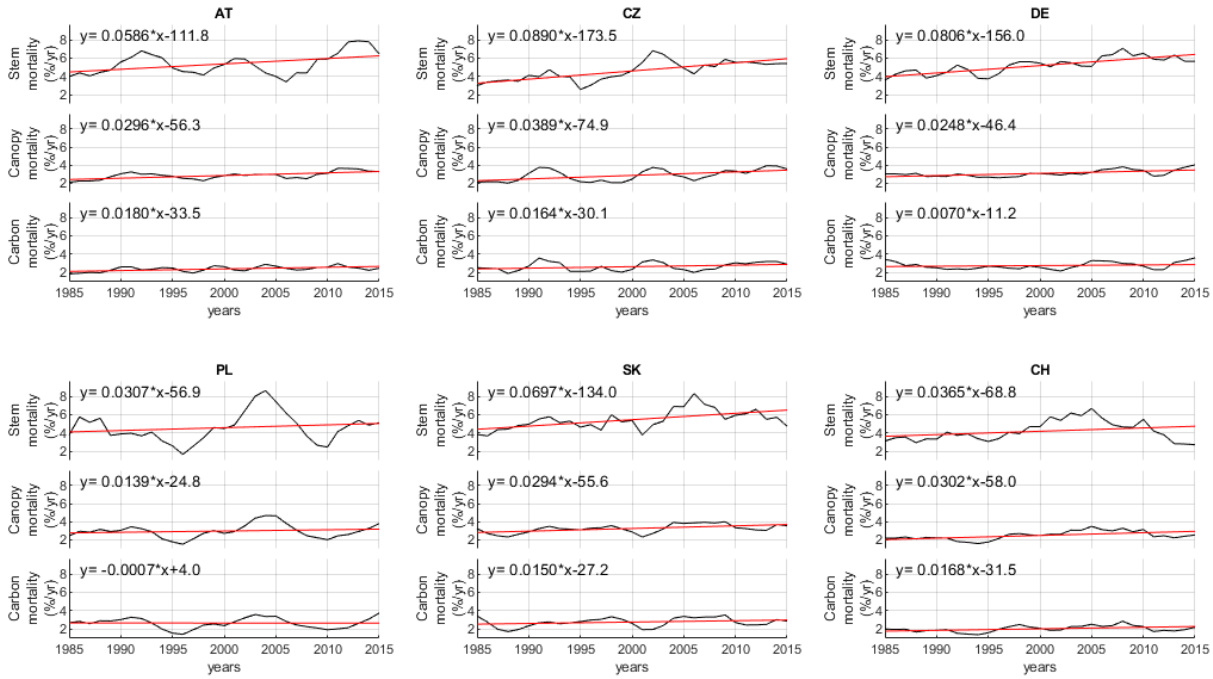

Figure 15. Stem, carbon and canopy mortality of the SIMCO2 are displayed over the time period 1985-2015. The red line shows the regression line, plotted using the MATLAB (The MathWorks Inc. 2019) function 'polyfit'. A running mean of 3 years was applied. The linear equations of the regression lines are displayed in the upper left corner of each subplot.

A significant correlation between NPP and mortality could be shown in the simulation with CO_2 fixed to levels of 1920 for Poland and Switzerland (Table 3). All mortality rates were significantly correlated for Poland, only canopy mortality was significantly correlated to NPP in Switzerland. The significant correlations are visually supported (Fig. 16).

Table 3. The significance (p-value) and strength (R_s^2) of the correlation between stem, carbon and canopy mortality and NPP are shown. Non-significant correlation values are printed in light grey.

	stem mortality		**canopy mortality**		**carbon mortality**	
	p-value	**R_s^2**	**p-value**	**R_s^2**	**p-value**	**R_s^2**
AT	0.1533	0.07	0.0141	0.19	0.1527	0.07
CZ	0.1131	0.08	0.1661	0.07	0.5475	0.01
DE	0.7990	0.00	0.2339	0.05	0.1759	0.06
PL	0.0075	0.23	0.0008	0.33	0.0045	0.25
SK	0.2894	0.04	0.6779	0.01	0.1640	0.07
CH	0.1377	0.07	0.0284	0.16	0.4698	0.02

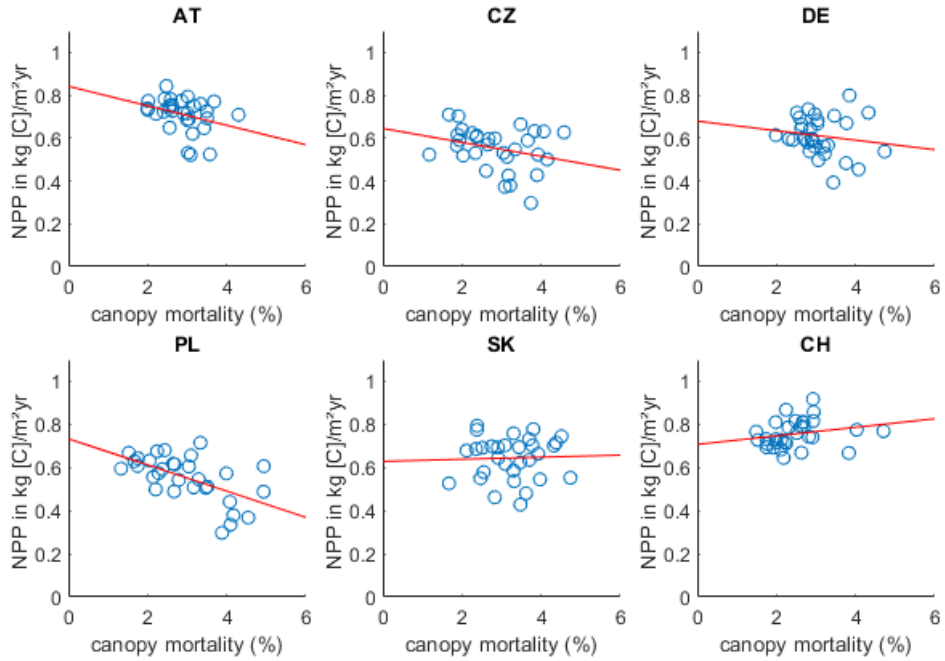

Figure 16. NPP and canopy mortality of the SIMCO2 in the time period 1985-2015 are plotted against each other, the values were simulated with historical climate data in which CO_2 concentration was fixed to the level of 1920. The red line shows the regression line that was plotted using the MATLAB (The MathWorks Inc. 2019) function 'polyfit'. A significant correlation was found for Poland and Switzerland.

3.3.1.5 Simulation investigating driver interactions (SIMall)

The trend of the NPP in the simulation with all drivers but nitrogen fixed to levels of 1920 decreased in all countries (Fig. S5; Table 2). The trends in Austria, Germany and Poland decreased compared to the historical simulation to values lower than 0.0005 kg [C] $m^{-2}yr^{-1}$, while the Czech Republic and Switzerland decreased to trends of 0.0008 kg [C] $m^{-2}yr^{-1}$ and 0.0010 kg [C] $m^{-2}yr^{-1}$ respectively. The trend in Slovakia decreased to a negative trend of -0.0007 kg [C] $m^{-2}yr^{-1}$ compared to the historical simulation. The mean NPP decreased in all countries, with by far largest decrease in Switzerland (-0.19 kg [C] $m^{-2}yr^{-1}$) compared to the historical simulation. Hence, the mean NPP in Switzerland was in the range of the mean NPP of the other countries in this simulation (Table S3).

Only regarding the averages of all countries, all mortality variable trends decreased in the simulation with all drivers except nitrogen fixed to their level in 1920 compared to the historical simulation (Fig. S6; Table S5, Fig. 12). The average trend in carbon mortality of all countries decreased by 0.0025% yr^{-1} compared to the historical simulation, thereby showing an overall slightly negative trend in this simulation (Table S5). The average trend in canopy mortality of all countries decreased by 0.0039% yr^{-1} compared to the historical simulation, the average of all countries was thereby still showing a slightly positive trend (Table S5). Also, the average trend of stem mortality of all countries decreased by 0.0281% yr^{-1} compared to the historical simulation, therefore, the average stem mortality trend of all countries was slightly positive with an annual increase over time of <0.01% (Table S5). The stem mortality rate in Switzerland increased the most compared to the historical simulation, up to a positive trend of 0.1413%yr^{-1} (Table S5). Interestingly, the stem mortality rate in the Czech Republic, Germany and Poland decreased the most compared to the historical simulation and showed relatively strong negative trends between -0.0582% yr^{-1} and -0.0977% yr^{-1} (Table S5). The mean mortality rates of the

countries were relatively similar to the historical simulation for canopy and carbon mortality (differences less than 0.5% yr^{-1}) (Table S4). However, for Austria, the Czech Republic and Slovakia the mean stem mortality decreased by more than 1% yr^{-1} and increased by 1.44% yr^{-1} for Switzerland compared to the historical simulation (Table S4). The Wilcoxon signed-rank test showed significant changes (α=0.05) between stem mortality of SIMall and SIMhist in all countries but Germany and Poland, and only in Austria for carbon mortality (Table S6).

When comparing the mortality trends in SIMall to the difference between SIMhist and the sum of differences between SIMhist and mortality trends of SIMtemp, SIMprecip and SIMCO2 (interactive trends), one can see that the interactive trends of all mortality rates were higher than the trends of SIMall in all countries but Poland (stem and carbon mortality showed negative trends) (Fig. 17). Furthermore, the interactive trends were generally more extreme than those in SIMhist and were partially showing an opposite trend in SIMall (e.g. carbon mortality trend, AT).

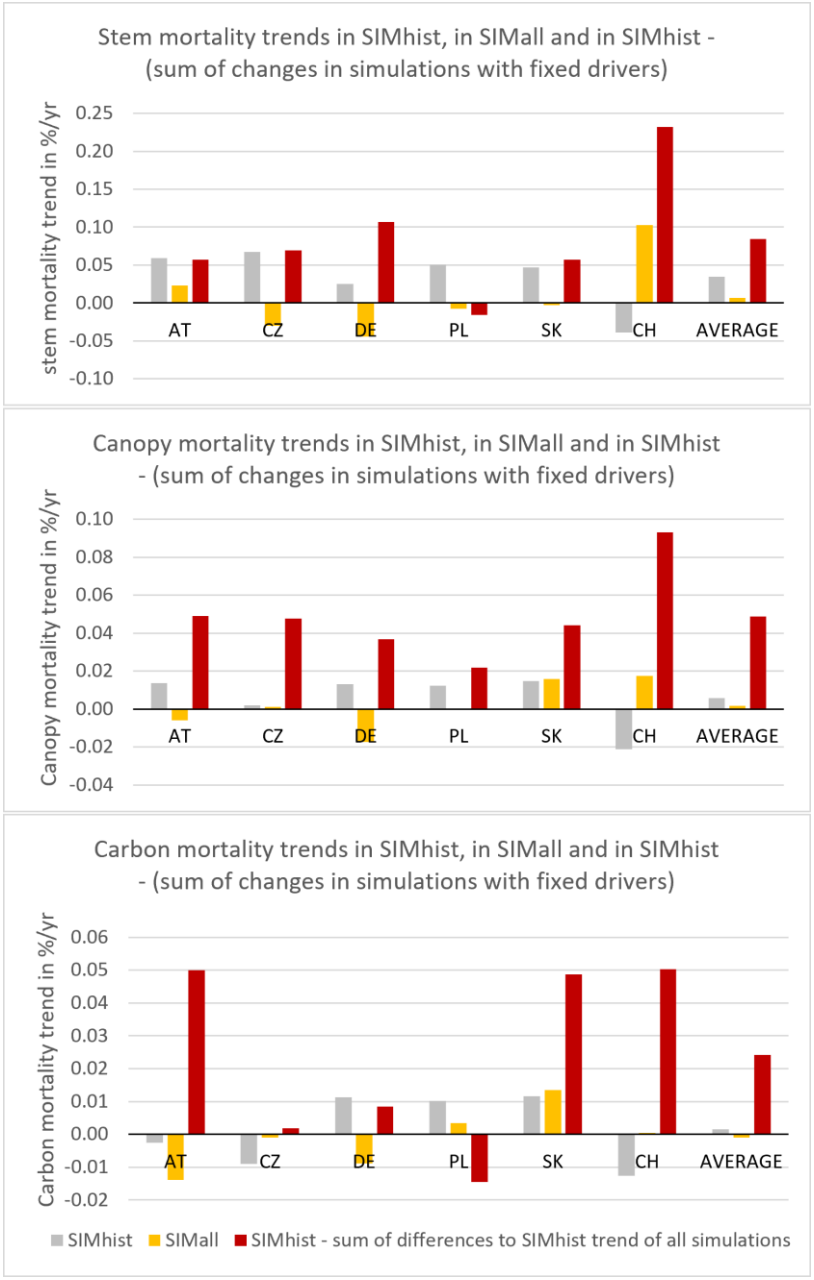

Figure 17. Stem, carbon and canopy mortality trends of SIMhist, SIMall and the difference between SIMhist and the sum of the differences of SIMprecip, SIMtemp and SIMCO2 to SIMhist are displayed for each country.

No significant correlation between NPP and mortality was found in any country in SIMall (Table S8).

3.3.2 Which mortalities caused the carbon loss in the different simulations?

3.3.2.1 Historical simulation (SIMhist)

The annual loss of carbon was in all countries largest due to stand-replacing disturbance mortality (average of all countries of 1.22% yr^{-1}) and lowest due to fire disturbance (zero in all countries but Switzerland) (Fig. 18; Table S9). Vitality mortality caused a slightly higher carbon loss than background mortality and moreover, showed a stronger positive trend over time. All carbon loss variables but the fire disturbance and stand-replacing disturbance showed a positive trend for the average of all countries over the time period (increases between 0.0037 % yr^{-1} and 0.0054 % yr^{-1}) (Table S10). The carbon loss was lowest in Switzerland for vitality and background mortality (Table S9). The highest mean loss due to vitality mortality could be seen in Poland and Germany (Table S9). Furthermore, Poland and Germany showed the strongest positive trend in carbon loss due to vitality mortality and Czechia the weakest (Fig. 18; Table S10).

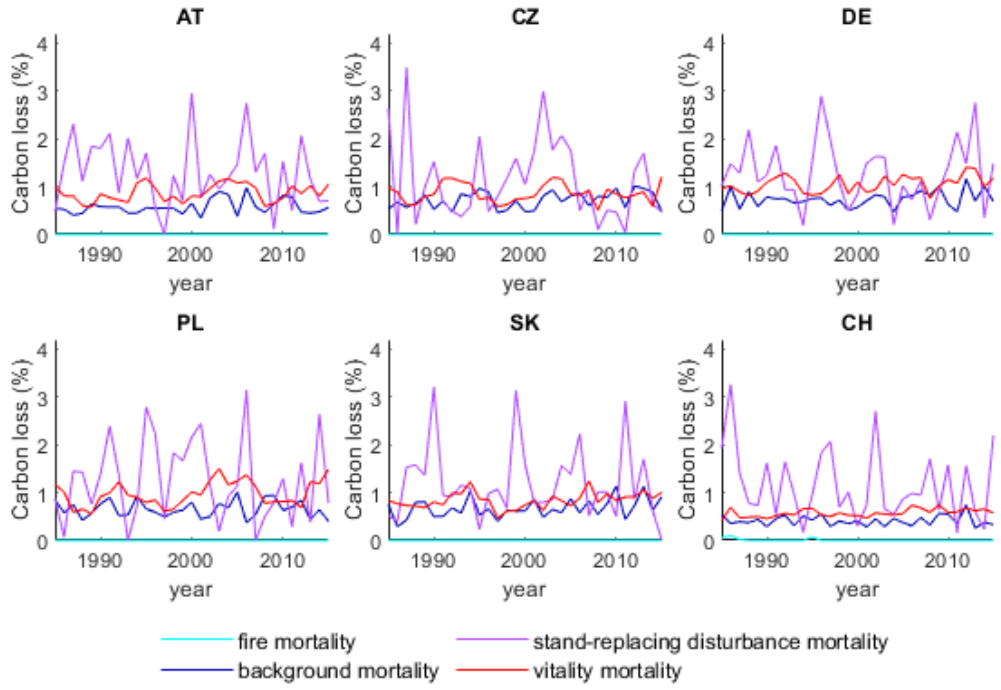

Figure 18. The causes of carbon loss in the historical simulation are quantified, including fire, vitality (growth-efficiency and self-thinning), background and stand-replacing disturbance mortality.

3.3.2.2 Simulation with fixed temperature (SIMtemp)

The trend of the carbon loss due to vitality mortality in the simulation with temperature fixed to levels of 1920 decreased by more than half of its value in SIMhist in all countries but Germany (decreased between -0.0017% yr^{-1} and -0.0120% yr^{-1}) and showed negative trends over the time period for the Czech Republic and Poland (Fig. 19; Table S10). Also, the mean

carbon loss due to vitality mortality decreased in all countries but Germany (increased by 0.08% yr^{-1}) compared to the historical simulation (Table S9).

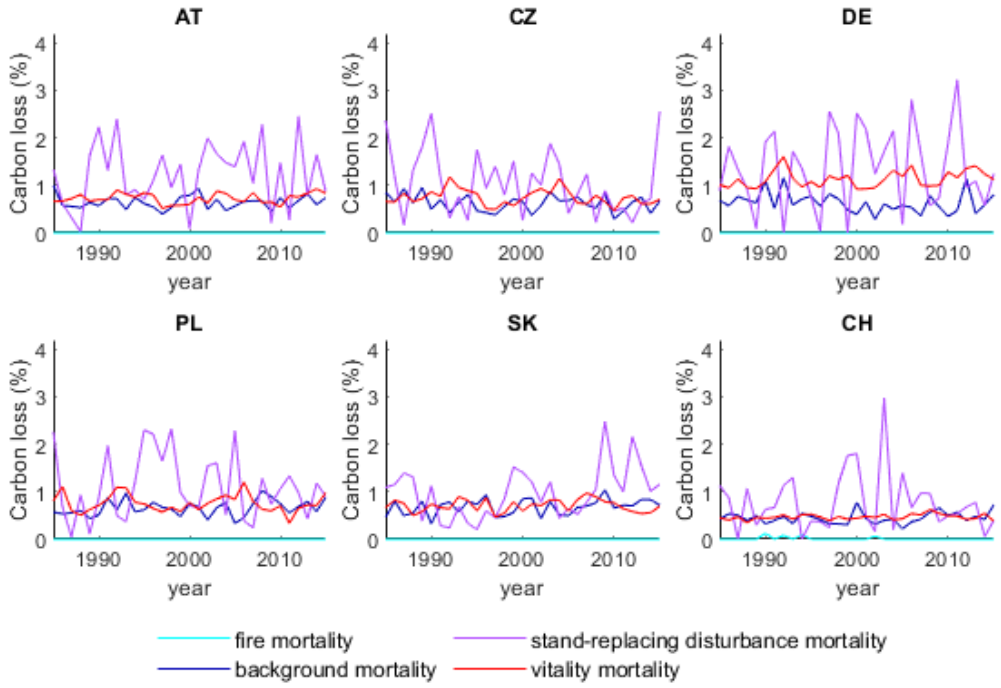

Figure 19. The causes of carbon loss in the simulation with temperature fixed to the level of 1920 are quantified, including fire, vitality (growth-efficiency and self-thinning), background and stand-replacing disturbance mortality.

3.3.2.3 Simulation with fixed precipitation (SIMprecip)

The mean carbon loss due to vitality mortality in SIMprecip decreased slightly in all countries but the Czech Republic compared to SIMhist and stayed thus generally very similar to the average carbon loss due to vitality mortality of all countries in SIMhist (Fig. S7; Table S9). The average trend of all countries of carbon loss due to vitality mortality reduced only slightly compared to the historical simulation. In Germany, Poland and Slovakia the trends decreased strongly compared to SIMhist (Table S10), while the trends increased in the other countries.

3.3.2.4 Simulation with fixed CO_2 concentration (SIMCO2)

The mean carbon loss due to vitality mortality decreased in all countries but Slovakia and Switzerland in SIMCO2 compared to SIMhist (Fig. 20; Table S9). The largest decrease in mean was seen in Poland with a decrease of 0.22% yr^{-1}. The average trend in carbon loss due to vitality mortality of all countries changed less than in SIMtemp (decreased by 0.0048% yr^{-1}), so that the average trend of all countries decreased by 0.0041% yr^{-1} in SIMCO2 compared to SIMhist (Table S10). However, compared to the SIMtemp, the strength of the decrease compared to the SIMhist was higher in SIMCO2 in Switzerland, Austria and Germany.

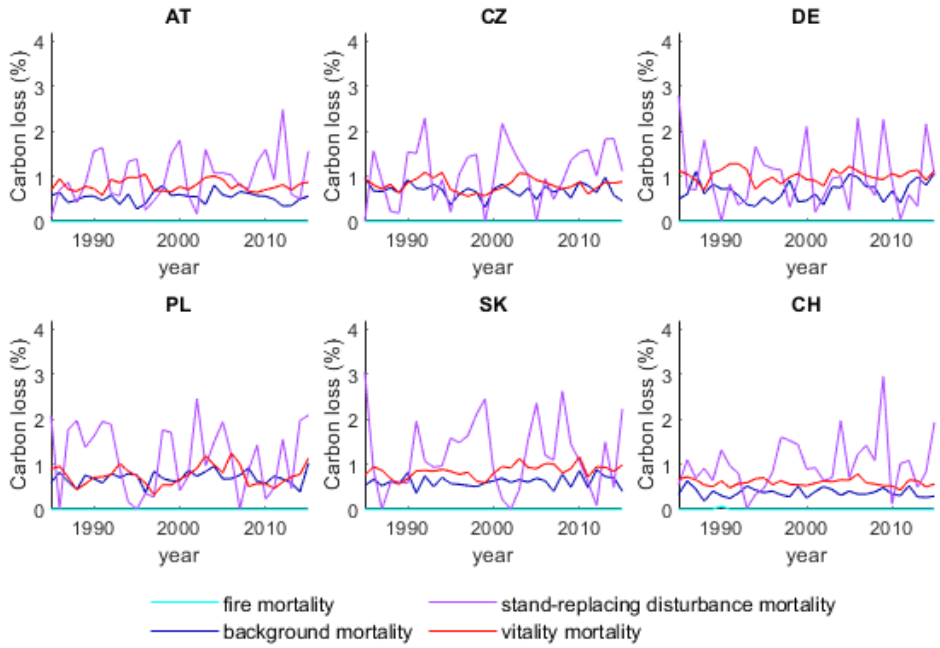

Figure 20. The causes of carbon loss in the simulation with CO_2 concentration fixed to the level of 1920 are quantified, including fire, vitality (growth-efficiency and self-thinning), background and stand-replacing disturbance mortality.

3.3.2.5 Simulation investigating driver interactions (SIMall)

In the simulation with all drivers but nitrogen fixed to 1920, the average carbon loss of all countries due to vitality mortality decreased compared to the historical simulation (Fig. S8; Table S9). However, mean vitality mortality decreased less in SIMall than in SIMtemp in Slovakia, Germany and Austria. The trend in carbon loss due to vitality mortality decreased in all countries, with the trends in Poland and Slovakia still showing positive trends. The decrease in trends in vitality mortality was less in SIMall than in SIMtemp in Slovakia, Germany and the Czech Republic. Interestingly, the average decrease in mean vitality mortality of all countries compared to SIMhist was less in SIMall than in SIMtemp. Additionally, the average trend of the carbon loss due to vitality mortality of all countries decreased compared to SIMhist as much as in SIMtemp.

3.3.3 Trends in NPP and mortality linked to changes in plant functional composition

3.3.3.1 Historical simulation (SIMhist)

The LAI of the PFTs seemed to have developed similarly in all countries but Switzerland over the time period 1985-2015 in the historical simulation (Fig. 21). However, Austria had continuously a larger share of boreal needle leaved evergreen trees (BNE) and boreal needle leaved evergreen shade-intolerant trees (BINE), while its forests consisted less of temperate (shade-tolerant) broadleaved summergreen tree (TeBS) (Table S11). The simulated LAI in forests in Switzerland was made up mostly by BNE and BINE, and the share of TeBS and boreal/temperate shade-intolerant broadleaved summergreen trees (IBS) together was roughly as much as the share of BINE (Table S11). The LAI of cool grass (C3G) was relatively high in Switzerland in 1985 compared to the other countries (Table S11), however, it showed a strong decline until 2015 (Table S12). IBS showed a positive trend in all countries (average of 0.02), while BNE showed a similar strong increase in trend but only in Switzerland (Table S12).

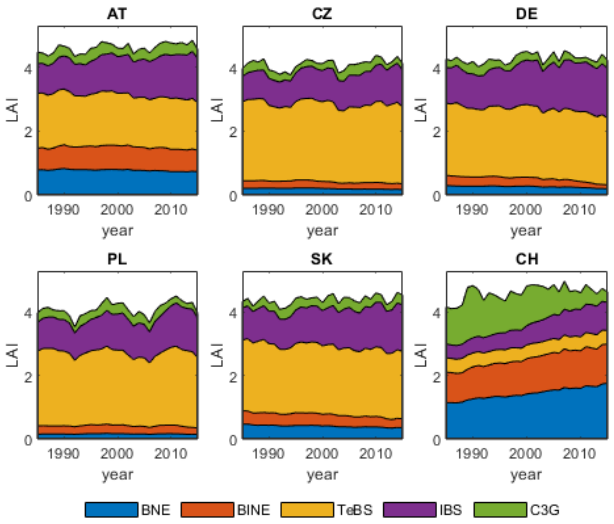

Figure 21. LAI of Plant Functional Types (PFTs) over the time period 1985-2015 in the historical simulation. BNE: PFT boreal needle leaved evergreen tree, BINE: PFT boreal needle leaved evergreen shade-intolerant tree, TeBS: PFT temperate (shade-tolerant) broadleaved summergreen tree, IBS: PFT boreal/temperate shade-intolerant broadleaved summergreen tree, C3G: PFT cool (C3) grass.

3.3.3.2 Simulation with fixed temperature (SIMtemp)

In the simulation with temperature fixed to 1920, the share of the PFTs of the LAI stayed similar to the historical simulation in 1985 (Fig. 22; Table S11). The LAI of IBS was still increasing in all countries, especially in Germany and Austria, but less than in SIMhist. The LAI of the PFTs in Switzerland was not showing large trends (Table S12).

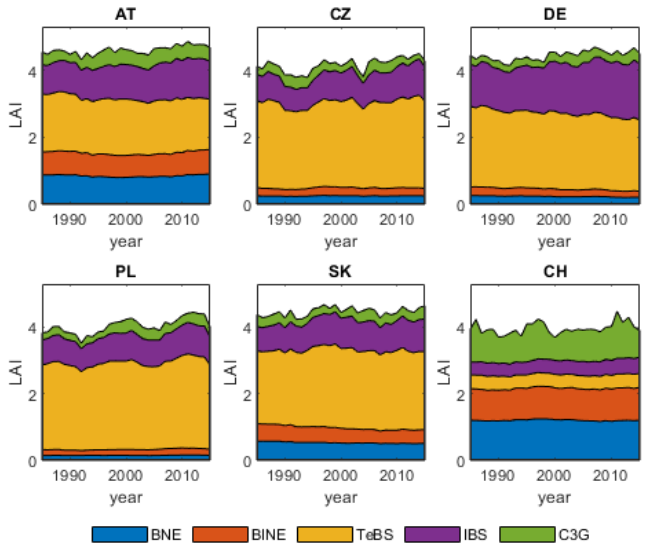

Figure 22. LAI of Plant Functional Types (PFTs) over the time period 1985-2015 in the simulation with fixed temperature. BNE: PFT boreal needle leaved evergreen tree, BINE: PFT boreal needle leaved evergreen shade-intolerant tree, TeBS: PFT temperate (shade-tolerant) broadleaved summergreen tree, IBS: PFT boreal/temperate shade-intolerant broadleaved summergreen tree, C3G: PFT cool (C3) grass.

3.3.3.3 SIMprecip, SIMCO2 and SIMall

Compared to the historical simulation, no large changes in LAI could be found in SIMprecip (Fig. S9) andSIMCO2 (Fig. S10). The share of PFTs stayed very similar (Table S11), while the strength of the increase of the LAI of IBS decreased slightly (Table S12). The LAI in SIMall showed very similar characteristics to SIMtemp (Fig. S11). However, the total LAI of IBS and TeBS decreased slightly, both compared to SIMhist and SIMtemp (Table S11). The trends in LAI and contribution of PFTs to it stayed relatively stable over time (Table S12).

4 Discussion

4.1 How well does the model simulate forest biomass density in the selected locations?

The model simulated the forest biomass (density) in the specific locations and scaled to country level well (Fig. 8), as the biomass (density) values proved to be significantly correlated to values by Thurner et al. (2013) on both country and grid cell level. Although, the R^2 values were similar for both the evaluation on grid cell and on country level, the significance of the correlation on grid cell level was much higher. As the average of the simulated forest carbon density for each country was derived from six samples only, a higher inaccuracy of the simulated biomass on country level is expected. Additionally, a larger sample size drawn from the same population inherently leads to a lower p-value (a higher confidence). Moreover, the biomass density values on grid cell level were much closer to the 1:1 line than on country level, as indicated by error bars crossing the 1:1 line for 23 out of 36 grid cells and only for 2 out of 6 country estimates. The higher inaccuracy on country level might particularly apply to larger countries and was thus observed in Germany (largest country) and the Czech Republic (third largest country) but not in Poland (second largest country) (Fig. 8b). However, the 'samples' were also more evenly distributed over entire Poland than over Germany and the Czech Republic (Fig. 5). The general overestimation of biomass on country level (slope of fitted line of 1.18) is contrary to the underestimation (slope of fitted line of 0.77) observed on grid-cell level and suggests a systematic sampling bias, which seems to be particularly strong in Germany and the Czech Republic (Fig. 8). A stratified random sampling strategy could inhibit this and is therefore suggested for further studies. Furthermore, the evaluation on country level has likely incorporated a higher uncertainty as the samples represent different proportions of the total vegetation in each country and each country has a different pedodiversity and variety in climatic conditions. Countries with more heterogenic conditions might thus be represented less accurately, which would reflect in a poorer agreement for larger countries. However, a poorer agreement in large countries is only seen in the ones with unevenly distributed 'samples', suggesting that the sampling method caused a larger bias than heterogenic conditions in large countries.

The evaluation of the biomass simulation is biased, since Thurner et al. (2013) estimated the biomass density of managed forest ecosystems, while the simulated vegetation is natural. Forest management can affect biomass production efficiency (Campioli et al. 2015), while harvest cycles change stand age and biomass. Regular harvests can thus lead earlier death of trees on average and lower the number and size of large trees. To dampen the effect of management on the forest biomass in the evaluation, the average biomass density of a grid cell was scaled by its estimated tree cover (eq. 8), since the average biomass density of a grid cell estimated by Thurner et al. (2013) included areas of low biomass density because of e.g., urban areas or agriculture. Nonetheless, this scaling does not account for structure and composition changes in forests, which can affect NPP and mortality rates (e.g., increased thinning might lower stress

mortality and increase growth rates (Gavinet et al. 2020; Manrique-Alba et al. 2020)). Also, the evaluation of simulated biomass density for both the grid cell and the country level, incorporates an error as it was scaled using a dataset estimating the tree cover fraction (eq. 8) in 2000, so ten years earlier than the year for which the simulation was evaluated. However, this error is likely relatively minor, as I am presuming that that time frame is rather short for large scale changes in forest cover over an entire country to happen. Also, the forest area in entire Europe has increased by 0.08% yr^{-1} between 1990 and 2011 (Forest Europe et al. 2011), which indicates an increase in forest area between 2000 and 2010 of about 0.8% over entire Europe.

4.2 What causes the differences between the canopy mortality simulated by the model and estimated by Senf et al. (2018)?

Answering the first research question, the tree mortality trends of the observations were not well reproduced using the LPJ-GUESS model. The simulated canopy mortality could not be shown to be significantly spatiotemporally correlated to the respective country's canopy mortality estimated by Senf et al. (2018) for any country (see section 3.2). The canopy mortality estimated by Senf et al. (2018) showed a positive trend for all examined countries. Positive trends were also seen in the historical simulation for all countries but Switzerland. However, the mortality was continuously about 3% yr^{-1} higher in the simulation compared to the estimate by Senf et al. (2018).

The stem mortality simulated by the LPJ-GUESS model when comparing its values to observed stem mortality values in Switzerland from 1990-2013 (Etzold et al. 2019) is just as the simulated canopy mortality values compared to the estimated values by Senf et al. (2018) roughly double the observed/estimated values. However, regarding this comparison one has to bear in mind that the minimum tree size of a Diameter at breast height (DBH) > 5 cm, applied by Etzold et al. (2019), differs from the dynamically assigned sapling size in the LPJ-GUESS model (based on the theoretical net photosynthesis at the ground). This might have further caused the very high stem mortality observed in the model, as a large number of young and small trees that die faster (due to increased NPP) inflates the stem mortality (since it is very sensitive to mortality of smaller trees). For comparability with field studies, it would therefore be beneficial if a minimum threshold for sapling size was applied when counting mortality losses in the model.

Based on the mortality rates estimated by Etzold et al. (2019), it can be assumed that the canopy mortality rates estimated by Senf et al. (2018) are more realistic, while the simulation overestimates the mortality values. The continuously higher mortality rates in the simulation may be explained by how the LPJ-GUESS model simulates tree growth. In the model, as a tree (representing a cohort) is simulated to grow, it follows rigidly the allometric functions defined for its particular PFT (eq. 1, eq. 2, eq. 3). This means that a certain height of a PFT cohort always leads to a particular stem diameter (eq. 1) and that a certain growth in stem diameter is necessarily leading to an increase in crown area up until a maximum crown area of shade intolerant PFTs of 50m^2 (eq. 3) (Smith et al. 2014). Additionally, sapwood cross-section and total leaf area are assumed to always maintain a certain (PFT-specific) proportion (eq. 2) (Smith et al. 2014). However, canopy size, shape and position are actually plastic and change depending on neighbourhood crowding (Muth and Bazzaz 2003; Jucker et al. 2015). This means that trees can adapt to a highly competitive neighbourhood by positioning their canopy in a location with better resource accessibility (e.g., light or space) or adapt the shape or size of their crown to fit better in a smaller available space. As these processes are not captured by the model, a certain neighbourhood crowding in the model might lead to an increased above-ground competition and thus a lower growth efficiency (and thereby an increased likelihood of

mortality), while in reality a tree would adapt to those conditions. Hence, the overestimation of mortality in the simulation might be due to a lack of crown and stem plasticity, as trees can survive (longer) under competitive circumstances by adapting crown size, shape and position (Muth and Bazzaz 2003; Jucker et al. 2015). This would have to be investigated further, and the simulations could be either supplemented by field research or by adopting a model, like the Perfect Plasticity Approximation (Purves et al. 2008), to assess the impact of crown rigidity on mortality rates. Furthermore, the LPJ-GUESS model counts canopy mortality from all trees (Smith et al. 2014). However, in reality, the largest trees of a stand are usually forming the canopy (unless there are gaps in the canopy) (de Carvalho et al. 2000), with smaller trees being seen as undergrowth or sub-canopy trees. Mortality of those is unlikely to be observed in Landsat images, such as those analysed by Senf et al. (2018). This might have also caused part of the large overestimation of canopy mortality in the simulations compared to Senf et al. (2018). This hypothesis could be tested further using the LPJ-GUESS model, by analysing how the simulated canopy mortality rates are distributed among tree sizes. If the hypothesis was supported in such an analysis, a threshold for tree size or canopy size could be applied to make simulated canopy mortality more comparable to field data.

Senf et al. (2018) analysed 4000 pixels (30m resolution) in each country for canopy mortality, therefore their analysis included data from varying biophysical gradients. Contrary to this, the 'samples' used in the simulation were rather few (50 per patch) and in Switzerland most of the simulated locations were situated in higher altitudes (Fig. 6). As vegetation in higher elevations is mostly limited in growth by temperature (Körner and Paulsen 2004; Takahashi 2010), those regions might benefit the most from increasing global temperatures and CO_2 concentrations (Zhao and Running 2010), due to a prolonged growing season and increased photosynthetic activity promoted by higher air temperature and increased CO_2 concentrations (Takahashi 2010). This can be observed for the simulation Switzerland, where both average temperatures increased by about 2°C over the time period 1985-2015 (similarly to the other countries) (Fig. 7) and where the simulated locations are situated at the highest altitudes (Fig. 6). In Switzerland, the canopy mortality showed a strong negative trend and the steepest increase in NPP was observed here. Additionally, the LAI of woody plants in Switzerland increased over time, indicating an increased growth of trees, thereby apparently increasingly outcompeting herbaceous undergrowth (Fig. 21). Hence, the negative trend in canopy mortality that was simulated in the locations of higher altitudes could have been expected due to the vegetation there being released from low-temperature stress by climate warming and a lengthening growing season. Moreover, this trend was likely not observed by Senf et al. (2018) because their random samples are from both low and high elevations to observe general trends in all countries. Also, the average elevation in Switzerland is about 800m a.s.l. (calculated using data from European Environmental Agency (2017)), so that if a large set of samples was taken from all levels of elevation their mean is likely to be similar and would thereby be below high elevations (defined as <1000 m a.s.l.). Based on this one could speculate that the results of the simulation might be consistent with the results by Senf et al. (2018) but that the number of samples and the weighing of the grid cell results to country level led to apparently different trends. To further investigate the impact of altitude on tree mortality, a reanalyse of the data by Senf et al. (2018) by altitude would therefore be beneficial. The same would hold for the simulated mortality trends, as that would avoid dampened or misleading trends at country level caused by averaging mortality trends of vegetation in higher and lower elevations (e.g., CH, AT).

Additionally, the trends estimated by Senf et al. (2018) showed a much steeper increase of canopy mortality over time than those of the simulation. A large part of the increase in forest mortality was suggested by Senf et al. (2018) to be caused by forests recovering from past land

use and harvest intensity increasing, particularly as thinning. Hence, the lower trends in the simulation compared to Senf et al. (2018) might be caused by the model simulating natural vegetation. For a more in-depth assessment of how much of the observed trends in canopy mortality are caused by changes in forest management, simulations trying to replicate stand structures in European forests would have to be analysed/conducted. However, the steeper increase in canopy mortality observed by Senf et al. (2018) compared to the simulations might also be attributed to the rigidity of the simulation of tree growth in the model. A higher plasticity of crowns allows the canopy to be packed more densely and for the canopy to show a higher complexity (Purves et al. 2007; Fotis et al. 2018). This was found to increase NPP (Fotis et al. 2018) and thereby competition, which might partially explain the higher increase in mortality observed by Senf et al. (2018).

Furthermore, no correlation was found between the simulated and observed canopy mortality in Europe (see section 3.2). The low sample size per country and the simple method of scaling the samples to country size by averaging them might have caused different patterns and did not catch the overall trends. However, if that was solely responsible for this, the smaller countries should have shown a more significant correlation with the canopy mortality estimated by Senf et al. (2018), which they did not. Moreover, the interannual variability of the simulated canopy mortality was constantly much higher than the observed (Fig. 9). Also, the interannual variability of simulated carbon loss caused by stand-replacing disturbance is very high, particularly compared to the carbon loss caused by background and vitality mortality (Fig. 18). The latter one is represented in the model as a certain likelihood of death that increases with low growth efficiency (eq. 5) and its stochasticity is thereby connected to climatic conditions. Opposed to that, stand-replacing disturbance is solely represented as a stochastic process in the model. As the 'samples' in the simulation are only six per country, which represent together an area of 30 ha, the stochasticity of the canopy mortality is likely not as dampened as in the observations by Senf et al. (2018), who analysed 4000 pixels (30m resolution) in each country for canopy mortality (an area of 360 ha per country). This is supported by the similarity of the amplitude of the interannual variability of the simulated canopy mortality of the different countries when visually comparing them. Furthermore, disturbances are often related to climate conditions and should thus generally show less random interannual variability in observations than in the simulations. Further studies using the LPJ-GUESS model would thus benefit from a larger sample size to dampen variability of mortality rates caused by stochasticity of disturbances. Otherwise, it would be advantageous to use a model linking disturbances with climatic conditions when using a small sample size.

4.3 Which driver is the most influential for the observed increase in mortality?

Answering the second research question, an increased competition in central European forests under climate change could be shown using the NPP as an indicator. The increase in simulated NPP over time shows that demographic processes are sped up in the forest. The trees can grow faster and e.g., a shaded tree is outcompeted faster. Thus, competition is indicated to increase, as does mortality in all countries but Switzerland. The very low tree density in Switzerland (Fig. 21) compared to the other countries is likely caused by climatic constraints and could therefore cause a possible exception to the increased NPP causing indicating an increased competition.

4.3.1 What causes the observed trends in mortality and NPP in SIMhist?

In the historical simulation a positive trend in NPP is shown for all countries (Fig. 10). In accordance with this, all tree mortality rates (except carbon in AT and CZ) increase in all

countries but Switzerland. Excluding Switzerland in the following, stem mortality, which is more sensitive to capture mortality of younger trees, shows the highest trends and absolute rates. Considering that the percentage of stem mortality will be much higher than the carbon mortality if e.g., 40 saplings die, both results are reasonable. Moreover, as smaller trees are more easily supressed and outcompeted than larger trees, the increase in NPP, stem mortality and carbon loss due to vitality mortality indicate an increased mortality due to higher competition. The canopy and carbon mortality are more sensitive towards the death of large, carbon-rich trees. Both variables were generally lower but displayed positive trends over time, besides the carbon mortality in Austria and the Czech Republic that showed negative trends. As larger trees are more sensitive to abiotic factors like water scarcity (due to larger and more exposed crowns they have a higher evaporation rate and suffer more easily from hydraulic failure than younger trees (the latter is not represented in the model)) (Bennett et al. 2015; McDowell and Allen 2015), these trends point towards increased mortality due to drought stress, although ambiguously in Austria and the Czech Republic. The shown increase in vitality mortality over time (except for CZ) supports the assumptions that mortality increases due to higher competition and due to increased stress. However, future studies would benefit if the vitality mortality rate could be broken down further to attribute how much of it is caused by direct resource stress (i.e., due to less available water caused by increased temperature or changed precipitation patterns) and how much is caused by indirect resource stress (i.e., increase in available resources increases neighbourhood crowding, thus causing stress). This would reduce uncertainties and assumptions when assessing the role of drivers causing increases in forest mortality. Furthermore, the LAI of the PFT IBS (boreal/temperate shade-intolerant broadleaved summergreen tree) showed a positive trend in all countries. As that PFT is shade-intolerant it is more vulnerable to growth efficiency and might thus be partially responsible for an increase in vitality mortality due to suppression.

The lack of correlation between both NPP and mortality, as well as NPP and climate drivers, was apparent, except for the significant correlations between canopy mortality and precipitation, and carbon mortality and NPP in Germany (Table S7). The significant correlations in Germany indicates a relationship between the increase of mortality of particularly larger trees and the increase of competition and changes in the precipitation patterns. The general lack of significant correlations, on the other hand, might be caused by the high variability of the mortality trends due to stand replacing disturbances being simulated only as stochastic processes. Furthermore, the lower increase of the simulated canopy mortality trends over time compared to estimations by Senf et al. (2018) might further explain a lack of significant correlation.

A particularly strong trend in NPP was observed in Switzerland. Also, the mean NPP is generally the highest in Switzerland, followed by Austria. Interestingly, those two countries include the simulated grid cells at the highest elevation (Fig. 6). Furthermore, all mortality rates in Switzerland show a downward trend over time (Fig. 11) and the LAI of woody PFTs increase over time in Switzerland on cost of the cool grass, C3G, PFT (Fig. 21). As vegetation at higher altitudes and along treelines is mostly temperature limited (Jolly et al. 2005; Harsch et al. 2009), the much stronger increase in NPP in these two countries can likely be ascribed to the increase in temperature over time and consequently, a shift of the treeline. This shift of the treeline is indicated by the succession of grass by woody PFTs in the LAI. Growth conditions that are commonly more stressful at higher altitudes seem to become less stressful (Harsch et al. 2009), thereby allowing vegetation that was too sensitive to the initially much more stressful conditions to migrate from lower elevations. The carbon loss due to vitality mortality does increase over time in Switzerland, but this can be explained by the warming-driven increase in tree biomass, with the result that death of fewer individual still results in more biomass loss. In Austria, the country that also includes grid cells at high altitudes, neither a treeline shift nor a

decrease in mortality can be observed. Such trends might be supressed by the trends in mortality in other grid cells at lower elevations in Austria. It would be advantageous to further investigate this by grouping trends according to the elevation of the grid cell.

4.3.2 What is the influence of temperature change on mortality and NPP?

The strength of the NPP trend increases compared to SIMhist in all countries (particularly the Czech Republic) but Slovakia and Switzerland. Also, the trends of carbon loss due to vitality mortality in SIMtemp decrease in all countries compared to SIMhist and show slightly negative trends over the time period for the Czech Republic and Poland. Therefore, the increase in NPP, and indicated competition, over the time period can be assumed to not be caused by increasing temperatures due to climate change but to be rather supressed by higher temperatures. This trend shows at the countries with the lowest median elevation (Fig. 6) and can hence be assumed to be only valid for forests at lower elevations. Furthermore, the mortality trends under temperatures at the level of 1920 increase slightly in all countries and the prevalent negative trend in Switzerland becomes less strong compared to the SIMhist. This is likely caused by the increase in NPP in SIMtemp compared to SIMhist, as generally steeper mortality trends in all countries but Slovakia and Switzerland were observed.

In Switzerland, the positive trend in NPP and the mean NPP decrease in strength compared to SIMhist, while in Slovakia only the positive trend decreases in strength. As in the other countries, the trend in carbon loss due to vitality mortality decreases in Switzerland compared to SIMhist, likely caused by the less steep increase of NPP over time compared to SIMhist. Moreover, the treeline shift shown in the change of LAI of PFTs in SIMhist cannot be observed in SIMtemp. This further supports that an increasing temperature is the main driver behind the treeline shift and steep increase in NPP observed in higher altitudes. For diffuse treelines with temperature as the main limiting factor, the former was also suggested by Harsch et al. (2009). However, the negative trend over time in mortality in Switzerland is still prevalent in this simulation and thereby other drivers also contributes to the decreasing mortality over time. Interestingly, the mean stem mortality in Switzerland nearly doubles compared to SIMhist, which indicates a much higher mortality of saplings. As saplings are more vulnerable to low temperatures than larger trees (they die if their tissue has not matured until winter) (Körner et al. 2016), the high stem mortality might be explained by generally lower temperatures in SIMtemp compared to SIMhist causing higher sapling mortality. This is supported, as the stem mortality rates were only significantly different from those in SIMhist in Switzerland and Slovakia.

4.3.3 What is the influence of precipitation change on mortality and NPP?

Changes in NPP and mortality are likely not dependent on the observed small changes in mean precipitation between 1920 and 2015 (Fig. 7) but are rather expected to be induced by changing patterns of seasonal precipitation. As observed in central Europe from 1951- 2000 (Schönwiese and Janoschitz 2008), overall, summer precipitation (precipitation in the growing season) in central Europe decreased. However, those patterns show quite large differences on a regional scale and might thus differ from the general trend. Additionally, as shown by Dulamsuren et al. (2017), European beech stands in Germany in lower elevations are mostly limited by precipitation, those in intermediate elevations (about 600 m a.s.l.) can be both temperature and precipitation limited and those at high elevations (about 1200 m a.s.l.) are mainly temperature limited.

The NPP trends decrease everywhere compared to SIMhist but in Poland and Austria, so that the overall trend of NPP in this simulation is still positive in all countries but very low in

Slovakia and Germany. The positive mortality trends in nearly all countries increase, the trends in canopy and carbon mortality show an especially strong increase. Additionally, the mean canopy and carbon mortality increase everywhere but in Slovakia and Switzerland. This indicates, contrary to the expected pattern (Schönwiese and Janoschitz 2008), a decrease of summer precipitation in SIMprecip compared to SIMhist. Based on this assumption, a more pronounced increase of mortality rates of larger trees due to less available water compared to SIMhist, is in accordance with literature (Bennett et al. 2015). That carbon and canopy mortality did not increase in Slovakia and Switzerland could be explained by those trees being rather temperature than water limited, as they lie in intermediate and high elevations respectively (Fig. 6) (Dulamsuren et al. 2017). As indicated by the LAI of the PFTs, the treeline shift at higher altitudes in Switzerland persists in this simulation, it thus supports that that region is mainly temperature limited.

However, the carbon loss trends due to vitality mortality increases in all countries but Germany, Poland and Slovakia, where it decreases strongly. This further supports that the observed changes in precipitation patterns in some countries is a decrease in summer precipitation compared to the SIMhist. This is leading to a lower NPP, a considerable increase in carbon and canopy mortality and an increase in vitality mortality in countries where this shift is particularly pronounced. As the vitality mortality only increases in some countries, one can suspect that not all countries experienced similarly strong decreases of summer precipitation compared to SIMhist. Therefore, a decrease in vitality mortality in some countries might be caused by decreasing competition mortality compared to SIMhist indicated by the decrease in NPP rates compared to SIMhist. The diverging model results stress that changes in seasonal precipitation patterns should be a priority for future investigations.

4.3.4 What is the influence of CO_2 concentration change on mortality and NPP?

The simulation with CO_2 concentrations fixed to levels of 1920 shows a large decrease of annual NPP trends in all countries compared to the SIMhist and the NPP shows a negative trend in all countries but Switzerland. This displays that CO_2 fertilisation is the main driver of the increase in NPP in all countries at lower elevation. SIMCO2 shows, that if no CO_2 fertilisation occurred, the climate change induced change of other drivers (i.e., mainly temperature) would strongly decrease NPP, as the lack of the increasing water-use efficiency caused by CO_2 fertilisation (Lo et al. 2019) would further increase abiotic stress induced mortality. However, at higher altitudes, the NPP increases nonetheless, while the treeline advances, mainly driven by temperature (Harsch et al. 2009).

Furthermore, the average trend in carbon loss due to vitality mortality of all countries decreases. However, that decrease is less than that observed in SIMtemp. Therefore, one can assume that the stress induced mortality due to increasing temperatures plays a slightly larger role in the observed increases in mortality than the competition induced mortality caused by CO_2 fertilisation. However, as the vitality mortality cannot be told apart with the applied model settings, increases in competition due to both CO_2 fertilisation and lengthened growing season as a consequence of higher temperatures might play a larger role together in the increasing mortality rates than the stress mortality caused by higher temperatures at low altitudes. Hence, further differentiation between causes of vitality mortality would be vital to answer the research question four more clearly.

Considering both the large decrease in NPP and the decrease in vitality mortality, although mortality generally increased in this simulation compared to SIMhist, it becomes apparent that direct competition induced mortality increases mainly as a consequence of CO_2 fertilisation. The mortality in this simulation shows the largest increase over time compared to the other

simulations with one driver fixed to 1920. This could be attributed to both the lower water-use efficiency of trees in this simulation compared to SIMhist and possibly to a higher stress induced competition in some countries (although the competition mortality due to CO_2 fertilisation was evidently higher in SIMhist than the stress mortality, when regarding the decrease of vitality mortality in this simulation compared to SIMhist).

4.3.5 How can driver interaction explain the observed trends in mortality and NPP in SIMall?

As the nitrogen deposition rates in the locations are not available, it is assumed that they have increased in all locations until the 1990s and declined since then (Schmitz et al. 2019). As the deposition rates were increasing until roughly 30 years ago, one can further assume that the nitrogen deposition rates – tough declining - continued to be at a high level. According to Lloyd (1999) NPP increase in temperate forests is doubled if an increase of CO_2 concentrations and nitrogen deposition are co-occurring, while when regarded individually the impact of increasing CO_2 concentrations are smaller than that of even low nitrogen depositions.

A considerable positive trend in NPP is still seen in the Czech Republic, Switzerland and Germany, while a negative trend can be observed in Slovakia. However, both the trend and the mean of NPP decrease in all countries compared to the historical simulation. As the only driver having a positive trend over time, increased nitrogen depositions can be assumed to be causing the positive trend observed. All of the three average mortality trends for all countries decrease compared to the historical simulation. However, stem and canopy mortality still show a slight increase in mortality over time, likely caused by the increase in competition indicated by the rising NPP. Interestingly, the decrease in means and trend strength of vitality mortality is less than that observed in SIMtemp (except for the trends in CH, PL, AT). Additionally, the carbon loss due to vitality mortality still shows a positive trend in Poland and Slovakia. This is likely caused by an increasing competition mortality, as mentioned above. A larger abiotic stress compared to SIMhist, on the other hand, has likely caused the large mortality reduction in all countries.

As seen in Fig. 17, driver interaction seems to greatly decrease mortality trends. As mentioned above NPP increase is doubled if an increase of CO_2 concentrations and nitrogen deposition are co-occurring (Lloyd 1999). These feedbacks also exist between other drivers: increased CO_2 concentrations fertilise trees, thus increasing growth rates (Ainsworth and Long 2005) and water-use efficiency (Frank et al. 2015), while temperature decreases water availability at lower altitudes but improves uptake of nitrogen (Friend et al. 2014) and lengthens the growing season (Myneni et al. 1997). Thus, the decrease in NPP trends (and often an associated increase in mortality) if one driver is not increasing over time will be much stronger due to the initial positive feedback strengthening the initially observed increase. Also, if NPP decreases because the increase of a driver like temperature causes resource stress (i.e., water stress), mortality rates might be dampened because of the opposite effects of some drivers. This might explain why the interactive mortality is always highest in Switzerland, where temperature has not caused water stress.

4.3.6 Which is the most important driver for the observed increase in mortality?

Answering the third research question, an increased tree mortality could be partially attributed to increased competition. It could only be shown at lower elevations, as the simulated areas in Switzerland showed a steep increase in NPP and a treeline shift that led to a decrease in stem mortality rates instead. The increase in competition at lower elevations can mainly be attributed to the increase in CO_2 concentration, and to a small part to the changed precipitation patterns

that seem to have increased available water in summer. Although increasing temperatures likely have a positive influence on NPP and thus increase competition mortality, the increase in temperature has mainly caused a decrease in NPP and an increase in stress mortality. How much the increase in NPP due to higher temperatures has thus possibly dampened the stress mortality cannot be told apart. An increase of NPP and competition mortality was seen in SIMall and thus attributed to increased nitrogen depositions. Due to all drivers being highly interactive, the strength of the influence of nitrogen depositions is uncertain.

The fourth research question, what the relative contribution of the individual drivers is in driving changes in tree mortality, can only be answered with high uncertainties. CO_2 concentrations are, as shown above the largest contributor to an increased competition mortality at lower elevations and that increase in mortality seems to be lower than the increase in stress mortality due to higher temperatures. The decrease in vitality mortality observed in SIMCO2 and SIMtemp was very similar but slightly larger in SIMtemp. Also, in SIMtemp, the NPP and the competition increased, the observed decrease of vitality mortality was thus probably dampened by competition mortality increasing, which increases the uncertainty of the assessment that temperature stress contributes more to the increasing mortality trends. The uncertainty is further increased, as SIMCO2 showed a high increase in mortality likely caused by CO_2 fertilisation decreasing the vulnerability of trees to temperature stress due to an increase in water-use efficiency and decreasing stress competition. The change in precipitation patterns caused by climate change seemed to have led to the opposite of what was expected, an increase in summer precipitation. Therefore, precipitation has increased NPP and competition mortality but was the smallest driver. An increase in both NPP and mortality over time could be shown to be related to increasing nitrogen deposition but due to the interactions of all drivers the scale of the competition mortality caused by nitrogen depositions is uncertain. Contrary, to the other countries, the mortality rates in Switzerland showed decreasing trends, which was attributed to its high elevation and the shift in treeline and the increasing NPP linked to this. The main driver of the trends seen in Switzerland was the temperature, followed by CO_2 concentrations and precipitation. Nitrogen was shown to influence the NPP in CH.

Further differentiation between causes of vitality mortality would need to be considered in further research to eliminate the currently very high uncertainties in the assessments of driver contribution to mortality. Distinction between vitality mortality because of direct resource stress and indirect resource stress because of neighbourhood crowding would immensely improve attribution of mortality trends to drivers.

4.4 Further limitations

Studies suggest that CO_2 fertilisation can cause immediate responses in tree growth rates but that responses of tree mortality rates are lagging (Brienen et al. 2020; Hubau et al. 2020; Needham et al. 2020). This is caused by increased growth rates decreasing carbon residence times, thus shortening the life-spans of trees (Körner 2017; Brienen et al. 2020). Therefore, current increases in canopy mortality worldwide are suggested to result from a lagged response of mortality to growth stimulation, which is projected to neutralise all current carbon gains due to higher growth rates (Brienen et al. 2020). Transferring that concept to this study, parts of the increased canopy mortality might be caused by the lagged mortality response. However, as other mortality rates are also observed to increase the lagged response does not seem to play a major role in European forests just yet. Nonetheless, it should be borne in mind when conducting further studies.

5 Conclusion

- The LPJ-GUESS model was able to reproduce the forest biomass (density) in the simulated locations and representative to the respective countries significantly well but seems to incorporate a systematic sampling bias for larger countries. Also, the observed canopy mortality by Senf et al. (2018) was not well reproduced, despite agreement between the model and observations of a positive trend in mortality for all countries except Switzerland. The simulated mortality values were overestimated, which might have been caused by a rigidity of the LPJ-GUESS model that does not allow crown plasticity, by no threshold being applied for sapling size in the model, by all crown deaths being seen as part of the canopy mortality rates in the model, and by the model only simulating natural vegetation. Whether those reasons are causing an overestimation of forest mortality is important to be further investigated. Moreover, the observed increase in canopy mortality by Senf et al. (2018) could not be shown for Switzerland and was less steep for all other countries in the simulation. The lower increase of mortality over time was likely related to the observed increase in mortality in Europe being linked to forests recovering from past land use and intensified harvest practices (Senf et al. 2018), which cannot be captured in a model simulating natural vegetation. Further studies analysing/simulating stand dynamics under forest management are therefore recommended.
- The entirely different trend in Switzerland from the observations was linked to the simulated grid cells being at high elevations (contrary to the observed samples) and a treeline shift decreasing mortality and increasing NPP rates. However, this would need to be further investigated, e.g., by re-evaluating the simulations and the data by Senf et al. (2018) by altitude.
- This study was able to show that an increased tree mortality in central Europe can be partially attributed to increased competition at lower elevations. The increase in competition was mainly attributed to the increase in CO_2 concentration, and to a low extent to changes in precipitation patterns that seem to have, contrary to expectations, increased available water. It is therefore of paramount importance to analyse changes in seasonal precipitation patterns more in-depth in future investigations. How strongly temperature and nitrogen have increased competition mortality could not be shown and should be further researched.
- Temperature (mainly increasing stress mortality) was shown to be the largest driver of mortality followed by CO_2 concentration (mainly increasing competition mortality). This assessment includes a large uncertainty. Precipitation changes have led to small increases in competition mortality. How strongly nitrogen depositions have increased competition mortality is uncertain but higher N was linked to higher competition and mortality. Driver interactions were shown to decreased mortality rates. Future studies breaking apart vitality mortality caused by direct resource stress and by indirect resource stress because of neighbourhood crowding are recommended. This would reduce current uncertainties and assumptions in assessing the role of drivers in increasing mortality rates.
- Understanding that increases in competition are partially responsible for an increase in tree mortality in European forests is an important contribution to understanding the current changes in the global carbon cycle and sink and could furthermore help to adapt forest management practices to those observed changes. This study also contributes to understanding and improving the LPJ-GUESS model.

6 References

Ainsworth, E. A., and S. P. Long. 2005. What have we learned from 15 years of free-air CO2 enrichment (FACE)? A meta-analytic review of the responses of photosynthesis, canopy properties and plant production to rising CO2. *New Phytologist,* 165**:** 351-372. DOI: https://doi.org/10.1111/j.1469-8137.2004.01224.x

Archambeau, J., P. Ruiz-Benito, S. Ratcliffe, T. Frejaville, A. Changenet, J. M. M. Castaneda, A. Lehtonen, J. Dahlgren, et al. 2020. Similar patterns of background mortality across Europe are mostly driven by drought in European beech and a combination of drought and competition in Scots pine. *Agricultural and Forest Meteorology,* 280. DOI: 10.1016/j.agrformet.2019.107772

Bellassen, V., N. Viovy, S. Luyssaert, G. Le Maire, M. J. Schelhaas, and P. Ciais. 2011. Reconstruction and attribution of the carbon sink of European forests between 1950 and 2000. *Global Change Biology,* 17**:** 3274-3292. DOI: 10.1111/j.1365-2486.2011.02476.x

Bennett, A. C., N. G. McDowell, C. D. Allen, and K. J. Anderson-Teixeira. 2015. Larger trees suffer most during drought in forests worldwide. *Nat Plants,* 1**:** 15139. DOI: 10.1038/nplants.2015.139

Bontemps, J. D., A. Denardou, J. C. Herve, J. Bir, and J. L. Dupouey. 2020. Unprecedented pluri-decennial increase in the growing stock of French forests is persistent and dominated by private broadleaved forests. *Annals of Forest Science,* 77. DOI: 10.1007/s13595-020-01003-6

Brienen, R. J. W., L. Caldwell, L. Duchesne, S. Voelker, J. Barichivich, M. Baliva, G. Ceccantini, A. Di Filippo, et al. 2020. Forest carbon sink neutralized by pervasive growth-lifespan trade-offs. *Nature Communications,* 11**:** 4241. DOI: 10.1038/s41467-020-17966-z

Campioli, M., S. Vicca, S. Luyssaert, J. Bilcke, E. Ceschia, F. S. Chapin Iii, P. Ciais, M. Fernández-Martínez, et al. 2015. Biomass production efficiency controlled by management in temperate and boreal ecosystems. *Nature Geoscience,* 8**:** 843-846. DOI: 10.1038/ngeo2553

Ciais, P., M. J. Schelhaas, S. Zaehle, S. L. Piao, A. Cescatti, J. Liski, S. Luyssaert, G. Le-Maire, et al. 2008. Carbon accumulation in European forests. *Nature Geoscience,* 1**:** 425-429. DOI: 10.1038/ngeo233

Cohen, W. B., Z. Yang, and R. Kennedy. 2010. Detecting trends in forest disturbance and recovery using yearly Landsat time series: 2. TimeSync — Tools for calibration and validation. *Remote Sensing of Environment,* 114**:** 2911-2924. DOI: https://doi.org/10.1016/j.rse.2010.07.010

de Carvalho, L. M. T., M. A. L. Fontes, and A. T. d. Oliveira-Filho. 2000. Tree species distribution in canopy gaps and mature forest in an area of cloud forest of the Ibitipoca Range, south-eastern Brazil. *Plant Ecology,* 149**:** 9-22. DOI: 10.1023/A:1009836810707

De Vries, W. I. M., G. J. Reinds, P. E. R. Gundersen, and H. Sterba. 2006. The impact of nitrogen deposition on carbon sequestration in European forests and forest soils. *Global Change Biology,* 12**:** 1151-1173. DOI: 10.1111/j.1365-2486.2006.01151.x

Dulamsuren, C., M. Hauck, G. Kopp, M. Ruff, and C. Leuschner. 2017. European beech responds to climate change with growth decline at lower, and growth increase at higher elevations in the center of its distribution range (SW Germany). *Trees,* 31**:** 673-686. DOI: 10.1007/s00468-016-1499-x

ESRI. 2012. ArcGIS Release 10.5.1. Redlands, CA.

Etzold, S., K. Ziemińska, B. Rohner, A. Bottero, A. K. Bose, N. K. Ruehr, A. Zingg, and A. Rigling. 2019. One Century of Forest Monitoring Data in Switzerland Reveals Species- and Site-Specific Trends of Climate-Induced Tree Mortality. *Frontiers in Plant Science,* 10. DOI: 10.3389/fpls.2019.00307

European Environmental Agency. 2017. Copernicus Land Monitoring Service - Reference Data: EU-DEM.

Eurostat. 2020. EuroGeographics for the administrative boundaries. European Commission.

FAO, 2012. FRA 2015 Terms and Definitions. The Food and Agricultural Organization of the United Nations (FAO), Report, Rome. [in Swedish, English summary]

Flechard, C. R., A. Ibrom, U. M. Skiba, W. de Vries, M. van Oijen, D. R. Cameron, N. B. Dise, J. F. J. Korhonen, et al. 2020. Carbon–nitrogen interactions in European forests and semi-natural vegetation – Part 1: Fluxes and budgets of carbon, nitrogen and greenhouse gases from ecosystem monitoring and modelling. *Biogeosciences,* 17**:** 1583-1620. DOI: 10.5194/bg-17-1583-2020

Forest Europe, UNECE, and FAO. 2011. State of Europe's Forests 2011 - Status and Trends in Sustainable Forest Management in Europe. In Ministerial Conference on the Protection of Forests in Europe.

Fotis, A. T., T. H. Morin, R. T. Fahey, B. S. Hardiman, G. Bohrer, and P. S. Curtis. 2018. Forest structure in space and time: Biotic and abiotic determinants of canopy complexity and their effects on net primary productivity. *Agricultural and Forest Meteorology,* 250-251**:** 181-191. DOI: https://doi.org/10.1016/j.agrformet.2017.12.251

Fowler, D., C. E. Steadman, D. Stevenson, M. Coyle, R. M. Rees, U. M. Skiba, M. A. Sutton, J. N. Cape, et al. 2015. Effects of global change during the 21st century on the nitrogen cycle. *Atmos. Chem. Phys.*, 15**:** 13849-13893. DOI: 10.5194/acp-15-13849-2015

Frank, D. C., B. Poulter, M. Saurer, J. Esper, C. Huntingford, G. Helle, K. Treydte, N. E. Zimmermann, et al. 2015. Water-use efficiency and transpiration across European forests during the Anthropocene. *Nature Climate Change,* 5**:** 579-+.

Friend, A. D., W. Lucht, T. T. Rademacher, R. Keribin, R. Betts, P. Cadule, P. Ciais, D. B. Clark, et al. 2014. Carbon residence time dominates uncertainty in terrestrial vegetation responses to future climate and atmospheric CO2. *Proceedings of the National Academy of Sciences of the United States of America,* 111**:** 3280-3285. DOI: 10.1073/pnas.1222477110

Gavinet, J., J. M. Ourcival, J. Gauzere, L. G. de Jalon, and J. M. Limousin. 2020. Drought mitigation by thinning: Benefits from the stem to the stand along 15 years of experimental rainfall exclusion in a holm oak coppice. *Forest Ecology and Management,* 473. DOI: 10.1016/j.foreco.2020.118266

Hansen, M. C., P. V. Potapov, R. Moore, M. Hancher, S. A. Turubanova, A. Tyukavina, D. Thau, S. V. Stehman, et al. 2013. High-Resolution Global Maps of 21st-Century Forest Cover Change. *Science,* 342**:** 850-853. DOI: 10.1126/science.1244693

Harsch, M. A., P. E. Hulme, M. S. McGlone, and R. P. Duncan. 2009. Are treelines advancing? A global meta-analysis of treeline response to climate warming. *Ecology Letters,* 12**:** 1040-1049. DOI: https://doi.org/10.1111/j.1461-0248.2009.01355.x

Hickler, T., K. Vohland, J. Feehan, P. A. Miller, B. Smith, L. Costa, T. Giesecke, S. Fronzek, et al. 2012. Projecting the future distribution of European potential natural vegetation zones with a generalized, tree species-based dynamic vegetation model. *Global Ecology and Biogeography,* 21**:** 50-63. DOI: https://doi.org/10.1111/j.1466-8238.2010.00613.x

Hubau, W., S. L. Lewis, O. L. Phillips, K. Affum-Baffoe, H. Beeckman, A. Cuni-Sanchez, A. K. Daniels, C. E. N. Ewango, et al. 2020. Asynchronous carbon sink saturation in African and Amazonian tropical forests. *Nature,* 579**:** 80-87. DOI: 10.1038/s41586-020-2035-0

Hyvönen, R., G. I. Agren, S. Linder, T. Persson, M. F. Cotrufo, A. Ekblad, M. Freeman, A. Grelle, et al. 2007. The likely impact of elevated [CO2], nitrogen deposition, increased temperature and management on carbon sequestration in temperate and boreal forest ecosystems: a literature review. *New Phytol,* 173**:** 463-480. DOI: 10.1111/j.1469-8137.2007.01967.x

Jolly, W. M., M. Dobbertin, N. E. Zimmermann, and M. Reichstein. 2005. Divergent vegetation growth responses to the 2003 heat wave in the Swiss Alps. *Geophysical Research Letters,* 32**:** n/a-n/a. DOI: 10.1029/2005gl023252

Jucker, T., O. Bouriaud, and D. A. Coomes. 2015. Crown plasticity enables trees to optimize canopy packing in mixed-species forests. *Functional Ecology,* 29**:** 1078-1086. DOI: https://doi.org/10.1111/1365-2435.12428

Körner, C. 2003. Slow in, Rapid out: Carbon Flux Studies and Kyoto Targets. *Science,* 300**:** 1242-1243.

Körner, C. 2017. A matter of tree longevity. *Science,* 355**:** 130-131. DOI: 10.1126/science.aal2449

Körner, C., D. Basler, G. Hoch, C. Kollas, A. Lenz, C. F. Randin, Y. Vitasse, N. E. Zimmermann, et al. 2016. Where, why and how? Explaining the low-temperature range limits of temperate tree species. *Journal of Ecology,* 104**:** 1076-1088. DOI: 10.1111/1365-2745.12574

Körner, C., and J. Paulsen. 2004. A world-wide study of high altitude treeline temperatures. *Journal of Biogeography,* 31**:** 713-732. DOI: https://doi.org/10.1111/j.1365-2699.2003.01043.x

Kunstler, G., S. Lavergne, B. Courbaud, W. Thuiller, G. Vieilledent, N. Zimmermann, J. Kattge, and D. Coomes. 2012. Competitive interactions between forest trees are driven by species' trait hierarchy, not phylogenetic or functional similarity: Implications for forest community assembly. *Ecology Letters,* 15**:** 831-840. DOI: 10.1111/j.1461-0248.2012.01803.x

Laubhann, D., H. Sterba, G. J. Reinds, and W. De Vries. 2009. The impact of atmospheric deposition and climate on forest growth in European monitoring plots: An individual tree growth model. *Forest Ecology and Management,* 258**:** 1751-1761. DOI: 10.1016/j.foreco.2008.09.050

Lloyd, J. 1999. The CO2 dependence of photosynthesis, plant growth responses to elevated CO2 concentrations and their interaction with soil nutrient status, II. Temperate and boreal forest productivity and the combined effects of increasing CO2 concentrations and increased nitrogen deposition at a global scale. *Functional Ecology,* 13**:** 439-459. DOI: 10.1046/j.1365-2435.1999.00350.x

Lo, Y. H., J. A. Blanco, E. G. de Andres, J. B. Imbert, and F. J. Castillo. 2019. CO2 fertilization plays a minor role in long-term carbon accumulation patterns in temperate pine forests in the southwestern Pyrenees. *Ecological Modelling,* 407. DOI: 10.1016/j.ecolmodel.2019.108737

Lu, L. L., H. C. Wang, S. Chhin, A. G. Duan, J. G. Zhang, and X. Q. Zhang. 2019. A Bayesian Model Averaging approach for modelling tree mortality in relation to site, competition and climatic factors for Chinese fir plantations. *Forest Ecology and Management,* 440**:** 169-177. DOI: 10.1016/j.foreco.2019.03.003

Luo, Y., and H. Y. H. Chen. 2015. Climate change-associated tree mortality increases without decreasing water availability. *Ecology Letters,* 18**:** 1207-1215. DOI: 10.1111/ele.12500

Manrique-Alba, A., S. Begueria, A. J. Molina, M. Gonzalez-Sanchis, M. Tomas-Burguera, A. D. del Campo, M. Colangelo, and J. J. Camarero. 2020. Long-term thinning effects on tree growth, drought response and water use ef ficiency at two Aleppo pine plantations in Spain. *Science of the Total Environment,* 728. DOI: 10.1016/j.scitotenv.2020.138536

McDowell, N. G., and C. D. Allen. 2015. Darcy's law predicts widespread forest mortality under climate warming. *Nature Climate Change,* 5**:** 669-672. DOI: 10.1038/nclimate2641

McMahon, S. M., G. G. Parker, and D. Miller. 2010. Evidence for a recent increase in forest growth. *Proceedings of the National Academy of Sciences,* 107**:** 3611 - 3615.

Mellert, K. H., J. Prietzel, R. Straussberger, K. E. Rehfuess, H. P. Kahle, P. Perez, and H. Spiecker. 2008. Relationships between long-term trends of air temperature, precipitation, nitrogen nutrition and growth of coniferous stands in Central Europe and Finland. *European Journal of Forest Research,* 127**:** 507-524. DOI: 10.1007/s10342-008-0233-7

Microsoft Corporation. 2018. Microsoft Excel version 16.0.

Muth, C. C., and F. A. Bazzaz. 2003. Tree canopy displacement and neighborhood interactions. *Canadian Journal of Forest Research,* 33**:** 1323-1330. DOI: 10.1139/x03-045

Myneni, R. B., C. D. Keeling, C. J. Tucker, G. Asrar, and R. R. Nemani. 1997. Increased plant growth in the northern high latitudes from 1981 to 1991. *Nature,* 386**:** 698-702. DOI: 10.1038/386698a0

Nagel, T. A., G. Iacopetti, J. Javornik, A. Rozman, P. De Frenne, F. Selvi, K. Verheyen, and M. Wulf. 2019. Cascading effects of canopy mortality drive long-term changes in understorey diversity in temperate old-growth forests of Europe. *Journal of Vegetation Science,* 30**:** 905-916. DOI: 10.1111/jvs.12767

Needham, J. F., J. Chambers, R. Fisher, R. Knox, and C. D. Koven. 2020. Forest responses to simulated elevated CO(2)under alternate hypotheses of size- and age-dependent mortality. *Global Change Biology,* 26**:** 5734-5753. DOI: 10.1111/gcb.15254

Neumann, M., V. Mues, A. Moreno, H. Hasenauer, and R. Seidl. 2017. Climate variability drives recent tree mortality in Europe. *Global Change Biology,* 23**:** 4788-4797. DOI: 10.1111/gcb.13724

Notaro, M., Z. Liu, R. Gallimore, S. J. Vavrus, J. E. Kutzbach, I. C. Prentice, and R. L. Jacob. 2005. Simulated and Observed Preindustrial to Modern Vegetation and Climate Changes*. *Journal of Climate,* 18**:** 3650-3671. DOI: 10.1175/jcli3501.1

Prentice, I. C., A. Bondeau, W. Cramer, S. P. Harrison, T. Hickler, W. Lucht, S. Sitch, B. Smith, et al. 2007. Dynamic Global Vegetation Modeling: Quantifying Terrestrial Ecosystem Responses to Large-Scale Environmental Change. In *Terrestrial Ecosystems in a Changing World,* eds. J. G. Canadell, D. E. Pataki, and L. F. Pitelka, 175-192. Berlin, Heidelberg: Springer Berlin Heidelberg.

Pretzsch, H., P. Biber, G. Schutze, and K. Bielak. 2014a. Changes of forest stand dynamics in Europe. Facts from long-term observational plots and their relevance for forest ecology and management. *Forest Ecology and Management,* 316**:** 65-77. DOI: 10.1016/j.foreco.2013.07.050

Pretzsch, H., P. Biber, G. Schutze, E. Uhl, and T. Rotzer. 2014b. Forest stand growth dynamics in Central Europe have accelerated since 1870. *Nat Commun,* 5**:** 4967. DOI: 10.1038/ncomms5967

Pugh, T. A. M., T. Rademacher, S. L. Shafer, J. Steinkamp, J. Barichivich, B. Beckage, V. Haverd, A. Harper, et al. 2020. Understanding the uncertainty in global forest carbon turnover. *Biogeosciences,* 17**:** 3961-3989. DOI: 10.5194/bg-17-3961-2020

Purves, D. W., J. W. Lichstein, and S. W. Pacala. 2007. Crown Plasticity and Competition for Canopy Space: A New Spatially Implicit Model Parameterized for 250 North American Tree Species. *PLOS ONE,* 2**:** e870. DOI: 10.1371/journal.pone.0000870

Purves, D. W., J. W. Lichstein, N. Strigul, and S. W. Pacala. 2008. Predicting and understanding forest dynamics using a simple tractable model. *Proceedings of the National Academy of Sciences,* 105**:** 17018-17022. DOI: 10.1073/pnas.0807754105

Rabin, S. S., J. R. Melton, G. Lasslop, D. Bachelet, M. Forrest, S. Hantson, J. O. Kaplan, F. Li, et al. 2017. The Fire Modeling Intercomparison Project (FireMIP), phase 1: experimental and analytical protocols with detailed model descriptions. *Geosci. Model Dev.*, 10**:** 1175-1197. DOI: 10.5194/gmd-10-1175-2017

Rozendaal, D. M. A., O. L. Phillips, S. L. Lewis, K. Affum-Baffoe, E. Alvarez-Davila, A. Andrade, L. E. O. C. Aragão, A. Araujo-Murakami, et al. 2020. Competition influences tree growth, but not mortality, across environmental gradients in Amazonia and tropical Africa. *Ecology*, 101**:** e03052. DOI: https://doi.org/10.1002/ecy.3052

Ruiz-Benito, P., E. R. Lines, L. Gómez-Aparicio, M. A. Zavala, and D. A. Coomes. 2013. Patterns and Drivers of Tree Mortality in Iberian Forests: Climatic Effects Are Modified by Competition. *PLOS ONE*, 8**:** e56843. DOI: 10.1371/journal.pone.0056843

Schelhaas, M.-J., G.-J. Nabuurs, and A. Schuck. 2003. Natural disturbances in the European forests in the 19th and 20th centuries. *Global Change Biology*, 9**:** 1620-1633. DOI: https://doi.org/10.1046/j.1365-2486.2003.00684.x

Schmitz, A., T. G. M. Sanders, A. Bolte, F. Bussotti, T. Dirnböck, J. Johnson, J. Peñuelas, M. Pollastrini, et al. 2019. Responses of forest ecosystems in Europe to decreasing nitrogen deposition. *Environmental Pollution*, 244**:** 980-994. DOI: https://doi.org/10.1016/j.envpol.2018.09.101

Schönwiese, C., and R. Janoschitz. 2008. Klima-Trendatlas Deutschland. Institut für Atmosphäre und Umwelt.

Seidl, R., M.-J. Schelhaas, W. Rammer, and P. J. Verkerk. 2014. Increasing forest disturbances in Europe and their impact on carbon storage. *Nature Climate Change*, 4**:** 806-810. DOI: 10.1038/nclimate2318

Senf, C., D. Pflugmacher, Y. Zhiqiang, J. Sebald, J. Knorn, M. Neumann, P. Hostert, and R. Seidl. 2018. Canopy mortality has doubled in Europe's temperate forests over the last three decades. *Nature Communications*, 9**:** 4978. DOI: 10.1038/s41467-018-07539-6

Smith, B. 2001. LPJ-GUESS-an ecosystem modelling framework. *Department of Physical Geography and Ecosystems Analysis. INES, Sölvegatan*, 12**:** 22362.

Smith, B., I. C. Prentice, and M. T. Sykes. 2001. Representation of vegetation dynamics in the modelling of terrestrial ecosystems: comparing two contrasting approaches within European climate space. *Global Ecology and Biogeography*, 10**:** 621-637. DOI: https://doi.org/10.1046/j.1466-822X.2001.t01-1-00256.x

Smith, B., D. Wårlind, A. Arneth, T. Hickler, P. Leadley, J. Siltberg, and S. Zaehle. 2014. Implications of incorporating N cycling and N limitations on primary production in an individual-based dynamic vegetation model. *Biogeosciences*, 11**:** 2027-2054. DOI: 10.5194/bg-11-2027-2014

Takahashi, K. 2010. Effects of altitude and competition on growth and mortality of the conifer Abies sachalinensis. *Ecological Research*, 25**:** 801-812. DOI: https://doi.org/10.1007/s11284-010-0710-6

The MathWorks Inc. 2019. MATLAB, version 9.7 (R2019b). Natick, Massachusetts, United States.

Thurner, M., C. Beer, M. Santoro, N. Carvalhais, T. Wutzler, D. Schepaschenko, A. Shvidenko, E. Kompter, et al. 2013. Carbon stock and density of northern boreal and temperate forests. *Global Ecology and Biogeography*, 23**:** 297-310. DOI: 10.1111/geb.12125

van Mantgem, P. J., N. L. Stephenson, J. C. Byrne, L. D. Daniels, J. F. Franklin, P. Z. Fule, M. E. Harmon, A. J. Larson, et al. 2009. Widespread Increase of Tree Mortality Rates in the Western United States. *Science*, 323**:** 521-524. DOI: 10.1126/science.1165000

Vilà-Cabrera, A., J. Martínez-Vilalta, J. Vayreda, and J. Retana. 2011. Structural and climatic determinants of demographic rates of Scots pine forests across the Iberian Peninsula. *Ecological Applications*, 21**:** 1162-1172. DOI: https://doi.org/10.1890/10-0647.1

Vilén, T., K. Gunia, P. J. Verkerk, R. Seidl, M. J. Schelhaas, M. Lindner, and V. Bellassen. 2012. Reconstructed forest age structure in Europe 1950–2010. *Forest Ecology and Management,* 286**:** 203-218. DOI: https://doi.org/10.1016/j.foreco.2012.08.048

Viovy, N. 2018. CRUNCEP Version 7 - Atmospheric Forcing Data for the Community Land Model. Boulder, CO: Research Data Archive at the National Center for Atmospheric Research, Computational and Information Systems Laboratory.

Westoby, M. 1984. The Self-Thinning Rule. In *Advances in Ecological Research Volume 14*, 167-225.

Zhao, M., and S. W. Running. 2010. Drought-Induced Reduction in Global Terrestrial Net Primary Production from 2000 Through 2009. *Science,* 329**:** 940-943. DOI: 10.1126/science.1192666

7 Appendices

7.1 Methods

Supplementary table 1. P-values and rho of the Pearson correlation to evaluate the fitted regression model of temperature and precipitation from 1920-2015. If the correlation is not significant (α=0.01), the values are printed in grey.

	temperature		**precipitation**	
	p-value	rho	p-value	rho
AT	3.5E-11	0.61	0.605	0.05
CZ	1.3E-08	0.54	0.423	-0.08
DE	3.4E-07	0.49	0.048	0.20
PL	2.2E-03	0.31	0.956	-0.01
SK	7.1E-09	0.55	0.800	-0.03
CH	2.4E-12	0.64	0.279	0.11

Supplementary table 2. Coordinates (in decimal degrees) and respective country of the 36 simulated areas.

Country	**Latitude**	**Longitude**
AT	47.25	13.75
AT	47.75	15.25
AT	48.25	13.75
AT	48.25	14.25
AT	48.25	14.75
AT	48.25	15.25
CZ	49.25	15.75
CZ	49.25	16.25
CZ	49.25	17.25
CZ	49.75	13.25
CZ	49.75	15.25
CZ	50.25	15.75
DE	50.25	11.75
DE	51.25	8.25
DE	51.25	9.75
DE	52.25	8.75

Country	**Latitude**	**Longitude**
PL	50.25	19.75
PL	50.75	21.75
PL	51.75	19.75
PL	52.75	17.75
PL	52.75	22.25
PL	53.75	21.25
SK	48.25	18.25
SK	48.75	18.25
SK	48.75	18.75
SK	48.75	19.25
SK	48.75	19.75
SK	48.75	20.25
CH	46.25	7.25
CH	46.75	7.25
CH	46.75	7.75
CH	46.75	8.25

DE	52.25	11.25	**CH**	46.75	8.75
DE	52.25	11.75	**CH**	47.25	8.75

7.2 NPP, mortality and correlation

Supplementary table 3. Mean NPP of different simulations.

Mean NPP (kg [C] $m^{-2}yr^{-1}$), 1985-2015					
	SIMhist	**SIMtemp**	**SIMprecip**	**SIMCO2**	**SIMall**
AT	0.79	0.78	0.79	0.71	0.72
CZ	0.63	0.64	0.65	0.55	0.58
DE	0.69	0.70	0.66	0.61	0.62
PL	0.64	0.62	0.63	0.55	0.57
SK	0.72	0.73	0.71	0.64	0.66
CH	0.81	0.68	0.82	0.76	0.62
AVERAGE	**0.71**	**0.69**	**0.71**	**0.64**	**0.63**

Supplementary table 4. Mean annual stem, canopy and carbon mortality of different simulations.

	SIMhist	**SIMtemp**	**SIMprecip**	**SIMCO2**	**SIMall**
Stem mortality					
AT	6.22%/yr	5.53%/yr	6.53%/yr	5.37%/yr	4.73%/yr
CZ	5.72%/yr	4.93%/yr	5.98%/yr	4.60%/yr	4.38%/yr
DE	5.87%/yr	5.96%/yr	5.18%/yr	5.19%/yr	5.06%/yr
PL	5.18%/yr	5.32%/yr	6.25%/yr	4.59%/yr	4.42%/yr
SK	5.81%/yr	4.66%/yr	5.71%/yr	5.46%/yr	4.73%/yr
CH	4.79%/yr	8.45%/yr	4.63%/yr	4.20%/yr	6.23%/yr
AVERAGE	**5.60%/yr**	**5.81%/yr**	**5.71%/yr**	**4.90%/yr**	**4.93%/yr**
Canopy mortality					
AT	2.86%/yr	3.11%/yr	3.29%/yr	2.86%/yr	2.81%/yr
CZ	2.87%/yr	2.90%/yr	3.35%/yr	2.87%/yr	2.80%/yr
DE	3.10%/yr	3.48%/yr	3.27%/yr	3.10%/yr	3.11%/yr
PL	2.97%/yr	2.93%/yr	3.32%/yr	2.97%/yr	2.96%/yr
SK	3.25%/yr	2.76%/yr	3.08%/yr	3.25%/yr	2.90%/yr
CH	2.48%/yr	2.71%/yr	2.32%/yr	2.48%/yr	2.75%/yr
AVERAGE	**2.92%/yr**	**2.98%/yr**	**3.10%/yr**	**2.92%/yr**	**2.89%/yr**

Carbon mortality					
AT	2.40%/yr	2.67%/yr	2.87%/yr	2.40%/yr	2.41%/yr
CZ	2.64%/yr	2.52%/yr	2.74%/yr	2.64%/yr	2.54%/yr
DE	2.76%/yr	3.18%/yr	2.97%/yr	2.76%/yr	2.81%/yr
PL	2.66%/yr	2.59%/yr	2.84%/yr	2.66%/yr	2.72%/yr
SK	2.77%/yr	2.43%/yr	2.65%/yr	2.77%/yr	2.51%/yr
CH	2.03%/yr	1.74%/yr	1.89%/yr	2.03%/yr	2.14%/yr
AVERAGE	**2.54%/yr**	**2.52%/yr**	**2.66%/yr**	**2.54%/yr**	**2.52%/yr**

Supplementary table 5. Differences in stem, canopy and carbon mortality trends as relative values to the historical simulation.

	SIMhist	**SIMtemp**	**SIMprecip**	**SIMCO2**	**SIMall**
Stem mortality					
AT	**0.0589**	-0.0137	0.0121	-0.0003	-0.0357
CZ	**0.0676**	-0.0667	0.0467	0.0215	-0.0977
DE	**0.0249**	0.0120	0.0142	0.0557	-0.0692
PL	**0.0506**	0.0141	-0.0603	-0.0198	-0.0582
SK	**0.0468**	-0.0213	0.0085	0.0230	-0.0494
CH	**-0.0387**	0.1456	0.0497	0.0752	0.1413
AVERAGE	**0.0350**	**0.0117**	**0.0118**	**0.0259**	**-0.0281**
Canopy mortality					
AT	**0.0136**	0.0072	0.0122	0.0160	-0.0194
CZ	**0.0020**	-0.0139	0.0227	0.0369	-0.0009
DE	**0.0130**	-0.0018	0.0139	0.0117	-0.0304
PL	**0.0122**	0.0077	0.0002	0.0017	-0.0128
SK	**0.0147**	0.0073	0.0075	0.0147	0.0013
CH	**-0.0213**	0.0292	0.0336	0.0515	0.0389
AVERAGE	**0.0057**	**0.0059**	**0.0150**	**0.0221**	**-0.0039**
Carbon mortality					
AT	**-0.0026**	0.0149	0.0171	0.0206	-0.0113
CZ	**-0.0090**	-0.0170	0.0025	0.0253	0.0080
DE	**0.0113**	-0.0038	0.0053	-0.0043	-0.0202
PL	**0.0102**	-0.0102	-0.0036	-0.0108	-0.0067
SK	**0.0117**	0.0141	0.0196	0.0033	0.0019
CH	**-0.0127**	0.0127	0.0208	0.0294	0.0131

AVERAGE	**0.0015**	**0.0018**	**0.0103**	**0.0106**	**-0.0025**

Supplementary table 6. The significance of differences in medians between SIMhist and all other simulations were calculated using the MATLAB (The MathWorks Inc. 2019) 'signedrank' function. P-values below 0.05 are significant, z-values show the change in median. If the difference in median between SIMhist and the respective simulation is not significant, the values are printed in grey.

p-values						
	AT	**CZ**	**DE**	**PL**	**SK**	**CH**
Stem mortality						
SIMtemp	0.2476	0.0573	0.9687	0.8141	0.0029	0.0001
SIMprecip	0.4217	0.5967	0.1641	0.0159	0.9219	0.5832
SIMCO2	0.0478	0.0057	0.1526	0.1038	0.4217	0.2811
SIMall	0.0013	0.0045	0.1313	0.1583	0.0415	0.0121
Canopy mortality						
SIMtemp	4.5E-06	1.7E-04	3.6E-05	2.9E-03	2.1E-06	3.4E-04
SIMprecip	1.3E-06	3.4E-06	2.3E-05	3.7E-06	3.4E-06	1.0E-05
SIMCO2	8.2E-05	2.5E-05	1.6E-06	5.9E-05	1.7E-04	1.2E-06
SIMall	7.5E-05	9.6E-05	8.6E-04	2.3E-04	1.0E-04	2.1E-06
Carbon mortality						
SIMtemp	0.4447	0.0778	0.7390	0.0684	0.0524	0.0108
SIMprecip	0.7390	0.8754	0.3369	0.6807	0.5832	0.1364
SIMCO2	0.0027	0.7688	0.0745	0.2397	0.8600	0.3570
SIMall	0.0360	0.2319	0.1416	0.2170	0.1583	0.4805
z values						
	AT	**CZ**	**DE**	**PL**	**SK**	**CH**
Stem mortality						
SIMtemp	-1.16	-1.90	0.04	0.24	-2.98	4.02
SIMprecip	0.80	0.53	-1.39	2.41	0.10	-0.55
SIMCO2	-1.98	-2.76	-1.43	-1.63	-0.80	-1.08
SIMall	-3.21	-2.84	-1.51	-1.41	-2.04	2.51
Canopy mortality						
SIMtemp	4.59	3.76	4.13	2.98	4.74	3.59
SIMprecip	4.84	4.64	4.23	4.62	4.64	4.41
SIMCO2	3.94	4.21	4.80	4.02	3.76	4.86
SIMall	3.96	3.90	3.33	3.68	3.88	4.74

Carbon mortality						
SIMtemp	-0.76	-1.76	0.33	-1.82	-1.94	-2.55
SIMprecip	-0.33	-0.16	-0.96	-0.41	-0.55	-1.49
SIMCO2	-3.00	-0.29	-1.78	-1.18	-0.18	-0.92
SIMall	-2.10	-1.20	-1.47	-1.23	-1.41	-0.71

Supplementary table 7. The significance and strength of the correlation between stem, carbon and canopy mortality and the driver NPP, precipitation, temperature and CO2 concentration in the historical simulation are shown. If the correlation is not significant, the values are printed in grey.

	p-values				**R_s^2**			
stem mortality	**NPP**	**Precipitation**	**Temperature**	**CO_2**	**NPP**	**Precipitation**	**Temperature**	**CO_2**
AT	0.6401	0.5338	0.5957	0.1086	0.01	0.01	0.01	0.09
CZ	0.9853	0.3121	0.4202	0.2135	0.00	0.04	0.02	0.05
DE	0.1709	0.0791	0.9439	0.3460	0.06	0.10	0.00	0.03
PL	0.3737	0.5352	0.9266	0.0957	0.03	0.01	0.00	0.09
SK	0.3121	0.8530	0.2261	0.2278	0.04	0.00	0.05	0.05
CH	0.2455	0.1463	0.7035	0.5013	0.05	0.07	0.01	0.02
Canopy mortality								
AT	0.1494	0.7197	0.9594	0.5702	0.07	0.00	0.00	0.01
CZ	0.7491	0.1975	0.7491	0.9991	0.00	0.06	0.00	0.00
DE	0.1307	0.0309	0.4725	0.3574	0.08	0.15	0.02	0.03
PL	0.3438	0.2583	0.8445	0.4434	0.03	0.04	0.00	0.02
SK	0.3905	0.9698	0.2321	0.2555	0.03	0.00	0.05	0.04
CH	0.0903	0.4473	0.1780	0.1824	0.10	0.02	0.06	0.06
Carbon mortality								
AT	0.4727	0.6078	0.8820	0.9043	0.02	0.01	0.00	0.00
CZ	0.9646	0.2278	0.2874	0.5747	0.00	0.05	0.04	0.01
DE	0.0342	0.0508	0.1469	0.4902	0.15	0.13	0.07	0.02
PL	0.3942	0.8310	0.6795	0.6448	0.02	0.00	0.01	0.01
SK	0.4820	0.9853	0.3714	0.6216	0.02	0.00	0.03	0.01
CH	0.3460	0.5629	0.1737	0.4591	0.03	0.01	0.06	0.02

Supplementary table 8. The significance and strength of the correlation between stem, carbon and canopy mortality and the driver NPP in the different simulations are shown. If the correlation is not significant, the values are printed in grey.

	p-value				R_s^2			
Stem mortality	**SIMtemp**	**SIMprecip**	**SIMCO2**	**SIMall**	**SIMtemp**	**SIMprecip**	**SIMCO2**	**SIMall**
AT	0.4645	0.3714	0.1533	0.4003	0.02	0.03	0.07	0.02
CZ	0.4605	0.3069	0.1131	0.1630	0.02	0.04	0.08	0.07
DE	0.1084	0.5658	0.7990	0.3893	0.09	0.01	0.00	0.03
PL	0.2716	0.4482	0.0075	0.5069	0.04	0.02	0.23	0.02
SK	0.6843	0.9043	0.2894	0.2500	0.01	0.00	0.04	0.05
CH	0.6779	0.6621	0.1377	0.6686	0.01	0.01	0.07	0.01
Canopy mortality								
AT	0.4698	0.1091	0.0141	0.6763	0.02	0.09	0.19	0.01
CZ	0.1106	0.8974	0.1661	0.0829	0.09	0.00	0.07	0.10
DE	0.8548	0.8974	0.2339	0.1546	0.00	0.00	0.05	0.07
PL	0.6747	0.6900	0.0008	0.2261	0.01	0.01	0.33	0.05
SK	0.2046	0.3563	0.6779	0.1096	0.05	0.03	0.01	0.09
CH	0.6939	0.8394	0.0284	0.6482	0.01	0.00	0.16	0.01
Carbon mortality								
AT	0.6231	0.6047	0.1527	0.7607	0.01	0.01	0.07	0.06
CZ	0.0811	0.6859	0.5475	0.1228	0.10	0.01	0.01	0.13
DE	0.9717	0.9853	0.1759	0.5055	0.00	0.00	0.06	0.05
PL	0.5167	0.2022	0.0045	0.8344	0.01	0.06	0.25	-0.01
SK	0.1716	0.2261	0.1640	0.2160	0.06	0.05	0.07	0.25
CH	0.5181	0.3349	0.4698	0.4515	0.01	0.03	0.02	0.25

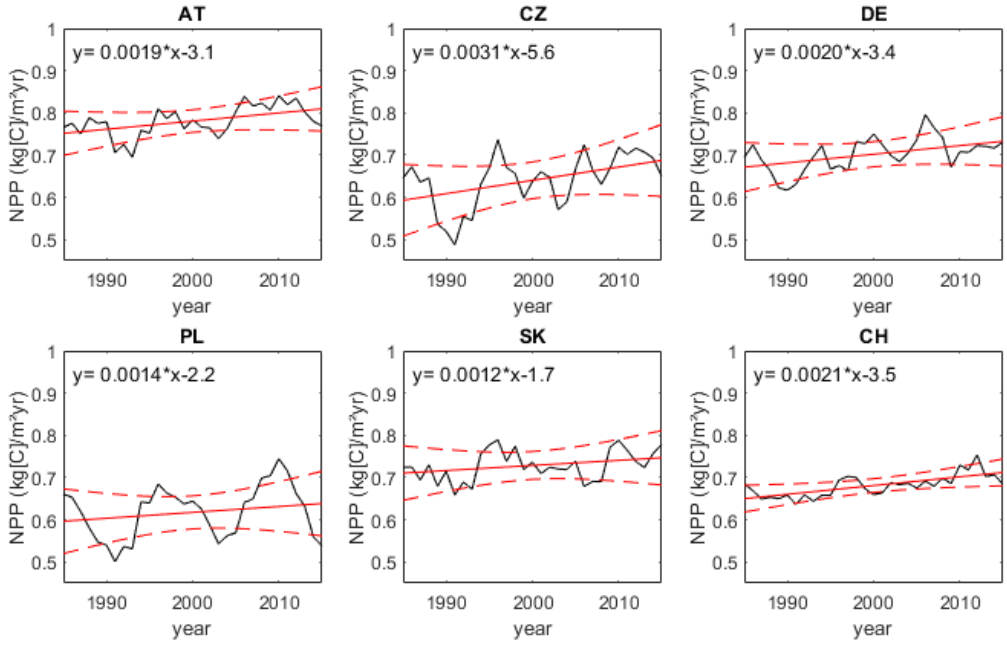

Supplementary figure 1. NPP of the simulation with fixed temperature is displayed in black with a moving average of 3 years applied. The continuous red line is the regression line and the dashed red lines show the 95% confidence interval. They were plotted using the MATLAB (The MathWorks Inc. 2019) functions 'polyfit' and 'polyval'.

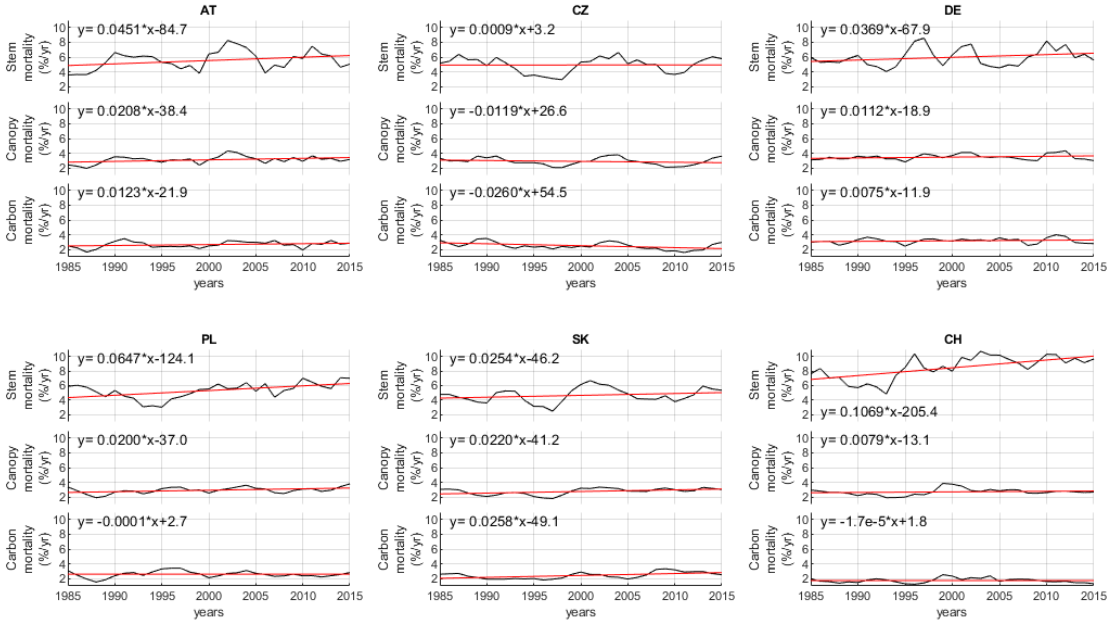

Supplementary figure 2. Stem, carbon and canopy mortality in the simulation with temperature fixed to levels of 1920 are displayed over the time period 1985-2015. The red line shows the regression line that was plotted using the MATLAB (The MathWorks Inc. 2019) function 'polyfit'. A running mean of 3 years was applied.

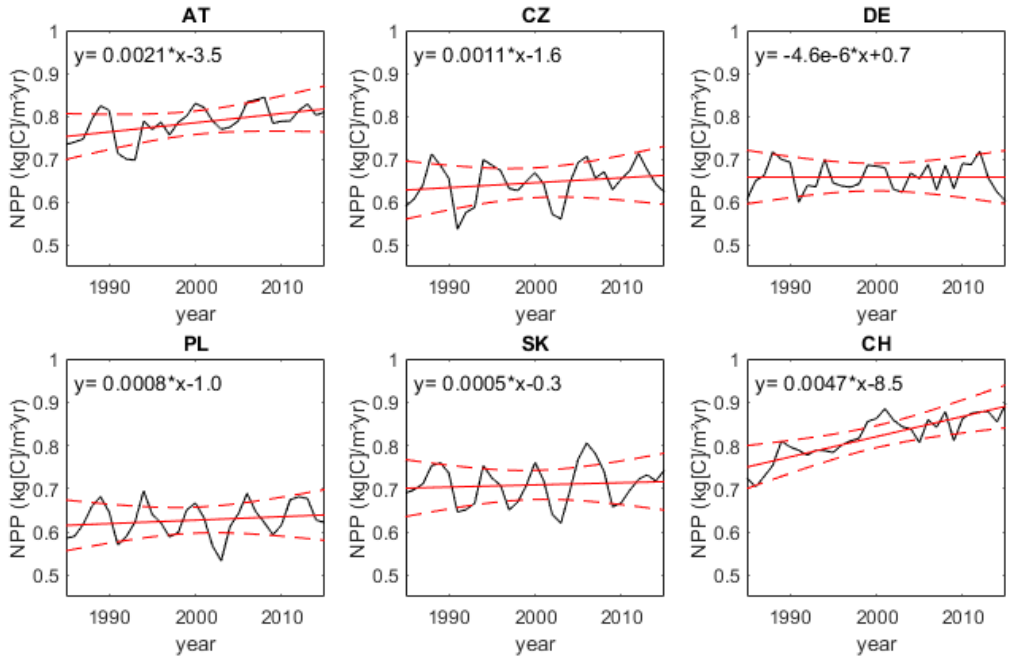

Supplementary figure 3. NPP of the simulation with fixed precipitation is displayed in black with a moving average of 3 years applied. The continuous red line is the regression line and the dashed red lines show the 95% confidence interval. They were plotted using the MATLAB (The MathWorks Inc. 2019) functions 'polyfit' and 'polyval'.

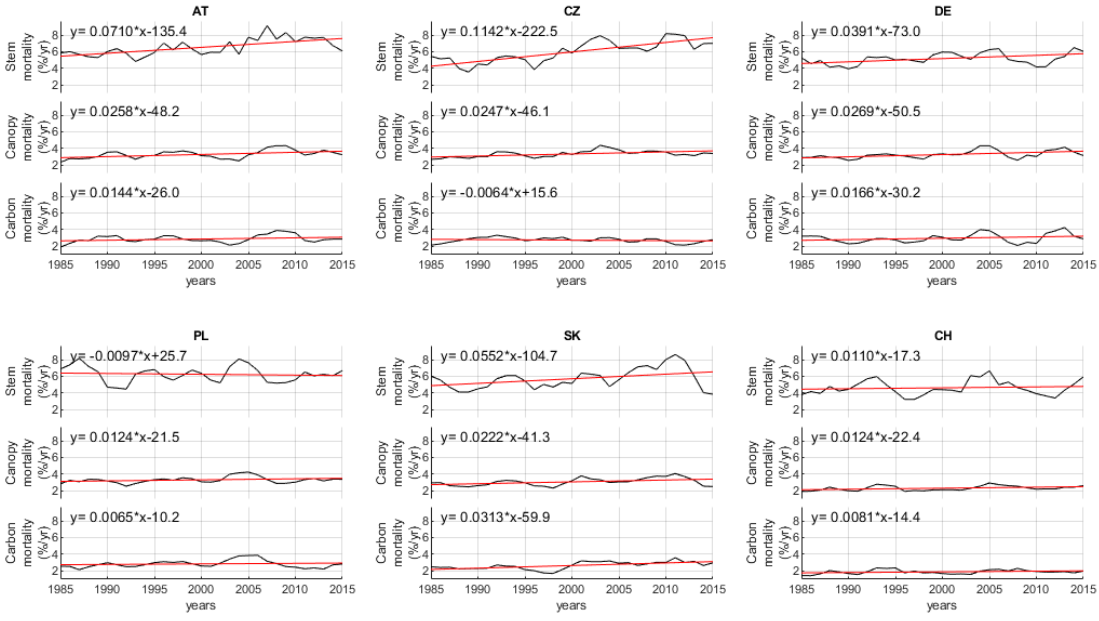

Supplementary figure 4. Stem, carbon and canopy mortality in the simulation with precipitation fixed to levels of 1920 are displayed over the time period 1985-2015. The red line shows the regression line that was plotted using the MATLAB (The MathWorks Inc. 2019) function 'polyfit'. A running mean of 3 years was applied.

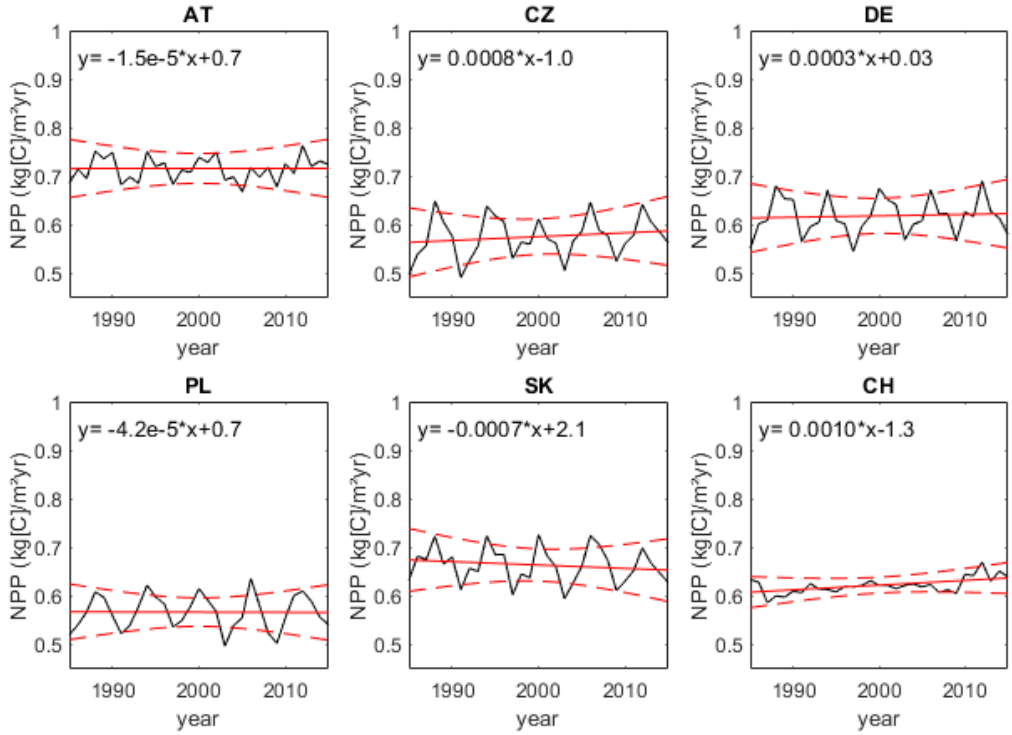

Supplementary figure 5. NPP of the simulation, with everything fixed to levels of 1920 but nitrogen deposition rates, is displayed in black with a moving average of 3 years applied. The continuous red line is the regression line and the dashed red lines show the 95% confidence interval. They were plotted using the MATLAB (The MathWorks Inc. 2019) functions 'polyfit' and 'polyval'.

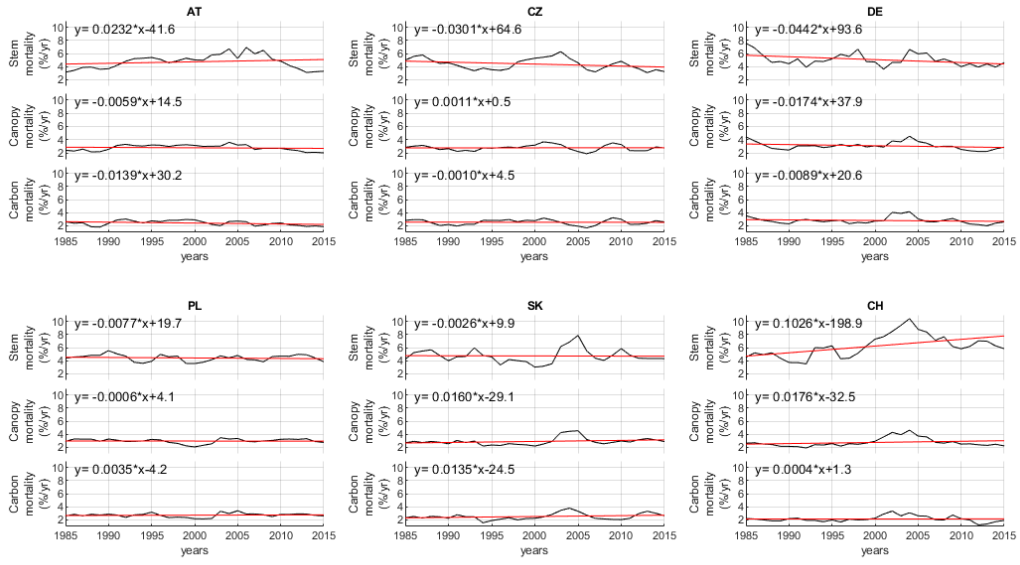

Supplementary figure 6. Stem, carbon and canopy mortality in the simulation with everything but nitrogen deposition rates fixed to levels of 1920 are displayed over the time period 1985-2015. The red line shows the regression line that was plotted using the MATLAB (The MathWorks Inc. 2019) function 'polyfit'. A running mean of 3 years was applied.

7.3 Carbon loss

Supplementary table 9. Mean of causes of carbon loss in all simulations.

	SIMhist	SIMtemp	SIMprecip	SIMCO2	SIMall
Mean carbon loss due to vitality mortality (%/yr), 1985-2015					
AT	0.86	0.73	0.86	0.79	0.76
CZ	0.86	0.75	0.94	0.81	0.75
DE	1.05	1.13	1.03	1.02	1.12
PL	0.97	0.76	0.82	0.75	0.88
SK	0.84	0.71	0.82	0.85	0.70
CH	0.57	0.47	0.57	0.59	0.49
AVERAGE	**0.86**	**0.76**	**0.84**	**0.80**	**0.78**
Mean carbon loss due to background mortality (%/yr), 1985-2015					
AT	0.57	0.64	0.57	0.53	0.59
CZ	0.71	0.62	0.64	0.68	0.75
DE	0.73	0.64	0.67	0.67	0.68
PL	0.66	0.66	0.73	0.70	0.64
SK	0.67	0.68	0.66	0.61	0.70
CH	0.41	0.45	0.36	0.37	0.39
AVERAGE	**0.63**	**0.61**	**0.60**	**0.60**	**0.62**
Mean carbon loss due to stand-replacing disturbance mortality (%/yr), 1985-2015					
AT	1.30	1.24	1.37	0.99	0.99
CZ	1.13	1.06	1.03	1.08	0.98
DE	1.28	1.37	1.21	1.00	0.98
PL	1.25	1.11	1.19	1.16	1.12
SK	1.20	0.98	1.07	1.21	1.04
CH	1.16	0.77	0.89	1.00	1.21
AVERAGE	**1.22**	**1.09**	**1.12**	**1.07**	**1.05**

Supplementary table 10. Trends in causes of carbon loss as relative values to the historical simulation.

	SIMhist	SIMtemp	SIMprecip	SIMCO2	SIMall
Annual change in vitality mortality (%/yr)					
AT	**0.0051**	-0.0033	0.0017	-0.0052	-0.0056
CZ	**-0.0001**	-0.0033	0.0004	-0.0006	-0.0008
DE	**0.0072**	-0.0017	-0.0088	-0.0062	-0.0084

PL	**0.0098**	-0.0120	-0.0035	-0.0076	-0.0073
SK	**0.0058**	-0.0055	-0.0044	0.0012	-0.0009
CH	**0.0047**	-0.0030	0.0003	-0.0065	-0.0057
AVERAGE	**0.0054**	**-0.0048**	**-0.0024**	**-0.0041**	**-0.0048**
Annual change in background mortality (%/yr)					
AT	**0.0040**	-0.0038	0.0034	-0.0043	-0.0021
CZ	**0.0062**	-0.0108	-0.0143	-0.0088	-0.0057
DE	**0.0045**	-0.0103	-0.0053	0.0022	-0.0062
PL	**-0.0007**	0.0057	-0.0024	0.0025	-0.0054
SK	**0.0081**	-0.0025	-0.0075	-0.0058	-0.0064
CH	**0.0001**	0.0027	0.0046	-0.0016	0.0020
AVERAGE	**0.0037**	**-0.0032**	**-0.0036**	**-0.0026**	**-0.0040**
Annual change in stand-replacing disturbance mortality (%/yr)					
AT	**-0.0127**	0.0224	0.0116	0.0300	-0.0033
CZ	**-0.0178**	-0.0005	0.0165	0.0363	0.0166
DE	**-0.0025**	0.0119	0.0192	-0.0018	-0.0029
PL	**-0.0018**	-0.0030	0.0036	-0.0040	0.0107
SK	**-0.0048**	0.0255	0.0338	0.0067	0.0116
CH	**-0.0186**	0.0150	0.0154	0.0365	0.0198
AVERAGE	**-0.0097**	**0.0119**	**0.0167**	**0.0173**	**0.0088**

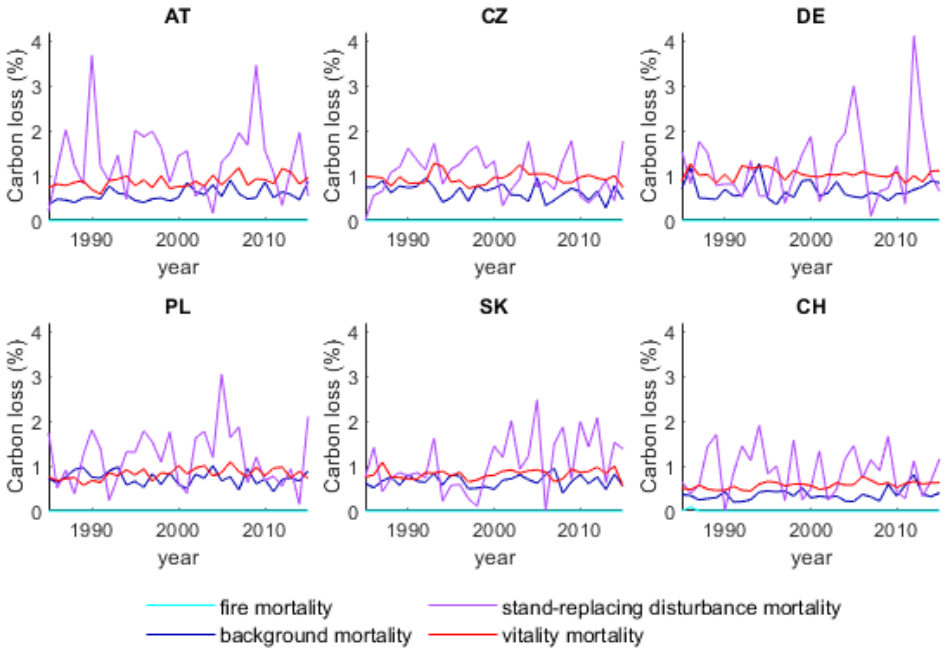

Supplementary figure 7. The causes of carbon loss in the simulation with fixed precipitation are quantified. 1: fire, 2: growth efficiency, 3: thinning mortality, 4: background mortality, 5: stand-replacing disturbance mortality.

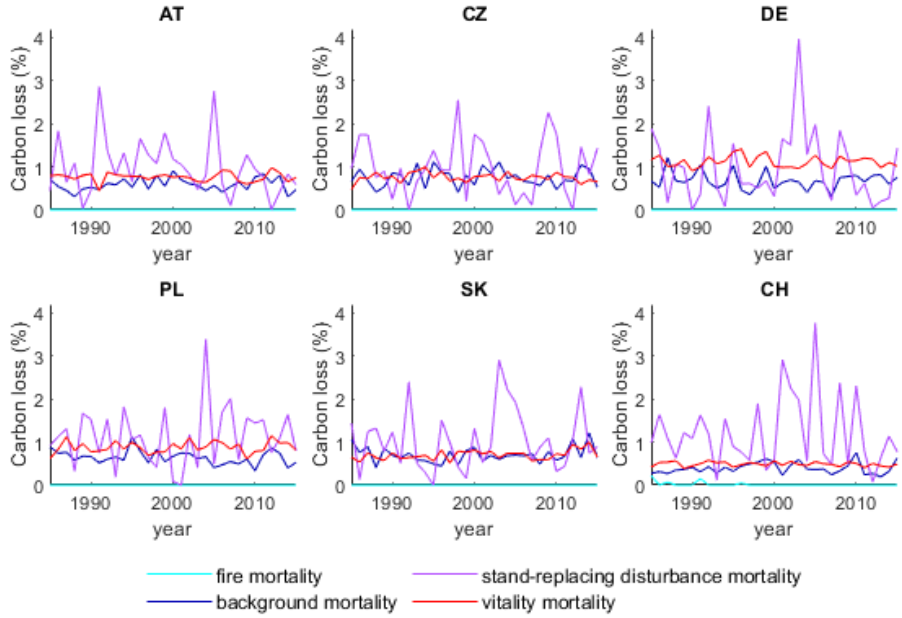

Supplementary figure 8. The causes of carbon loss in the simulation, with all divers fixed but nitrogen deposition rates, are quantified. 1: fire, 2: growth efficiency, 3: thinning mortality, 4: background mortality, 5: stand-replacing disturbance mortality.

7.4 LAI

Supplementary table 11. Mean LAI of the different PFTs in all simulations.

BNE	SIMhist	SIMtemp	SIMprecip	SIMCO2	SIMall
AT	0.77	0.84	0.64	0.74	0.84
CZ	0.20	0.25	0.24	0.20	0.24
DE	0.26	0.23	0.23	0.25	0.22
PL	0.16	0.14	0.18	0.17	0.17
SK	0.40	0.53	0.34	0.36	0.53
CH	1.43	1.20	1.45	1.42	1.10
AVERAGE	**0.54**	**0.53**	**0.51**	**0.52**	**0.52**
BINE					
AT	0.72	0.69	0.69	0.66	0.74
CZ	0.22	0.24	0.21	0.22	0.24
DE	0.25	0.22	0.24	0.25	0.22
PL	0.26	0.18	0.21	0.22	0.20
SK	0.36	0.45	0.33	0.36	0.51
CH	1.10	0.96	1.20	1.05	0.92

AVERAGE	**0.48**	**0.45**	**0.48**	**0.46**	**0.47**
TeBS					
AT	1.63	1.63	1.72	1.71	1.56
CZ	2.45	2.55	2.34	2.40	2.30
DE	2.19	2.27	2.23	2.19	2.16
PL	2.32	2.62	2.41	2.36	2.35
SK	2.16	2.34	2.25	2.10	2.02
CH	0.44	0.41	0.47	0.39	0.40
AVERAGE	**1.86**	**1.97**	**1.90**	**1.86**	**1.80**
IBS					
AT	1.16	1.02	1.20	0.90	0.82
CZ	0.98	0.85	1.10	0.70	0.72
DE	1.32	1.45	1.22	1.05	1.14
PL	1.09	0.82	0.97	0.68	0.82
SK	1.17	0.87	1.16	0.97	0.75
CH	0.65	0.42	0.64	0.57	0.32
AVERAGE	**1.06**	**0.91**	**1.05**	**0.81**	**0.76**
C3G					
AT	0.33	0.41	0.34	0.27	0.33
CZ	0.25	0.28	0.25	0.23	0.26
DE	0.25	0.27	0.22	0.20	0.23
PL	0.28	0.28	0.30	0.27	0.26
SK	0.30	0.29	0.29	0.28	0.32
CH	1.00	0.98	0.87	0.94	0.94
AVERAGE	**0.40**	**0.42**	**0.38**	**0.37**	**0.39**

Supplementary table 12. Total trends in LAI of the different PFTs in all simulations.

BNE	**SIMhist**	**SIMtemp**	**SIMprecip**	**SIMCO2**	**SIMall**
AT	-0.0024	0.0001	-0.0035	-0.0011	-0.0024
CZ	-0.0015	0.0003	-0.0010	-0.0005	0.0010
DE	-0.0026	-0.0017	-0.0034	-0.0024	0.0010
PL	-0.0001	0.0004	0.0000	0.0010	0.0002
SK	-0.0035	-0.0025	-0.0036	-0.0028	-0.0002
CH	0.0200	-0.0004	0.0213	0.0168	-0.0015

AVERAGE	0.0016	-0.0006	0.0016	0.0018	-0.0003
BINE					
AT	-0.0002	0.0005	-0.0022	-0.0011	0.0000
CZ	-0.0020	0.0005	-0.0030	-0.0017	-0.0002
DE	-0.0058	-0.0025	-0.0065	-0.0064	0.0000
PL	-0.0009	0.0014	-0.0004	0.0019	-0.0005
SK	-0.0040	-0.0045	-0.0043	-0.0046	0.0003
CH	0.0106	0.0015	0.0082	0.0053	-0.0009
AVERAGE	-0.0004	-0.0005	-0.0014	-0.0011	-0.0002
TeBS					
CZ	-0.0059	-0.0061	-0.0032	-0.0020	-0.0041
AT	-0.0008	0.0059	-0.0044	-0.0041	-0.0016
DE	-0.0018	-0.0071	-0.0040	-0.0003	-0.0024
PL	-0.0015	0.0057	-0.0098	-0.0039	-0.0036
SK	-0.0037	0.0057	-0.0094	-0.0076	-0.0061
CH	0.0001	0.0001	-0.0005	-0.0010	-0.0014
AVERAGE	-0.0023	0.0007	-0.0052	-0.0031	-0.0032
IBS					
AT	0.0168	0.0107	0.0149	0.0050	0.0018
CZ	0.0120	0.0100	0.0107	0.0041	0.0024
DE	0.0185	0.0175	0.0108	0.0066	0.0023
PL	0.0137	0.0059	0.0096	0.0055	-0.0015
SK	0.0162	0.0063	0.0123	0.0106	0.0016
CH	0.0186	0.0031	0.0110	0.0084	0.0009
AVERAGE	0.0160	0.0089	0.0116	0.0067	0.0013
C3G					
AT	0.0007	0.0041	0.0027	-0.0021	0.0002
CZ	-0.0010	-0.0028	-0.0009	-0.0005	-0.0002
DE	-0.0031	0.0044	0.0012	-0.0021	-0.0007
PL	-0.0024	0.0044	-0.0020	-0.0043	0.0019
SK	0.0013	0.0010	0.0009	0.0011	0.0010
CH	-0.0345	0.0018	-0.0302	-0.0273	0.0122
AVERAGE	-0.0065	0.0022	-0.0047	-0.0059	0.0024

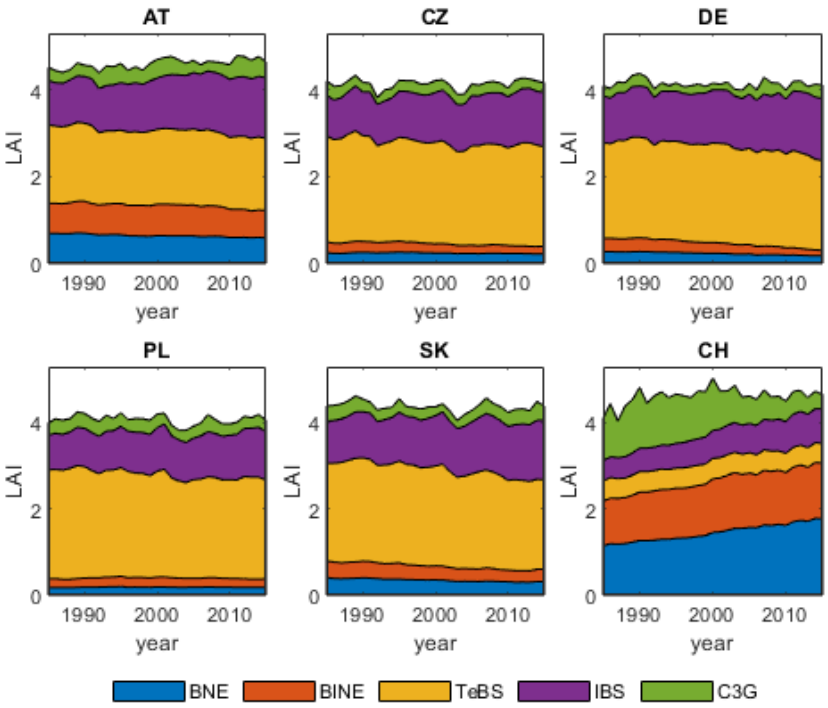

Supplementary figure 9. LAI of Plant Functional Types (PFTs) over the time period 1985-2015 in the simulation with fixed precipitation. BNE: PFT boreal needle leaved evergreen tree, BINE: PFT boreal needle leaved evergreen shade-intolerant tree, TeBS: PFT temperate (shade-tolerant) broadleaved summergreen tree, IBS: PFT boreal/temperate shade-intolerant broadleaved summergreen tree, C3G: PFT cool (C3) grass.

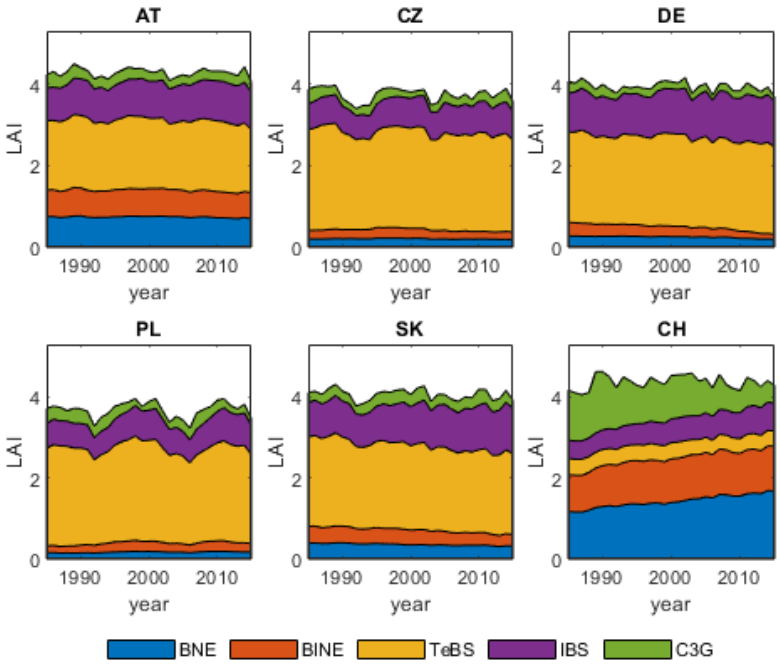

Supplementary figure 10. LAI of Plant Functional Types (PFTs) over the time period 1985-2015 in the simulation with fixed CO2 concentration. BNE: PFT boreal needle leaved evergreen tree, BINE: PFT boreal needle leaved evergreen shade-intolerant tree, TeBS: PFT temperate (shade-tolerant) broadleaved summergreen tree, IBS: PFT boreal/temperate shade-intolerant broadleaved summergreen tree, C3G: PFT cool (C3) grass.

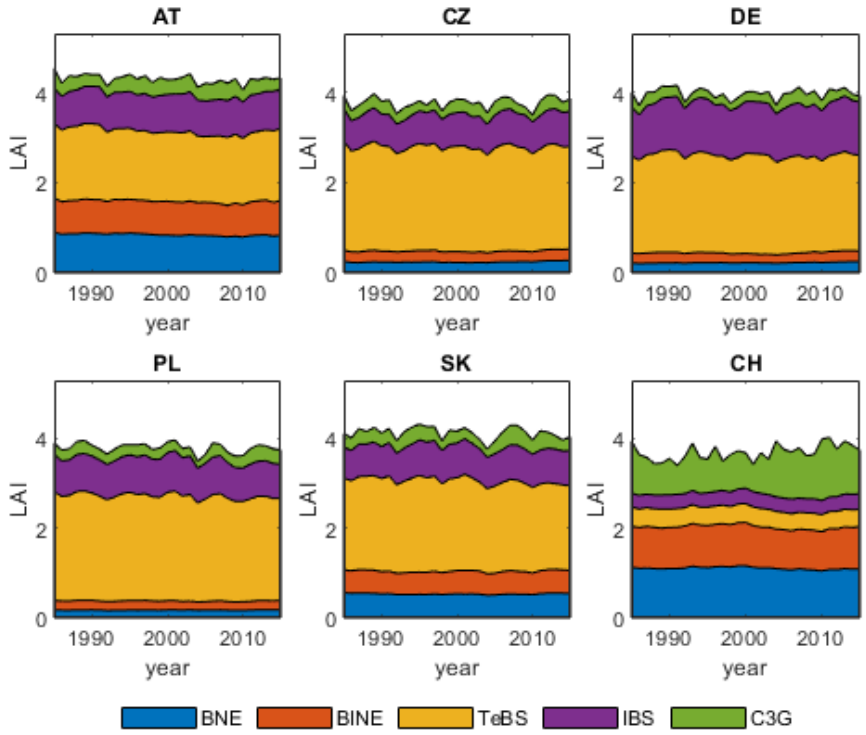

Supplementary figure 11. LAI of Plant Functional Types (PFTs) over the time period 1985-2015 in the simulation with all drivers but nitrogen fixed. BNE: PFT boreal needle leaved evergreen tree, BINE: PFT boreal needle leaved evergreen shade-intolerant tree, TeBS: PFT temperate (shade-tolerant) broadleaved summergreen tree, IBS: PFT boreal/temperate shade-intolerant broadleaved summergreen tree, C3G: PFT cool (C3) grass.